

University of Alberta

**Characterization and Upgrading of a Rutile Concentrate
Produced from the Oil Sands Tailings**

By

Francis Chachula



A thesis submitted to the Faculty of Graduate Studies and Research in partial fulfillment
of the requirements for the degree of Master of Science

In

Materials Engineering

Department of Chemical and Materials Engineering

Edmonton Alberta

Fall, 2002



National Library
of Canada

Acquisitions and
Bibliographic Services

395 Wellington Street
Ottawa ON K1A 0N4
Canada

Bibliothèque nationale
du Canada

Acquisitions et
services bibliographiques

395, rue Wellington
Ottawa ON K1A 0N4
Canada

Your file Votre référence

Our file Notre référence

The author has granted a non-exclusive licence allowing the National Library of Canada to reproduce, loan, distribute or sell copies of this thesis in microform, paper or electronic formats.

The author retains ownership of the copyright in this thesis. Neither the thesis nor substantial extracts from it may be printed or otherwise reproduced without the author's permission.

L'auteur a accordé une licence non exclusive permettant à la Bibliothèque nationale du Canada de reproduire, prêter, distribuer ou vendre des copies de cette thèse sous la forme de microfiche/film, de reproduction sur papier ou sur format électronique.

L'auteur conserve la propriété du droit d'auteur qui protège cette thèse. Ni la thèse ni des extraits substantiels de celle-ci ne doivent être imprimés ou autrement reproduits sans son autorisation.

0-612-81377-0

Canada

University of Alberta

Library Release Form

Name of Author: Francis Chachula

Title of Thesis: Characterization and Upgrading of a Rutile Concentrate
Produced from the Oil Sands Tailings

Degree: Master of Science

Year this Degree Granted: 2002

Permission is hereby granted to the University of Alberta Library to reproduce single copies of this thesis and to lend or sell such copies for private, scholarly or scientific research purposes only.

The author reserves all other publication and other rights in association with the copyright in the thesis, and except as herein before provided, neither the thesis nor any substantial portion thereof may be printed or otherwise reproduced in any material form whatever without the author's prior written permission.



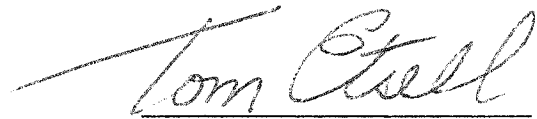
Francis Chachula
Apt. 1203 T2
4604 106A St.
Edmonton, AB
T6H 5J4
Canada

Date: September 24, 2002

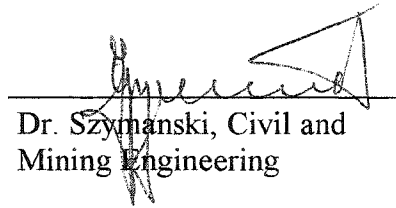
University of Alberta

Faculty of Graduate Studies and Research

The undersigned certify that they have read, and recommend to the Faculty of Graduate Studies and Research for acceptance, a thesis entitled **Characterization and Upgrading of a Rutile Concentrate Produced from the Oil Sands Tailings** in partial fulfillment of the requirements for the degree of **Master of Science in Materials Engineering**.



Dr. T. Etsell, Chemical and
Materials Engineering



Dr. Szymanski, Civil and
Mining Engineering



Dr. Qi Liu, Supervisor,
Chemical and Materials
Engineering

Date: September 24, 2002

ABSTRACT

A rutile concentrate, recently produced from a novel process developed by Syncrude Canada Ltd. and Lakefield Research Ltd., was characterized and upgraded in this research.

The major contaminants in the rutile concentrate were found to be altered ilmenite and siliceous minerals such as quartz. The altered ilmenite was found to be removable by magnetic separation. In order to remove the siliceous minerals, a reverse flotation process was developed which involved the use of cationic collectors for the siliceous minerals, and several polysaccharides as depressants for rutile. The reverse flotation process was applied to the rutile concentrate after magnetic separation. It was found that the free liberated quartz grains could be completely floated into the flotation concentrate. However, the upgraded rutile still contained moderate amounts of SiO_2 . Mineralogical and SEM/EDX analysis showed that intimate association (interlocking) between the minerals was the main reason that caused the siliceous minerals to remain in the rutile concentrate. Further process options were proposed based on the results.

ACKNOWLEDGMENTS

I would like to acknowledge the contributions of my supervisor, Dr. Qi Liu for his unwavering and unequivocal guidance and supervision throughout the project.

Financial support provided to this project by Alberta Energy Research Institute and Syncrude Canada Ltd is gratefully acknowledged.

During the course of this research project technicians and my fellow students have helped me with the testwork. Tina Barker performed the SEM/EDX analyses, Yahui Zhang built the laboratory suspension flotation machine, and Shiraz Merali provided all-around help with day-to-day laboratory needs and operations.

TABLE OF CONTENTS

1	INTRODUCTION.....	1
2	Literature Survey.....	3
2.1	Alberta Oil Sands.....	3
2.1.1	Heavy Minerals in Alberta Oil Sands.....	3
2.1.2	Clark Hot Water Process.....	4
2.1.3	Concentration of Heavy Minerals in Froth Treatment Tailings.....	7
2.2	Titanium: Resource and Utilization.....	8
2.2.1	Titanium Mineralogy.....	8
2.2.2	Titanium Mineral Formation Geology.....	10
2.2.3	World Titanium Dioxide Resources Supply and Demand.....	13
2.2.4	Use of Titanium Minerals.....	15
2.2.5	Processing of Titanium Minerals.....	16
2.2.5.1	Synthetic Rutile.....	17
2.2.5.2	Slag Processes.....	19
2.2.5.3	Upgrading of Titanium Mineral Concentrates.....	20
2.2.5.4	The Chloride Process: Titanium Tetrachloride.....	21
2.2.5.5	Production of Titanium Dioxide Pigments.....	22
2.2.5.6	Production of Titanium Metal.....	23
2.3	Previous Studies to Recover Heavy Minerals From the Oil Sands.....	25
2.3.1	Typical Techniques Used in Heavy Mineral Separation.....	25
2.3.1.1	Gravity Concentration.....	25
2.3.1.2	Magnetic Separation.....	26
2.3.1.3	Electrostatic and High-Tension Separation.....	28
2.3.1.4	Froth Flotation.....	29
2.3.1.4.1	Collectors.....	32
2.3.1.4.2	Regulators or Modifiers.....	33
2.3.1.4.3	Frothers.....	34
2.3.1.5	Surface Charge for Oxide Minerals.....	34
2.3.1.5.1	Development of the Surface Charge.....	34

2.3.1.5.2	The Electric Double Layer	37
2.3.2	Typical Processing Flowsheets for Heavy Minerals.....	42
2.3.3	Previous Studies to Recover Heavy Minerals from Alberta Oil Sand	
	Tailings	45
3	OBJECTIVE.....	54
4	EXPERIMENTAL	55
4.1	Sample Characterization.....	55
4.2	Magnetic Susceptibility Measurement	55
4.3	Magnetic Separation	56
4.4	Electrostatic Separation	56
4.5	Froth Flotation	56
4.5.1	Flotation of Quartz and Rutile Single Minerals.....	57
4.5.2	LR Rutile Flotation	59
4.5.2.1	Scaling up Suspension-Cell Flotation Machine	60
4.6	Zeta Potential Measurements.....	60
4.7	Adsorption Measurements.....	61
4.8	SEM/EDX Analysis.....	62
5	RESULTS AND DISCUSSION	63
5.1	Characterization of the LR Rutile.....	63
5.1.1	Particle Size	63
5.1.2	Chemical Analysis	63
5.1.3	Petrographical Analyses.....	64
5.2	Upgrading of the LR Rutile by Magnetic Separation - Removal of Iron	65
5.2.1	Low Intensity Dry Magnetic Separation.....	65
5.2.2	High Intensity Dry Magnetic Separation	68
5.3	Upgrading of the LR Rutile by Electrostatic Separation-Removal of Siliceous Minerals	69
5.4	Upgrading of the LR Rutile by Froth Flotation - Removal of Siliceous Minerals	70
5.4.1	Quartz Single Mineral Flotation	70
5.4.2	Rutile Single Mineral Flotation	72

5.4.3	Flotation of Artificial Mineral Mixtures	73
5.4.4	Mechanisms of the Flotation Separation of Quartz from Rutile.....	76
5.4.4.1	Zeta Potential Measurements	76
5.4.4.2	Adsorption Density of Starch.....	81
5.5	Reverse Flotation of Siliceous Minerals from the LR Rutile	82
5.5.1	The Effect of Concentration of Dodecylamine Acetate (DDAA)	83
5.5.2	The Effect of Concentration of Rutile Depressant – Wheat Starch.....	84
5.5.3	Other Test Conditions.....	85
5.6	Analysis of the Flotation Products.....	86
5.6.1	Optical Analysis.....	86
5.6.2	Chemical Analyses.....	87
5.6.3	Petrographical Analyses.....	88
5.6.4	SEM/EDX Analysis.....	89
6	CONCLUSIONS.....	95
7	RECCOMENDATIONS FOR FURTHER RESEARCH	97
8	REFERENCES.....	98
9	Appendix	102
9.1	Appendix I: Adsorption Measurements.....	102
9.1.1	Determination of Adsorption Density.....	103

List of Tables

Table 1	Typical Composition of Athabasca Heavy Mineral Assemblage (Owen,1996).....	8
Table 2	Production of Titanium Minerals by Country (Gambogi, 2002)	14
Table 3	Separation Characteristics of Heavy Minerals	26
Table 4	Rutile Concentrate Specifications for the Chloride Process	45
Table 5	Grades of Rutile Concentrates Produced in Previous Studies.....	48
Table 6	Grades of Ilmenite and Leucoxene Concentrates Produced in Previous Studies	48
Table 7	Grades of Zircon Concentrates Produced in Previous Studies.....	48
Table 8	Polysaccharides Used in the Flotation Testwork	58
Table 9	Whole Rock Analysis of the LR Rutile.....	63
Table 10	Magnetic Separation of LR Rutile at 2000 Gauss.....	66
Table 11	Magnetic Separation of LR Rutile at 6000 Gauss, with Cleaning	67
Table 12	Magnetic Separation of LR Rutile at 12000 Gauss.....	68
Table 13	Whole Rock Analyses of the Magnetic Separation Products.	69
Table 14	Effect of DDAA Concentration on the Reverse Flotation of Rutile Concentrate	83
Table 15	Effect of Wheat Starch Concentration on the Reverse Flotation of Rutile Concentrate.....	84
Table 16	Reverse Flotation of Rutile Concentrate using Armeen [®] 18D.....	86
Table 17	Whole Rock Analysis of Typical Flotation Tails.....	87

List of Figures

Figure 1 Simplified Syncrude Extraction and Froth Treatment Plant (Owen, 1996)	6
Figure 2 Titanium Resources of the World (Garnar and Stanaway, 1994)	13
Figure 3 Synthetic Rutile Processes (Padmanabhan et al, 1990).....	18
Figure 4 QIT Process Schematic (QIT, www.qit.ca , 2001).....	20
Figure 5 Titanium Ingot Manufacture (Smith, 1993)	24
Figure 6 Contact Angle Between a Bubble and Particle in an Aqueous Media (Wills, 1997)	31
Figure 7 Schematic Representation of the Diffuse Part of the Electric Double Layer (Shaw, 1992)	37
Figure 8 The Electric Double Layer According to Stern's Theory (Shaw, 1992).....	40
Figure 9 Particle Charge Reversal Due to the Presence of a Surfactant (Hunter, 1993) ..	41
Figure 10 Generalized Mineral Processing Flowsheet of Heavy Minerals (Wills, 1997).43	
Figure 11 Associated Minerals Consolidated Ltd. of Australia (Wills, 1997)	44
Figure 12 Trevoy & Schutte Flowsheet.....	47
Figure 13 MDL Process Flowsheet	49
Figure 14 MDA Process Flowsheet.....	50
Figure 15 Lakefield Research Ltd. (LRL) Process Flowsheet (reconstructed from Oxenford et al (2001)).....	51
Figure 16 A Typical Field of LR Rutile Under Cross-Polarized Light.	64
Figure 17 Low Intensity Magnetic Separation	66
Figure 18 Low Intensity Magnetic Separation with Cleaning.....	67
Figure 19 Flotation Recovery of Quartz Single Minerals	71
Figure 20 Flotation Recovery of Quartz and Rutile Single Minerals with Selected Depressants.....	73
Figure 21 Flotation Recovery of Quartz and Rutile Artificial Mixtures with Selected Depressants.....	74
Figure 22 Flotation Recovery of Quartz and Rutile Artificial Mixtures	75
Figure 23 Zeta Potential Measurements of Quartz and Rutile	77
Figure 24 Effect of DDAA on Zeta Potential for Quartz and Rutile.....	78

Figure 25 Effect of 10 ppm Wheat Starch on Zeta Potential for Quartz and Rutile.....	79
Figure 26 Effect of 10 ppm Wheat Starch and 10^{-6} M DDAA on the Zeta Potential for Quartz and Rutile	80
Figure 27 Adsorption Density of Wheat Starch on Quartz and Rutile.....	82
Figure 28 Typical Field of Flotation Tail by Plane Polarized Light.....	89
Figure 29 SEM Image of the Surface of a Rutile Particle	90
Figure 30 SEM Image of a Rutile Particle, Showing a Trelliswork Structure	93
Figure 31 A Typical SEM Image of the Rutile Concentrate	94
Figure 32 Another SEM Image of the Rutile Concentrate	94

1 INTRODUCTION

The Athabasca oil sands in the Fort McMurray region have long been known to contain heavy minerals (mainly titanium and zirconium minerals). The Mineral Development Agreement (MDA) studies, recently completed in 1996 by the Federal and Alberta Provincial governments, defined the extent of the heavy mineral resources contained in the oil sands. According to this study, the average concentration of TiO_2 and ZrO_2 in the oil sands is about 0.35% and 0.032%, respectively (McCosh, 1996).

At these grades, the oil sands are not economic resources for the titanium and zirconium heavy minerals. However, during the commercial Clark hot water process, which is currently employed by Syncrude Canada Ltd and Suncor Energy Inc to extract bitumen from the oil sands, the titanium and zirconium minerals are enriched in the bitumen froths. Subsequent treatment of the bitumen froths generated a froth product that contains mostly bitumen and froth treatment tailings that consist of mostly water and mineral solids. The froth treatment tailings thus obtained contain high concentrations of the titanium and zirconium minerals. The MDA study has shown that the average TiO_2 content in the froth treatment tailings is about 10 – 11%, and the average ZrO_2 content is about 3 – 4 % (Alberta Chamber of Resources, 1996), which are substantially higher than in the original oil sands feed. In fact, at these concentrations, the Alberta oil sands tailings are the second richest heavy mineral resource in the world (Alberta Chamber of Resources, 1996). According to Oxenford et al (2001), the TiO_2 and zircon contained in the oil sands tailings that can potentially be recovered amount to about 6% of the world's TiO_2 production and about 9% of the world's zircon consumption. However, despite the rich and enormous resources, currently, these heavy minerals are not recovered and are discarded straight to tailings ponds.

While it may be argued that the absence of a recovery operation for the heavy minerals is due to a lack of interest from the oil sands operators, the lack of a viable technological process is the main contributing factor. Since the 1970s there have been continuous efforts to extract and recover the heavy minerals. However, the processes that were

proposed were inadequate to produce marketable heavy mineral concentrates. Typically, a roasting step was used in these processes to remove the residual bitumen present in the froth treatment tailings. The heavy minerals are then upgraded by gravity, magnetic and electrostatic separation techniques that are typical in the alluvial sands processing industry. The inability of these processes to produce market-grade heavy mineral concentrates has re-enforced the widely held suspicion that there must be some major metallurgical challenges to extract the heavy minerals from the Athabasca oil sands tailings.

Based on these previous studies, recently Lakefield Research Ltd and Syncrude Canada Ltd developed a novel process from which saleable concentrates of ilmenite and zircon were produced (Oxenford et al, 2001). The novel part of this process is that froth flotation was used to separate zircon from the titanium minerals, which is different from any of the previous studies. As will be seen from the next chapter, froth flotation is the most appropriate technique to separate the zirconium minerals from the titanium minerals in the Athabasca oil sands. It is therefore expected that the Lakefield and Syncrude process will form the basis for any subsequent studies in recovering heavy minerals from the oil sands tailings.

Although the ilmenite and zircon are saleable, the high-grade titanium mineral concentrate produced from the Lakefield and Syncrude process, i.e., the rutile concentrate, was not saleable due to its very low grade. As part of the effort to modify this process, we took this rutile concentrate and studied the possibility of upgrading it to marketable grade. The research results are summarized in this thesis.

2 LITERATURE SURVEY

2.1 Alberta Oil Sands

The Athabasca region of northern Alberta contains large deposits of oil sands. The oil sands deposits are of the Cretaceous age and cover an area in Alberta of over 30,000 square kilometers. The McMurray Formation is an oil bearing quartz sand containing up to 18% by weight of extra-heavy oil or bitumen. This deposit is one of the largest hydrocarbon accumulations in the world, with an estimated 2500×10^9 barrels of contained oil and 175×10^9 barrels of reserves (National Energy Board, 2000). Currently, Syncrude Canada Ltd and Suncor Energy Inc are the two commercial operators who extract the oil contained in these sands for sale on the oil market. Two other operators, Albian Sands Energy Inc. and True North Energy L.P., are going to enter the oil sands industry in 2002 and 2004, respectively. In 2001, Syncrude produced 81.4 million barrels (223,000 barrels per day) of Syncrude Sweet Blend (www.syncrude.ca, 2001). With proposed expansions, by 2008 total annual production from Syncrude is expected to double to 170 million barrels of Syncrude Sweet Blend. Suncor has increased production capacity to 225,000 barrels of oil per day, more than doubling 1999 production (www.suncor.ca, 2002).

2.1.1 *Heavy Minerals in Alberta Oil Sands*

The presence of heavy minerals in the Athabasca oil sands has been known for some time (Blair, 1950; Scotland and Benthin, 1954). In the mid-1990's, the Federal Government of Canada entered into Minerals Development Agreements (MDA's) to assist in the development of new non-energy mineral resources. One of the sponsored projects was an assessment of the potential of heavy minerals from the oil sands. The proposed project was to include an assessment of the geology, mineral distribution, metallurgical processes and potential markets.

The MDA study examined core samples from virtually all the geological facies within the leases of Syncrude Canada Ltd., Gulf Oil and Suncor Energy Ltd. The heavy mineral concentrations were found to be fairly consistent over most of the Athabasca McMurray Formation, with no very rich concentrations being found. McCosh (1996) concluded that the heavy minerals in the oil sands were controlled by the natural sorting of the grains during deposition in the Cretaceous period. The heavy minerals are typically fine grained (d_{50} less than 100 μm) with non post-depositional re-working of sediments as is typical of most other heavy mineral deposits (Oxenford et al, 2001). The post-depositional environment is reducing with secondary mineralization being common. These secondary minerals can occur as intergrowths or inclusions in other minerals (Owen, 1996).

Titanium concentrations average about 0.35% (as TiO_2) in feed grade oil sands, but can vary from 0.08% to 1.6% in some samples (Oxenford et al, 2001). No significant variation of titanium content has been found in different leases, or in different areas of the McMurray Formation. The zirconium assays are more variable than the titanium values, and zirconium ranges from about 0.0002% to 0.18% with an average of 0.032% ZrO_2 (Oxenford et al, 2001). Other valuable minerals that were identified in the oil sands include rare earth elements in the form of monazite, as well as trace amounts of palladium, platinum and gold.

2.1.2 Clark Hot Water Process

The process utilized by the two current oil sands operators is the Clark Hot Water Process. In the Syncrude operation, bitumen is extracted from the oil sand in extraction plants located at both the Mildred Lake and Aurora sites while the final upgrading in the froth treatment plant takes place at Mildred Lake. The following description of the Syncrude process was obtained from the Syncrude Canada Ltd. website (www.syncrude.ca, 2001).

At the Mildred Lake site, 50 percent of the oil sand processed is transported by conveyor and enters the tumblers (large horizontal, rotating drums). The oil sand is slurried by

steam, hot water and caustic soda to condition it for bitumen separation. The rotary action also aerates the slurry. The slurry from the tumblers is discharged onto vibrating screens where large materials such as rocks and lumps of clay are rejected. The slurry is then diluted in pump boxes and pumped to the "Superpot" distributor where it is blended with the slurry from the North mine hydrotransport system. (Currently, some 50 percent of oil sand processed at Mildred Lake arrives at the extraction plant as a hydrotransport slurry. This will increase to 100 percent by 2006.)

The blended slurry is fed to the four Primary Separation Vessels (PSVs) and the two Auxiliary Settling Areas (ASAs), which are smaller versions of the PSVs. In the PSVs and ASAs, bitumen floats to the surface as primary froth. The sand settles out and the middlings and underflow streams are pumped to the Tailings Oil Recovery (TOR) vessels. These deep cone vessels recover most of the remaining bitumen using Syncrude-developed technology. Froth from the TOR vessels is recycled to the PSVs to improve its quality.

Bitumen recovery is further improved by the secondary flotation plant, which processes middlings from the TOR vessels. Froth from the secondary flotation plant is combined with the primary froth stream from the PSVs, deaerated and heated, and fed to the froth treatment plant.

At Aurora, oil sand slurry is hydraulically transported by pipeline at a rate of 8,000 tonnes of oil sand per hour. By the time the slurry travels the three to five kilometers to extraction facilities at Aurora, it has already been conditioned for bitumen separation. Aurora produces bitumen slurry with a low energy extraction process. The low energy extraction process operates at 25°C to 35°C, which consumes 40 percent less energy than the original 80°C operation. Following extraction, the bitumen froth enters a 36-inch buried pipeline and travels 35 kilometers to the Mildred Lake operation for froth treatment and bitumen upgrading.

Froth treatment minimizes the water and solids going to the upgrader. Froth is diluted with naphtha and this diluted bitumen is either put through inclined plate settlers (IPS) or through two stages of centrifuges. The combined product from the inclined plate settlers and centrifuges is then put through another set of centrifuges to remove the water and solids as tailings before going to the upgrader. A simplified flowsheet of the froth treatment plant is shown in Figure 1 (Owen, 1996). A Naphtha Recovery Unit (NRU) recovers naphtha from all froth treatment tailings.

Figure 1 shows that two tailings streams are produced from the oil sands operations: the Extraction Plant Tailings (also called Primary Tailings) and the Centrifuge Tailings (also called Froth Treatment Tailings). While generally both tailings contain mineral solids, water, silt and residual bitumen, the Extraction Plant Tailings contain primarily clays, fine solids and water, and the Centrifuge Tailings contain mostly coarse and fine mineral sands and residual bitumen. As can be seen from Figure 1, the TiO_2 content in the Centrifuge Tailings is 11.5%, which makes them the second richest titanium mineral resources in the world.

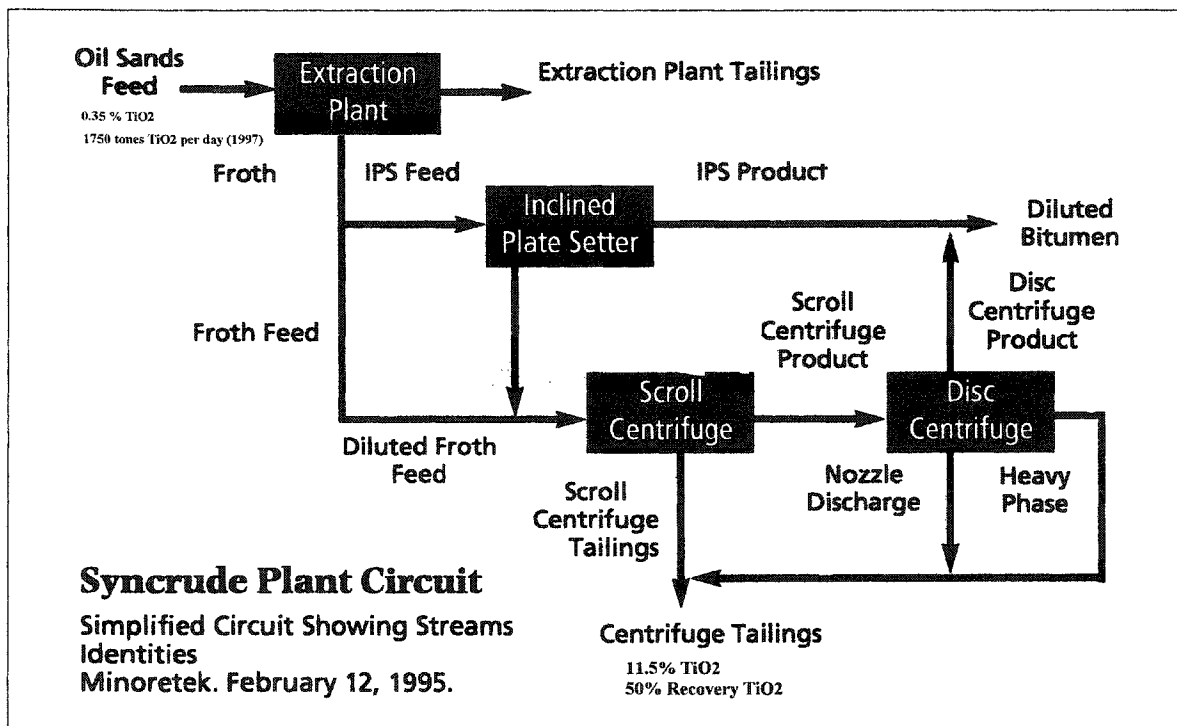


Figure 1 Simplified Syncrude Extraction and Froth Treatment Plant (Owen, 1996)

2.1.3 Concentration of Heavy Minerals in Froth Treatment Tailings

As already discussed, the heavy minerals contained in the Alberta oil sands are well below economic mining grades, however it is known that the titanium and zirconium minerals are concentrated together with the bitumen. Therefore, as the bitumen is extracted into the froth products in the Clark Hot Water process, the heavy minerals are enriched in the froth treatment tailings when the froths are de-sanded and de-watered. According to the MDA study, the froth treatment tailings contained 11.5% TiO_2 and 3.40% ZrO_2 , and recovered about 50% of the TiO_2 and 85% of the ZrO_2 from the oil sands feed (Owen, 1996).

Therefore, although the oil sands feed does not seem to be an economic source for heavy minerals, the oil sands tailings, at a grade of 11.5% TiO_2 and 3.40% ZrO_2 , are significant heavy mineral resources. In fact, the froth treatment tailings are claimed to be the second richest titanium resource in the world (Owen, 1996). The recoverable TiO_2 and zircon in the froth treatment tailings, at 220,000 tonnes and 80,000 tonnes per year, respectively, at the current production levels of Syncrude and Suncor, represent approximately 6% of the world's production of TiO_2 and approximately 9% of the world's zircon production (Oxenford et al, 2001).

Previous studies attempting to separate the heavy minerals have completed a basic feed analysis of the froth treatment tailings (Owen, 1996). However there are significant discrepancies about the mineral composition in the Athabasca oil sands. It is agreed that the mineral grains themselves are well liberated. Titanium dioxide is 75% liberated with 73 % in the optimal size range for flotation (Owen, 1996). Zircon is 96% liberated with 95 % in the optimal size range for flotation (Owen, 1996). This makes developing the oil sand tailings as heavy mineral resources very attractive.

The most comprehensive characterization data were obtained by the MDA study on the oil sands and are presented below in Table 1 using XRD techniques (Owen, 1996). Their

study determined that the heavy minerals comprised the following mineral suite and their weight percentages, excluding silica and fine clay (< 4 µm).

Table 1 Typical Composition of Athabasca Heavy Mineral Assemblage (Owen, 1996)

Mineral	Weight Percent
Rutile	26.8
Ilmenite	16.3
Siderite	15.5
Anatase	9.8
Pyrite	9.0
Zircon	7.7
Tourmaline	5.2
Garnet	2.6
Magnetite	1.9
Monazite	1.4
Kyanite	1.1
Staurolite	1.0
Mica	0.9
Chlorite	0.8

2.2 Titanium: Resource and Utilization

2.2.1 Titanium Mineralogy

Titanium is the ninth most abundant element on Earth, and is found in more than 45 different minerals, but most commonly occurs as titanomagnetite, ilmenite and rutile (Garnar and Stanaway, 1994). Titanomagnetite normally contains less than 10% TiO₂, making it of little or no value as an ore of titanium. Titanium is only found in an oxide form and often occurs with the silicate and iron forming minerals. The following mineral definitions were referenced from Garnar and Stanaway (1994).

Ilmenite: Ilmenite (FeOTiO₂) forms an incomplete series with geikielite (MgTiO₂) and pyrophanite (MnTiO₂). Ilmenite and its alteration products are the most abundant TiO₂ sources on Earth. There are different ore types of ilmenite. The primary sources are hard

rock deposits associated with gabbros, diorites and orthosites. These deposits are primarily mined to produce TiO_2 slag. Hard rock ilmenite deposits may be strongly magnetic due to their association with magnetite but may also be weakly magnetic or paramagnetic. Fresh unaltered ilmenite is black with a metallic or submetallic luster. Ilmenite alters very slowly from crystalline FeOTiO_2 to an amorphous mixture of FeO , Fe_2O_3 , and TiO_2 . During this process some of the iron oxides are leached out of the grains thereby increasing the TiO_2 content. The end product of this alteration is either rutile or anatase. Fresh unaltered ilmenite is soluble in H_2SO_4 and HCl , but as alteration progresses, its solubility decreases proportionally until the end products, which are insoluble in acids.

Leucoxene (Pseudorutile): As the ilmenite alteration process continues, the grains lighten in color and signs of recrystallization become detectable by x-ray diffraction techniques. At this stage of alteration the mineral grains are tan or gray and have a waxy luster. The color can be enhanced for identification by heating to 1000°C for ten minutes in an oxidizing atmosphere. The mineral grains at this stage of decomposition have an increased TiO_2 content of 80 - 90%. The resulting grains are only partially soluble in acids and are only slightly paramagnetic.

Anatase: Anatase occurs in nature as one of the three polymorphs of TiO_2 , but more commonly occurs as the end product of the ilmenite alteration process in beach sands. Large anatase deposits are found in carbonatites in Brazil where they occur as pseudomorphs with intergrowths of fine quartz. In beach sand deposits, anatase grains are slightly translucent and are yellowish to gray in color.

Rutile: Rutile is the primary mineral used in the titanium industry today, which can be found in two forms: primary rutile and secondary rutile. The primary rutile makes up the major portion. The majority of primary rutile is mined from beach sand deposits in Australia and the Republic of South Africa and from some continental deposits such as the one found in Sierra Leone. Secondary rutile is found in beach sand deposits and is the end product of the ilmenite alteration process.

Pseudobrookite: Pseudobrookite (Fe_2TiO_5) is not a commercial ore of titanium because of its low TiO_2 content. It commonly occurs as a pneumatolytic or fumarolic product in volcanic igneous rocks. It can also form when ilmenite or altered ilmenite is heated above 1400°C .

Perovskite: Perovskite (CaTiO_3) deposits have been of interest as a source of titanium for several years, though there is currently no economic process to effectively process this ore. Limited success has been achieved in producing a TiO_2 pigment from perovskites using an acid sulfation method.

Sphene: Sphene (CaTiSiO_5) has no economic importance and is considered a gangue mineral associated with titanium mineral deposits.

2.2.2 Titanium Mineral Formation Geology

Titanium mineral deposits can form by two processes: the first is immiscible, high specific gravity molten droplets in cooling magmas, the second weathering-resistant, high specific gravity mineral grains sorted during clastic sedimentation. These formation processes are described below and referenced from Garnar and Stanaway (1994), unless otherwise stated.

Magmatic Segregation Deposits: Magmatic segregation of TiO_2 takes place in tholeiitic basaltic magmas that pond under the crust and slowly crystallize, de-gas and fractionate to yield molten residuals increasingly enriched in titanium, phosphorus and iron. The increasing titanium and iron concentrations finally result in the formation of immiscible liquid oxide droplets that descend due to their higher specific gravity to the base of the magma chamber where layering of the mineral deposit slowly builds up. The end result of the titanium-iron oxide deposits is an accumulation of minerals that form as lenses in depressions on the magma chamber floor. An example of this type of deposit is found in the San Gabriel Mountain ilmenite deposits of California.

There are several other types of deposits that form in the same manner as the one mentioned above. These deposits include alkalic intrusive deposits and contact-metamorphic deposits. The largest difference between these types of deposits is the molten source material that was available to form the mineral grains when the molten immiscible liquids cooled, segregated and subsequently crystallized.

Relict Titanium Dioxide Deposits: Under normal crustal conditions titanium is immobile via either solution in aqueous phases or solid state diffusion. Thus relict titanium dioxide deposits containing minerals such as pseudorutile, rutile, brookite and anatase will be formed when certain elements are leached or diffused away while the titanium remains immobile. This usually takes place during rock weathering when calcium and silica leach from perovskite and sphene to form anatase. A deposit of this nature can be found in Brazil. A similar type of process can also take place in oxidizing acidic sediments where pseudorutile replaces ilmenite to form altered ilmenite and leucoxene in placer deposits such as those found in Florida.

Placer Deposits (Garnar and Stanaway, 1994; Birkeland and Larson, 1989): Moving water can sort mineral grains according to size in gravel deposits, sands or silts, by shape in micaceous and non-micaceous silts, or according to specific gravity to give placer deposits. To form a placer deposit, the appropriate source rock, weathering and appropriate flow regimes are necessary to sort the mineral grains. These types of deposits are also known as heavy mineral (HM) sands. Two types of deposits are noted. The first type is called a trap placer, which is rarely more than one meter thick. This type of deposit forms from the reworking of sediment and the failing of a flow regime to effectively remove the bulk placer component. The second type is called a bed placer, which can reach tens of meters in thickness. These result from the higher specific gravity minerals accumulating in direct response to the fluid and grain flow regimes operating at or close to the time of the initial mineral deposition. These two types of deposits can often occur together; however, trap placers are important for high value minerals such as

gold while bed placers can supply volumes necessary for bulk commodities such as ilmenite and zircon.

Shoreline Deposits (Garnar and Stanaway, 1994; Birkeland and Larson, 1989):

Mechanical processes that result in the accumulation of titanium bearing heavy minerals such as ilmenite and rutile on beaches can form shoreline deposits. The processes that form these types of deposits are similar to those that form placer type deposits.

Hydrodynamics and wave mechanics deposit minerals upon a shoreline where the heavy minerals are concentrated, the lighter minerals are swept away. As marine regression changes over time the resulting heavy mineral deposit can also be further subjected to erosional forces such as water and wind erosion. Often these deposits eroded by wind form large dunes inland where the minerals are concentrated over time. Dune migration inland often segregates the lighter minerals leaving the heavy minerals behind. If extensive migration continues the heavy minerals can also be eroded leaving many small dunes over a very large area negating the potential for an economic deposit.

Alluvial (Garnar and Stanaway, 1994; Birkeland and Larson, 1989): Despite the prominence of beach and dune placers, river deposits can also be sources of potential economic deposits. These deposits are often found in areas where the flow conditions of the river change such as in the alluvial fan where rivers empty into larger bodies of water. As the flow characteristics of the river changes, the segregation and deposition of the heavy minerals occurs first while the lighter minerals are continuously swept downstream. Such deposits can be found at Gbangbama in Sierra Leone, Richards Bay in South Africa as well as the deposits found in the Kiev District of the Ukraine.

Offshore: Deposits found offshore can arise not only by the drowning of shoreline and alluvial deposits, but also as submarine deposits that form from the flow regimes outlined for alluvial deposits. During large storms, wave energy penetrates to greater depths than normal that can set in motion huge masses of sand by liquefaction. The titanium minerals are separated and concentrated from any lighter minerals that are present.

2.2.3 World Titanium Dioxide Resources Supply and Demand

Titanium dioxide can be found on every populated continent in the world. Figure 2 shows a map of the titanium resources of the world (Garnar and Stanaway, 1994). From this map it can be seen that there are deposits located on every continent, though only a third of these resources have ever or are currently being recovered. On this map, names that are underlined are locations of deposits that have or are currently in production. The majority of the rest pose some sort of a technological metallurgy processing deficiency where the desired titanium product cannot be recovered satisfactorily to invest in the deposit.

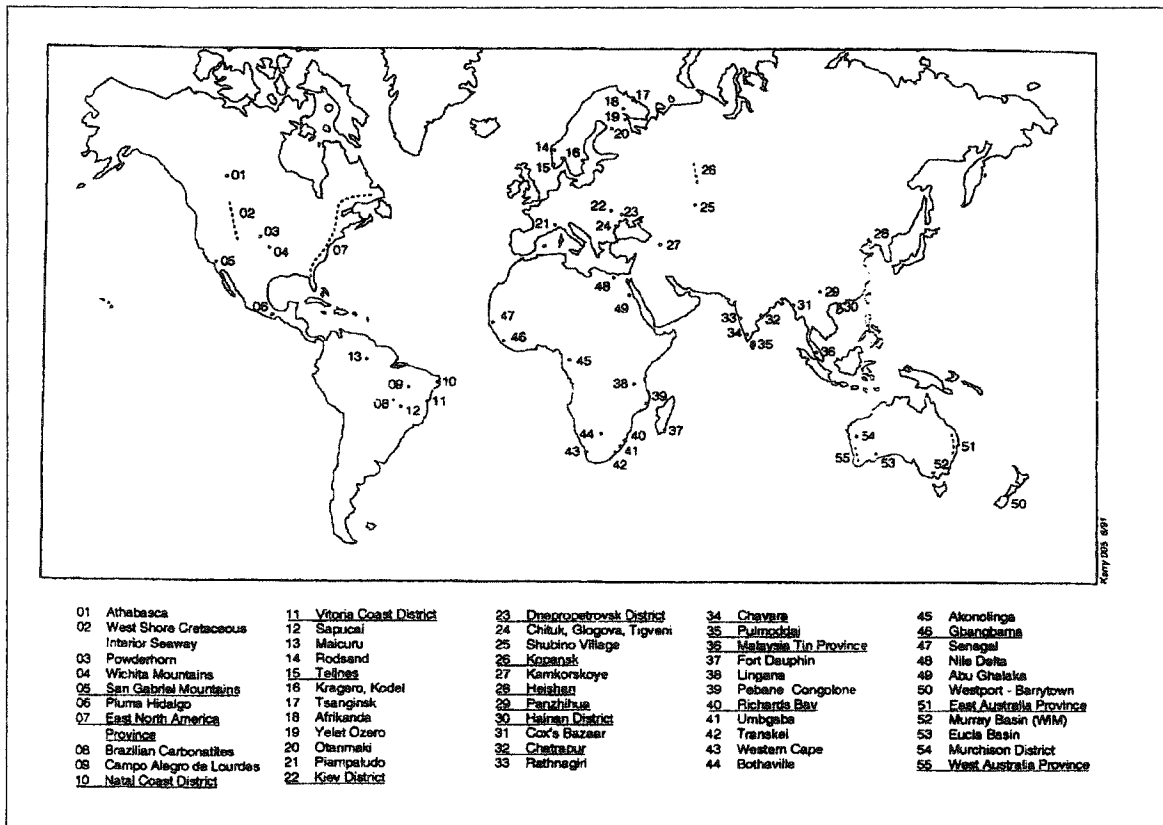


Figure 2 Titanium Resources of the World (Garnar and Stanaway, 1994)

The United States Geological Survey (USGS) surveys the mining industries from around the world every year and composes a mineral commodity summary, part of which for year 2002 is shown in Table 2 (Gambogi, 2002). Ilmenite, its altered products and rutile are the only current mineralogical sources for titanium dioxide. Ilmenite, leucosene, rutile, slag and synthetic rutile compete as feedstock sources for producing TiO₂ pigment, titanium metal and welding rod coatings. In the future, commercial processes may be developed to use perovskite deposits. Ilmenite supplies about 90% of the world's demand for titanium minerals (Gambogi, 2002). In Canada, mine production is primarily used to produce titaniferous slag from ilmenite. The world ilmenite resources total about 1 billion tons of titanium dioxide. Identified world resources of rutile (including anatase) total about 230 million tons of contained TiO₂. Worldwide exploration and development efforts continue in Australia, Canada, The Gambia, India, Kenya, Mozambique, South Africa and the United States.

Table 2 Production of Titanium Minerals by Country (Gambogi, 2002)

Unit: kilo tones of TiO₂

	Mine Production		Reserves	Reserve Base
	2000	2001		
Ilmenite:				
United States	300 ^a	300 ^a	13000	59000
Australia	1230	1190	110000	130000
Canada	760	720	31000	36000
India	205	200	30000	38000
Norway	275	270	40000	40000
South Africa	935	1000	63000	63000
Ukraine	242	240	5900	13000
Other Countries	331	320	49000	84000
World Total	4300	4200	340000	470000
Rutile:				
United States	(^a)	(^a)	750	1800
Australia	225	220	21000	32000
India	16	15	6600	7700
South Africa	94	90	8300	8300
Ukraine	56	55	2500	2500
Other Countries	4	4	8000	17000
World Total	4700	4600	380000	540000

^a: Included with ilmenite

2.2.4 Use of Titanium Minerals

The primary consumption of titanium minerals is in the production of titanium dioxide (TiO₂) pigments. TiO₂ pigment producers consumed about 95% of titanium mineral concentrates produced in 2002 (Gambogi, 2002). The remainder was used in welding rod coatings and for manufacturing titanium metal, carbides and chemicals.

Titanium dioxide pigments are primarily used in paints, lacquers, paper, plastics, ink, rubber, textiles, cosmetics, sunscreens, leather, food coloring, and ceramics (Mineral Sands, www.minerals.org.au, 1999). The high refractive index, absorption of UV light and low toxicity of titanium dioxide makes it an ideal additive in these products, especially since weathering, fading damage and degradation normally caused by the sun can be negated by the addition of the pigment (www.richardsbayminerals.co.za, 2002).

Titanium dioxide pigments are relatively easy to manufacture either by precipitation by hydrolysis from a sulfate solution or from oxidation of titanium tetrachloride. Specific properties such as luster, opacity, brightness and hardness can be controlled through the selective addition of specific compounds and subsequent controlled nucleation and growth of the oxide. The high demand for white titanium dioxide pigment resulted when many governments around the world banned the use of lead carbonates in paint manufacture (Mineral Sands, www.minerals.org.au, 1999). The resultant effect was to create an enormous demand for titanium dioxide pigments in the 1980s to the point where additional world capacity was required to meet the increased demand (Garnar and Stanaway, 1994). In 2001, however, a slowing world economy led to a moderate decrease in global consumption of titanium dioxide pigments (Gambogi, 2002).

Titanium metal was discovered in 1791 and four years later was named after the Titans of Greek mythology (Weast and Astle, 1981). Titanium metal was first produced in 1910, but not utilized commercially until the 1950s when it was nicknamed the "Wonder Metal of the Age" (Garnar and Stanaway, 1994). Titanium and its alloys are attractive since they have a high strength-to-weight ratio, high elevated-temperature properties to about

550°C and excellent corrosion resistance, particularly in oxidizing acids and chloride media as well as most natural environments (Smith, 1993). Unfortunately titanium and its alloys cost substantially more than common metals such as aluminum and steel because they are difficult to extract from their ores and sophisticated melting and fabricating techniques must be used in their manufacture. The higher cost of titanium fabrication is principally the result of the metal's high reactivity and affinity for interstitial elements such as oxygen, nitrogen, hydrogen and carbon (Smith, 1993). Despite these limitations, titanium and its alloys do compete effectively where their high strength-to-weight ratios and high elevated-temperature properties make them the ideal choice in many applications.

The largest industrial use of titanium has been in the manufacture of aircraft and missile engines, frames and skins (Winter, www.webelements.com, 1993). The high strength to weight ratio makes titanium an ideal choice for aircraft. In upcoming years the demand for titanium metal in aircraft will increase dramatically as commercial aircraft become out dated and the military starts building its new fleet of strike planes. The F22, Eurofighter, JointStrike Fighter and Rafale Fighter will maintain titanium demand from the military. The F22 due to start production in 2004 will be constructed out of 39% by weight titanium (Roskill, www.roskill.co.uk/timet.html, 2001). Recently the largest consumer use of titanium metal has been in the manufacture of sports equipment, particularly in golf clubs and tennis racquets (Roskill, www.roskill.co.uk/timet.html, 2001).

2.2.5 Processing of Titanium Minerals

As described earlier, there are two types of titanium mineral concentrates produced, the ilmenite series, which still contain significant amounts of iron, and the rutile concentrates which are relatively pure titanium dioxide. Each of these streams needs to be further processed to produce titanium dioxide pigments or titanium metal.

2.2.5.1 Synthetic Rutile

Ilmenite mineral concentrates are usually processed to produce “synthetic rutile” that is utilized as a feed for titanium pigment production by the chloride process (Lefond, 1983). Synthetic rutile is created when the iron from ilmenite, altered ilmenite or leucoxene is removed from the lattice structure leaving a relatively pure titanium dioxide as the final product. However, certain impurities in these mineral concentrates, such as silicate and aluminosilicate minerals, cannot be removed by acid leaching.

For the chloride process to function properly impurities such as iron, calcium, silicon, aluminum, phosphorus, magnesium, vanadium, barium and strontium, as well as radionuclides such as thorium and uranium need to be removed (Chao and Senkler, 1992). Alkaline earth metals such as magnesium and calcium oxides are especially undesirable in the chloride pigment process as their oxides form magnesium and calcium chlorides that form paste like condensates which tend to foul the fluidizing reactors and other downstream equipment (Mishra and Kipouros, 1996). There are several processing methods for accomplishing the removal of iron and some of the impurities from the ilmenite feed, as summarized in Figure 3 (Padmanabhan et al, 1990).

Various companies around the world are currently using most of these processes. However, as environmental regulations become more stringent some of these processes are being re-evaluated. The sulfate process, also known as the Ishihara process, is being phased out due to disposal problems of spent sulfuric acid (Padmanabhan et al, 1990). In this process the ilmenite mineral is reduced with coke around 900-1000°C to decompose the iron oxides. Leaching is then carried out at 130°C with sulfuric acid to remove the iron, and the resultant leach residue typically contains greater than 95% titanium dioxide. The advantage of this process is that there are no rigid specifications for feed materials regarding the TiO₂ content. However, certain impurities such as chromium, vanadium, niobium, manganese, and phosphorus are known to seriously impair pigment properties (Lefond, 1983). It is important that the feed contain low amounts of these elements as well as being capable of being dissolved in sulfuric acid at practical temperatures.

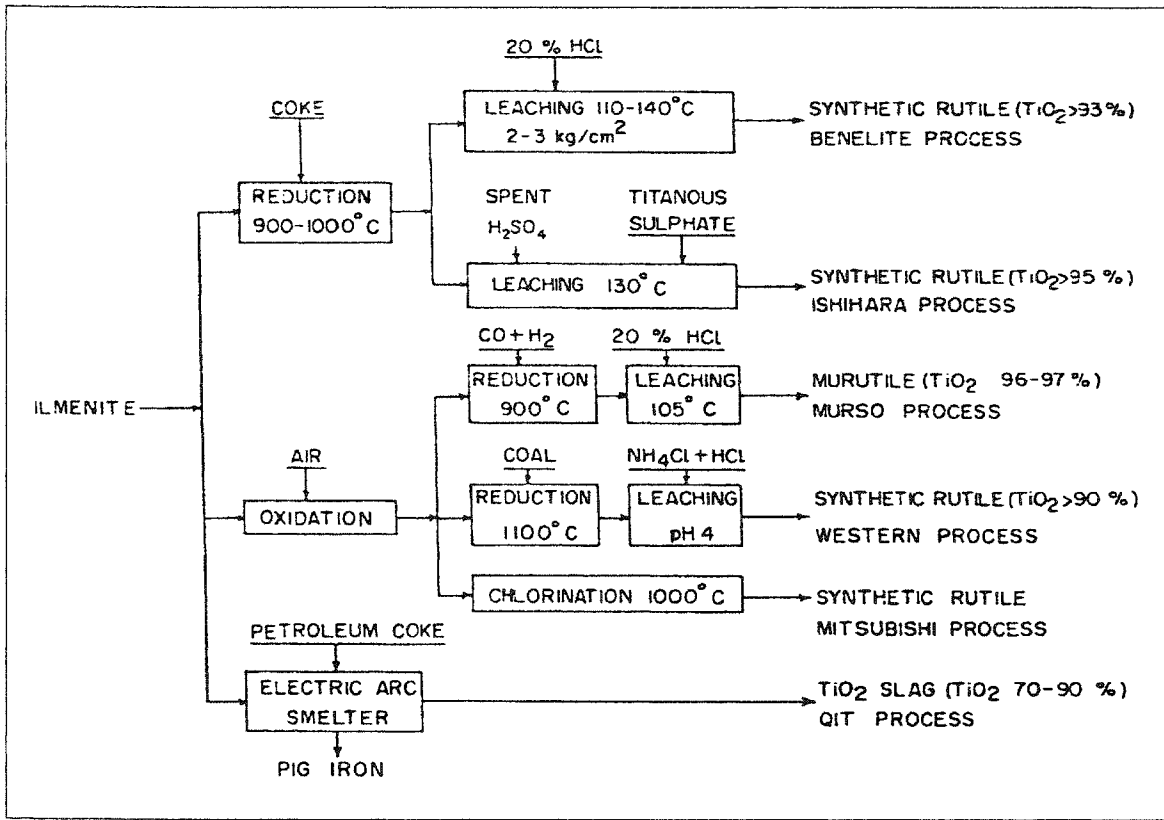


Figure 3 Synthetic Rutile Processes (Padmanabhan et al, 1990)

A similar process that is becoming more favorable is to use hydrochloric acid instead of sulfuric acid. Hydrochloric acid is easier to recycle and regenerate than sulfuric acid solutions. This process is called the Benelite process in which a 20% hydrochloric acid solution is used to leach ilmenite between 110-140°C. Dhrangadhra Chemical Works produces synthetic rutile using this process at their plants in Tamil Nadu as well as Indian Rare Earth's Limited (IRE) at Chatrapur, India. Kerr-McGee Chemical Corporation located near Mobile, AL in the US uses the Benelite process and has been the only producer of synthetic rutile in the US since 1977 (Garnar and Stanaway, 1994). The Murso process and the Western process are both variations of the Benelite process.

An alternative method for producing synthetic rutile is to mix petroleum coke with the ilmenite before being fed into a fluidized bed reactor. Chlorine gas is then injected and the mixture is heated to (and chlorinated) at 1000°C (Fukushima et al, 1976). The feed materials can consist of both ilmenite and titanium slag. Thermodynamic calculations indicated that the chlorination of iron is more favorable than the chlorination of titanium (Rhee and Sohn, 1990). Thus under stringent controls the selective chlorination of iron to a gas phase (iron chloride) can be accomplished leaving porous synthetic rutile behind (Sohn and Zhou, 1998). The solid is collected and removed from the reactor for further processing by carbochlorination. This process is called the Mitsubishi process and is used in Japan. This process is becoming more favorable as controls and reaction kinetics become better understood. The process is simple with less pretreatment stages and less expensive equipment. The final product of titanium tetrachloride can be used as direct feed for pigment manufacture or titanium metal.

2.2.5.2 Slag Processes

A process that is significantly different from the processes mentioned above is used by Quebec Iron and Titanium Ltd. (QIT) and its subsidiary in South Africa called Richards Bay Minerals (RBM). In this process petroleum coke is mixed with the ilmenite feed before being fed into an electric arc furnace. The iron in the ilmenite is reduced to pig iron and the titanium dioxide forms a slag (Borowiec et al, 1998). This slag is known by the trade name Sorelslag™. The QIT process produces a slag with 80% titanium dioxide (QIT, www.qit.com, 2001). Sulfate titanium pigment producers primarily used the Sorelslag™ produced by the QIT process. As markets changed in the 1990s, QIT needed to revamp its process to stay competitive with the chloride process producers. Production of a higher-grade slag was necessary. As a result, the process was changed in 1997 to the UGS™ process to allow the production of a UGS™ slag which contained 94.5% titanium dioxide (QIT, www.qit.com, 2001). This slag is suitable as a direct feed for the chloride titanium pigment process due to its low impurities. A schematic representation of the QIT process can be seen below in Figure 4 (QIT, www.qit.com, 2001).

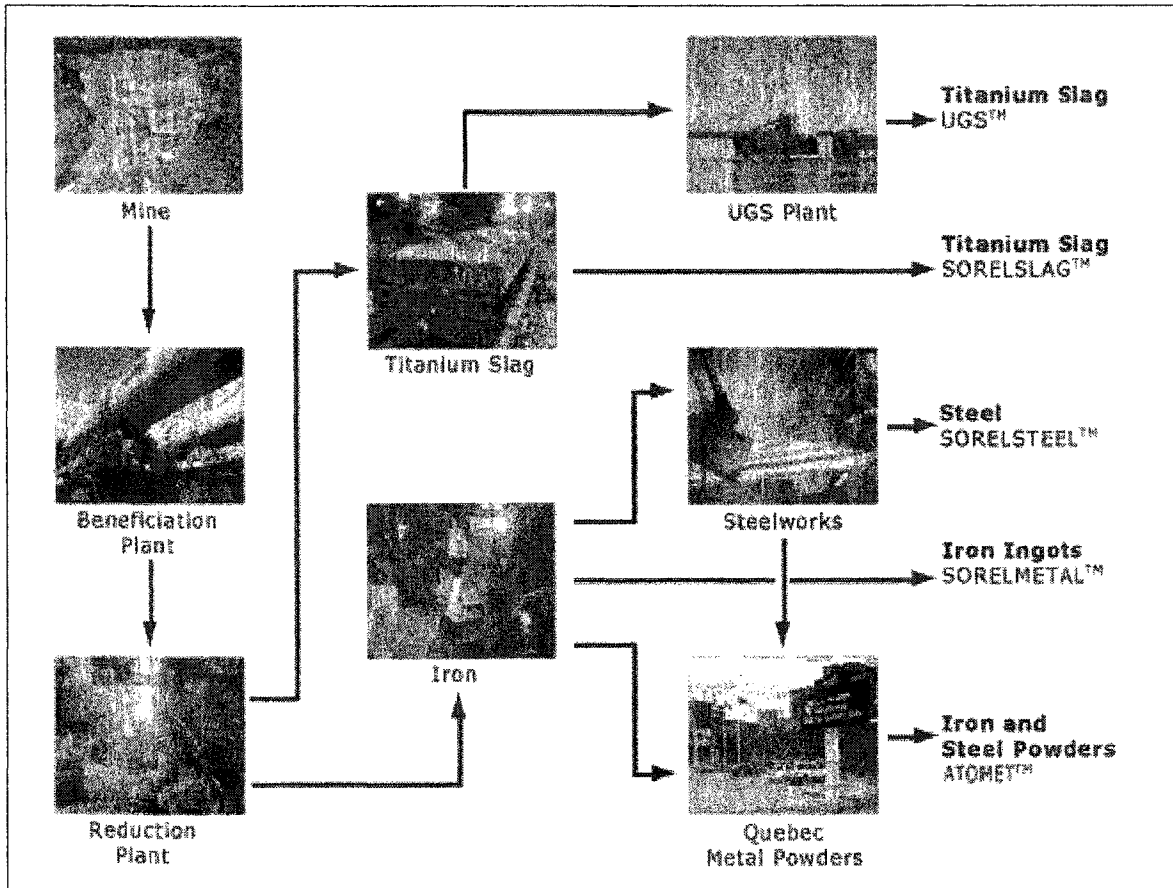


Figure 4 QIT Process Schematic (QIT, www.qit.ca, 2001)

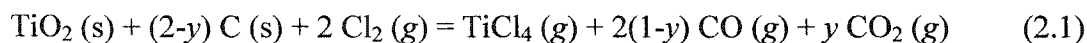
2.2.5.3 Upgrading of Titanium Mineral Concentrates

Several U.S. Patents, such as 5,085,837 (Chao and Senkler, 1992) and 5,885,536 (Hollitt, 1999), disclose processes by which impurity elements can be removed by leaching. These involve the use of a mineral acid and an aqueous solution of an alkali metal compound. The first part of the process is similar to the Benelite process described above. The patents claim the solubilization of iron, alkali metal, alkaline earth metal, rare earth metal, aluminum, phosphorus, thorium, uranium, chromium, manganese, silicon, vanadium and yttrium. Hydrochloric acid leaching is used at 10-20% by weight based on the total weight of the solution. Leach times are about 20-40 minutes at 120°C under 1 – 2 atmosphere pressure. Leaching with sodium hydroxide is used at 20-30% by weight

based on the total weight of the solution at 180-210°C under 9 - 18 atmosphere pressure for about 20-40 minutes. Between each leaching stage the slurry is filtered and washed with hot water to remove the dissolved impurities. The leachants are then purified by selective precipitation of the dissolved elements. Sodium hydroxide leachant is purified by the addition of lime to precipitate solid calcium silicate compounds that are removed by filtration. The upgraded titanium concentrate can be used as a direct feed for the chloride titanium pigment process.

2.2.5.4 The Chloride Process: Titanium Tetrachloride

Rutile concentrates and the synthetic rutile produced from ilmenite contain over 91% TiO₂. These products need further processing to produce titanium pigments. Today both synthetic rutile and rutile concentrates are further processed by carbochlorination to form titanium tetrachloride. This gaseous product is produced by mixing coke and chlorine gas in a fluidized bed reactor. The reaction can be expressed as (Yang and Hlavacek, 1998):



or simply,



The resulting titanium tetrachloride from equation 2.2 is then purified by fractional condensation or chemical precipitation techniques. The condensed titanium tetrachloride is removed under inert atmosphere to avoid contamination by oxygen or moisture in the air and is stored for further processing to either titanium dioxide pigments or titanium metal.

2.2.5.5 Production of Titanium Dioxide Pigments

There are currently two major process routes for the production of titanium dioxide pigments, i.e., the sulfate process and the chloride process.

The sulfate process produces a filter cake containing titanium dioxide and a solution containing dissolved iron. The filter cake is then dissolved in dilute acid to yield titanyl sulfate (TiOSO_4) and iron sulfate (Lefond, 1983). Any ferric iron present is reduced to the ferrous state by adding scrap iron. This is done to avoid precipitation of ferric iron later in the hydrolysis process and to facilitate washing of the precipitated titania (TiO_2) since ferrous iron is less strongly adsorbed. After reduction of the iron, the solution is clarified by settling and filtration. The solution is then concentrated and the titania is precipitated by hydrolysis, filtered, washed, calcined between 900-1000°C to the oxide form and further treated before the finished pigment stage (Garnar and Stanaway, 1994). The nature of the various special treatments determines the grade and type of the finished pigment. These include the anatase or rutile form, chalking or nonchalking, oil or water dispersible, etc (Lefond, 1983).

In the chloride process, the purified titanium tetrachloride is converted directly to titanium dioxide by oxidizing the TiCl_4 with air or oxygen at high temperatures around 1000°C (Lefond, 1983; Garnar and Stanaway, 1994)). These operations can be carried out both with large-scale continuous reactors or small-scale batch reactors, depending on the desired products. Spray calcination can also be used to produce TiO_2 pigment particles between 150-250 nm (Gurav et al, 1998). Additives such as aluminum chloride are introduced at the oxidation step to improve pigment characteristics and to ensure that virtually all of the titanium is oxidized into the rutile crystalline form. The chlorine gas formed during oxidation is recovered and recycled back into the chlorination process. The resulting fine-grained TiO_2 is calcined between 500-600°C to remove any residual chlorine and hydrochloric acid that may have formed during oxidation (Lefond, 1983).

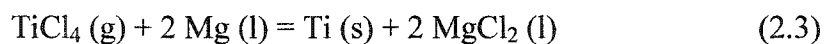
The calcination also helps to improve the pigment characteristics such as the final brightness and luster.

Depending on the end use of the pigment other special treatments are available to enhance specific properties of the pigment. These can include special coatings such as aluminum phosphate coatings for improved light fastness in laminates (Banford et al, 1998), and silica, alumina and zirconia phosphates for improved durability and gloss (Hiew and Chegwiddden, Jan. 29, 2002). Treatments by organic chemicals are also available for improving the wettability, dispersibility and gloss characteristics of the pigments that are suitable for use in water-thinnable paint systems (Orth-Gerber et al, 2002).

2.2.5.6 Production of Titanium Metal

Less than ten percent of world titanium mineral production is used to make titanium metal sponge. There are only two economic processes available to produce the sponge, the Kroll process and the Hunter Process (Smith, 1993). The two processes are similar except in the reactants used, the Hunter process uses molten sodium and the Kroll process uses molten magnesium.

In the Kroll process, TiCl_4 is reacted with molten magnesium between 773-873°C in a closed stainless-steel vessel under an inert argon atmosphere. The end products of the reaction are titanium sponge, magnesium chloride (MgCl_2), and some excess magnesium. The chemical reaction is:



The porous aggregate known as titanium sponge consists of tightly connected Ti particles about 20 μm in diameter. The byproduct MgCl_2 and the residual Mg are contained in the fine porosity inside the sponge. They are removed by evacuation at 1000°C for several days.

The titanium sponge is then crushed and compacted into electrode compacts which are welded together to form a long consumable electrode for vacuum arc melting (Deura et al, Dec. 1998). Alloying elements can be added during crushing and compacting if certain properties are desired in the ingot. Vacuum arc melting is necessary since titanium is highly reactive with the oxygen and nitrogen in the air (Smith, 1993). The consumable electrode becomes the anode in the vacuum arc furnace and a water-cooled copper crucible serves as the cathode. An arc is struck between the compacted electrode and the copper crucible and the molten metal collects and solidifies in the copper crucible (Deura et al, 1998; Smith, 1993). A diagram of this process can be seen in Figure 5. Ingots up to 10 tons with diameters of 91.4 cm can be produced (Smith, 1993). Finished titanium products are made from the ingots.

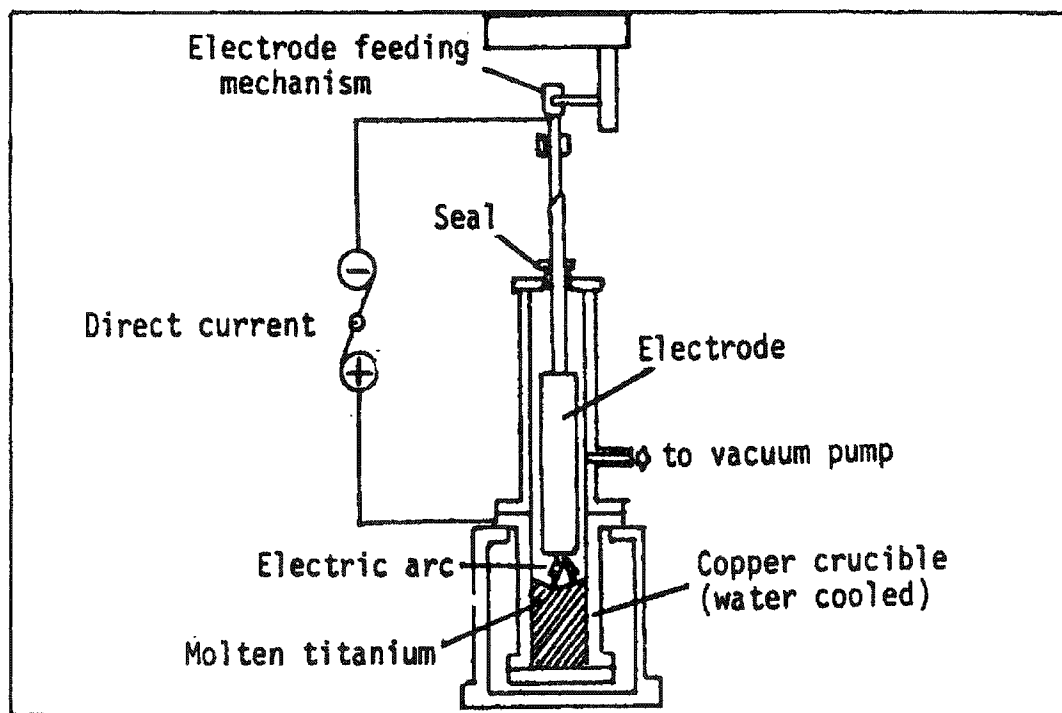


Figure 5 Titanium Ingot Manufacture (Smith, 1993)

2.3 Previous Studies to Recover Heavy Minerals From the Oil Sands

2.3.1 Typical Techniques Used in Heavy Mineral Separation

Ores that are mined usually need to be processed to form individual mineral concentrates of the desired grades before further processing can take place. The various processing stages that can be used depend on the mineral properties contained in the ore body. By utilizing the mineral properties certain gangue minerals can be rejected while keeping the desired minerals for further processing. Properties such as density, magnetic properties, electrical conductivity and surface wettability can be used to concentrate minerals from their ores.

Table 3 highlights the separation characteristics of heavy minerals typically contained in alluvial type heavy mineral deposits such as the Alberta oil sands. From Table 3 it can be seen that heavy minerals and the associated gangue have different properties, some minerals share the same magnetic and electrical properties; yet have significant differences in their specific gravity. Mineral processing equipment is designed to utilize the differences in these properties and mineral processing plants are methodically designed to systematically remove undesirable minerals by placing the individual equipment in a specific order. However the order the equipment is placed can vary from plant to plant due to the variations in the components in the ore body.

2.3.1.1 Gravity Concentration

Gravity concentration is the oldest form of mineral processing. This process utilizes the differences in specific gravity among minerals and their movement in response to gravitational or centrifugal force and the fluid drag of a process medium (air or water). In order to effect a separation there has to be a sufficient density difference between the mineral and the gangue. The following concentration criteria applies:

$$e = (D_h - D_f) / (D_l - D_f) \quad (2.4)$$

where D_h is the specific gravity of the heavy mineral, D_l is the specific gravity of the light mineral and D_f is the specific gravity of the fluid medium. When the concentration criteria quotient e is greater than 2.5, gravity separation is relatively easy. The efficiency of the separation decreases as the value of the quotient decreases. The efficiency of gravity concentration processes is also dependent on the particle size. Particle size will affect how a particle moves in a fluid, thus for an efficient separation the particles should have a similar size.

Table 3 Separation characteristics of heavy minerals

Mineral	Specific Gravity	Magnetic Property	Electrostatic Conductivity
Ilmenite	4.5 - 5.0	Magnetic	Conductor
Altered Ilmenite	4.0 - 5.0	Magnetic	Conductor
Leucoxene	3.5 - 4.5	Weakly Magnetic	Conductor
Rutile	4.2	Non-magnetic	Conductor
Anatase	4.2	Non-magnetic	Conductor
Zircon	4.6 - 4.7	Non-magnetic	Non-conductor
Pyrite	4.9 - 5.2	Weakly Magnetic	Conductor
Tourmaline	3.0 - 3.2	Weakly Magnetic	Non-conductor
Garnet	3.4 - 4.2	Weakly Magnetic	Non-conductor
Staurolite	3.7 - 3.8	Weakly Magnetic	Non-conductor
Monazite	4.9 - 5.4	Weakly Magnetic	Non-conductor
Quartz	2.65	Non-magnetic	Non-conductor

There are many different types of gravity concentration equipment for just about any size of particle or type of feed. These machines include jigs, cones, spirals, tables and centrifugal equipment such as hydrocyclones and centrifugal separators.

2.3.1.2 Magnetic Separation

Magnetic separation is based on the exploitation of the difference in magnetic properties of minerals. This separation technique can be used to separate magnetic minerals from non-magnetic minerals, or minerals possessing different degree of magnetic susceptibilities.

Nearly all materials are affected in some way when placed into a magnetic field and can be classified into two main groups depending on whether they are attracted or repelled by a magnetic field, i.e., diamagnetic and paramagnetic.

Diamagnetic materials are repelled along the lines of magnetic force to a point where the field intensity is smaller. The forces involved are very small and currently there is no effective process to concentrate diamagnetic materials (Wills, 1997).

Paramagnetic materials are attracted along the lines of magnetic force to points of greater field intensity. Paramagnetics can be concentrated in high intensity magnetic separators. Minerals currently being separated in commercial magnetic separators include ilmenite, wolframite, monazite, siderite, pyrrhotite, chromite, and hematite as well as manganese minerals (Wills, 1997).

Ferromagnetism is regarded as a special case of paramagnetism involving very high forces. Ferromagnetic materials have very high susceptibility to magnetic forces and retain some magnetism, called remanence, when removed from the field. These materials can be concentrated in low-intensity magnetic separators. The principal ferromagnetic material separated is magnetite (Fe_3O_4), although hematite (Fe_2O_3) and siderite (FeCO_3) can be converted to magnetite by roasting at elevated temperatures (Wills, 1997).

Magnetic separation of materials is possible by inducing a magnetic force on a particle large enough to make the particle move in a desired direction. The unit of measurement of magnetic flux density or magnetic induction is (B), and the number of lines of force passing through a unit area of material is called the Tesla (T). The magnetizing force which induces the lines of force through a material is called the field intensity (H) and has the units of ampere/meter ($1 \text{ ampere/meter} = 4\pi \times 10^{-7} \text{ Tesla}$). In vacuum, the magnetic flux density is given as:

$$B = \mu_0 H \quad (2.5)$$

where μ_0 is the permeability of vacuum and has the value of $4\pi \times 10^{-7}$ Tm/A.

The magnetic susceptibility (S) is the ratio of the intensity of magnetization produced in the material to the magnetic field that produces the magnetization. The formula is given by:

$$S = \frac{M}{H} \quad (2.6)$$

The capacity of a magnet to lift a particular mineral is dependent not only on the value of the field intensity, but also on the field gradient, the rate at which the field intensity increases towards the magnet surface. The higher the magnetic susceptibility of a mineral, the higher the field density in the particle and the greater the attraction up the field gradient towards increasing magnetic field strength. The force exerted on a particle can be given as:

$$F \propto H \frac{dH}{dl} \quad (2.7)$$

where F is the magnetic force exerted on the particle, H is the field intensity and $\frac{dH}{dl}$ is the field gradient.

2.3.1.3 Electrostatic and High-Tension Separation

Both electrostatic and high-tension separation utilizes the difference in electrical conductivity among the various minerals in a feed to effect a separation. Though nearly all minerals show a difference in electrical conductivity, the applications of this type of concentration is somewhat limited. The only real application of this technology has been in the processing of heavy mineral sands. The feed to these separators must be dry, have a clean mineral surface and be fed in a monolayer for efficient operation (Wills, 1997). And due to these restrictions, these separation techniques have a limited throughput.

Electrostatic separation works by the attraction of particles carrying one kind of charge towards a DC electrode of the opposite charge that causes a lifting effect. A thin charged wire induces a charge on the conductor particles, which passes the opposite charge through them onto a separation drum resulting in a net opposite charge on the conductor particles. This opposite charge causes the conductors to be lifted from the separating surface towards the electrode effecting a separation.

High-tension separation utilizes a pinning effect to cause a separation. The pinning effect is created by the ionization of gas molecules through a corona effect. The ionized gases in the charged corona accelerate to the separation drum where conductors pass the charge through them. The non-conducting mineral particles, having received a net charge from the electrode, retain this charge and are pinned to the oppositely charged separator (drum) surface.

2.3.1.4 Froth Flotation

Flotation is the most important and versatile mineral processing technique that exists today with its applications being expanded to treat greater tonnages of ore and to cover new areas. Patented in 1906, the invention of flotation has led to the ability to process low-grade and complex ore bodies that would otherwise be considered uneconomic (Wills, 1997).

Flotation is a relatively new technique for the separation of heavy minerals. This is due to the fact that most heavy mineral deposits mined until now are alluvial or placer deposits and have consisted of well liberated and well-rounded grains of minerals. It is easy to recover these minerals by gravity, electrostatic and magnetic separation techniques. As the newer ore bodies become more disseminated and particle sizes get finer, the traditional gravity/magnetic/electrostatic combinations gradually lose their efficiencies and froth flotation has been studied recently (Mao, et al, 1999). At present flotation is not being used on a commercial scale to float any heavy minerals from the beach sands.

The theory of froth flotation is complex and not completely understood, though the general principle utilizes the differences in the physico-chemical surface properties of the various minerals (Wills, 1997). To achieve a separation, the surfaces of the minerals need to be treated with reagents to change the desired or undesired wettability by water. For flotation to take place, an air bubble must be able to attach itself to a particle and lift it to the water surface. Thus particle size also plays an important role in flotation; if the mineral particles are too large, then the adhesion between the particle and the bubble will be less than the particle weight and will not lift its load to the surface. If particles are too small, then they have the tendency to float very easily (called “entrainment”) resulting in non-selective flotation.

Air bubbles can only attach to mineral surfaces if they can displace the water away from the mineral surface. This can only happen if the surface is rendered water repellent or hydrophobic. Most minerals are hydrophilic, i.e., not water repellent, in their natural state and flotation reagents (collectors and regulators) must be added to make them selectively hydrophobic and thus to effect a separation. Once the air bubbles are attached, they will lift the particle to the air-water interface where a stable froth must be formed to prevent the air bubbles from dropping their mineral load. The stability of the froth layer, or its ability to hold minerals once they have been floated, can be increased by the addition of frothers.

The activity of a mineral surface in relation to flotation reagents in water depends on the forces that operate on that surface. Flotation is a three phase system in which air, water and a solid contact each another. The tensile forces between these interfaces lead to the development of an angle between the mineral surface and the bubble surface. At equilibrium, Young's equation applies:

$$\gamma_{s/A} = \gamma_{s/w} + \gamma_{w/A} \cos\theta \quad (2.8)$$

where $\gamma_{s/A}$, $\gamma_{s/w}$ and $\gamma_{w/A}$ are the surface energies between solid-air, solid-water and water-air, respectively, and θ is the contact angle between the mineral surface and the bubble. Figure 6 shows a representation of Young's equation. The work required to break the particle-bubble interface is called the work of adhesion, $W_{s/A}$, and is equal to the work required to separate the solid-air interface and produce separate air-water and solid-water interfaces.

$$W_{s/A} = \gamma_{w/A} + \gamma_{s/w} - \gamma_{s/A} \quad (2.9)$$

Combining the above two equations results in:

$$W_{s/A} = \gamma_{w/A} (1 - \cos\theta) \quad (2.10)$$

From this equation, it can be seen that the greater the contact angle, the greater the work of adhesion between the particle and bubble which increases the stability of the system. By increasing the contact angle, the floatability of a mineral can be increased by rendering the surface more hydrophobic.

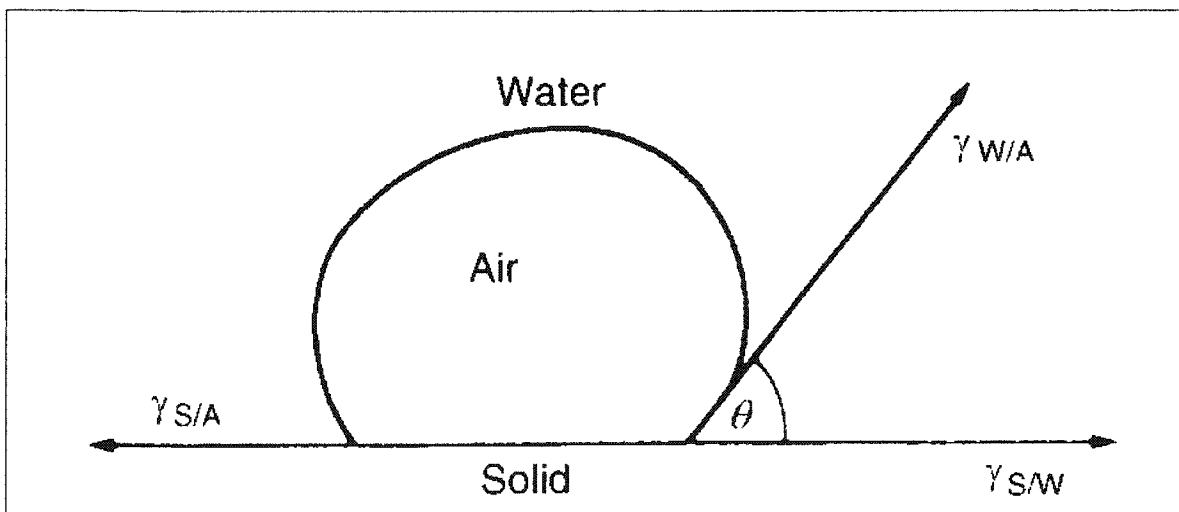


Figure 6 Contact Angle between a Bubble and Particle in an Aqueous Media (Wills, 1997)

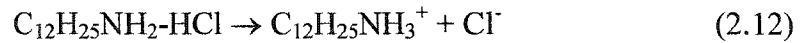
2.3.1.4.1 Collectors

The purpose of collectors is to change the mineral/water interface from hydrophilic to hydrophobic. The requirements of a collector are that part of the molecule is in itself hydrophobic, while part of it will interact selectively with mineral surfaces. This interaction may be purely physical adsorption or a surface chemical reaction, though sometimes a combination of both processes is involved.

Collectors can be classified into two general groups. The first ionizes in aqueous solution to give a negatively charged radical and the second ionizes to give a positively charged radical. These are known more commonly as anionic and cationic collectors, respectively. Another type of collector is a non-ionizing collector that is practically insoluble in water and renders the mineral water repellent by covering the mineral surface with a thin film. The most widely used collectors are of the ionizing type.

Because of chemical, electrical or physical attraction between the polar portions and surface sites, collectors adsorb on the particles with their non-polar ends orientated towards the bulk solution, thereby imparting hydrophobicity to the mineral particles (Wills, 1997). Collectors are usually used in small amounts, typically at concentrations that form less than a monomolecular layer on the mineral surface. Anionic collectors can be broken down further into two groups, oxyhydril, based on organic and sulpho acid groups and sulphhydril, based on bivalent sulfur (Wills, 1997). The oxyhydril collectors have functional groups based on the carboxylic or the fatty acids and soaps, sulphates and sulphonates. The sulphhydril collectors have functional groups based on the xanthates and dithiophosphates. Cationic collectors are primarily based on the amine group and are used extensively in oxide mineral flotation. They can be thought of as ammonia with one or more of the hydrogen atoms replaced by a hydrocarbon chain (Manser, 1975). The extent of this replacement can classify them into groups as, primary, secondary or tertiary amines. The most common type of cationic collector contains between 12-18 carbon atoms in the hydrocarbon chain and is almost totally insoluble in water. Laurylamine (dodecylamine, $C_{12}H_{25}NH_2$) may be taken as a typical example of this group. Amines are

generally converted to the hydrochlorides or acetates before addition to a flotation circuit, for example:



2.3.1.4.2 Regulators or Modifiers

Regulators or modifiers are extensively used in flotation to modify the action of the collector, either by intensifying or reducing its water-repellant effect on the mineral surface (Wills, 1997). The end result is to make the collector more specific to one type of mineral over another. Regulators can be used as activators, depressants or pH modifiers. A surface modifier that increases the hydrophilic character of a mineral is known as a depressant and one that increases the hydrophobic character an activator. Some chemicals may act as either an activator or a depressant depending on the conditions under which they are used. For example, the fluoride ion, which is used as a modifier in oxide flotation, behaves as a depressant if used in conjunction with anionic collectors but as an activator if used in conjunction with cationic collectors (Manser, 1975).

Depressants are used to increase the selectivity of flotation by rendering certain minerals hydrophilic, thus preventing their flotation. There are many types of depressants and their actions are complex and not well understood. Slime coating is an example of the most naturally occurring form of depression. A slime coating is produced from grinding and crushing an ore or by the adsorption of specific ions on the mineral surface (Wills 1997). Slimes coat the mineral particle preventing collector adsorption.

Other depressants act by reducing or eliminating the adsorption of the collector on to the mineral surface, as well as possibly increasing the hydrophilic character of the mineral through a hydrophilic coating. To be effective, a modifier of any type must be selective

by accentuation differences between mineral species. The most common inorganic modifiers include acids and alkalis for pH modification. Various multivalent cations, especially calcium and ferric ions, as well as numerous anions such as fluoride, sodium silicate, silicofluoride, sulfide, phosphate, chromate, cyanide and ferricyanide are among the most common (Manser, 1975). Organic modifiers include various complexing agents such as citrate ions though the largest group of organic modifiers is the polymer colloids. This group contains various tannin products and quebracho as well as starch products derived from various sources and their degradation products such as dextrin, gums and glues.

2.3.1.4.3 Frothers

In mineral processing frothers are as important as collectors, and often most collectors are strong frothers, though ideally a frother should have no collecting power (Wills, 1997). The purpose of a frother is to stabilize the air-water interface and reduce the surface tension to produce a froth layer that is just stable enough to facilitate transfer of a floated mineral from the cell surface. Frothers can be acids, amines and alcohols, though alcohols are the most widely used due to their low collecting power. The most common frothers are pine oil, an aromatic alcohol ($C_{10}H_{17}OH$) and cresol (cresylic acid) ($CH_3C_6H_4OH$). Synthetic alcohols are also increasingly being used due to their consistency of the chemical composition. A widely used synthetic alcohol frother is methyl isobutyl carbinol (MIBC). Another range of synthetic frothers is based on polyglycol ethers such as Dowfroth 250, Cyanamid R 65 and Union Carbide PG 400. These frothers produce a stronger froth layer than the alcohols (Wills, 1997).

2.3.1.5 Surface Charge for Oxide Minerals

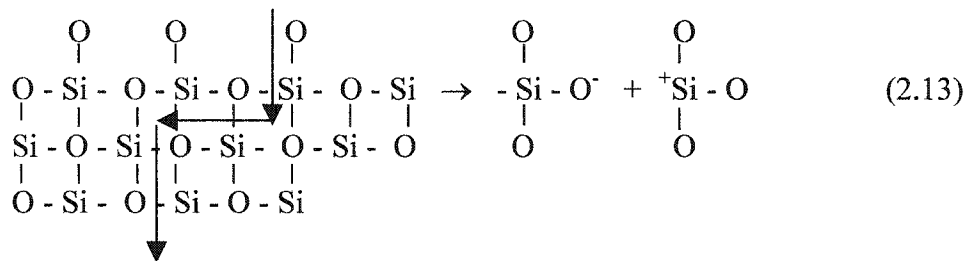
2.3.1.5.1 Development of the Surface Charge

Surface charge of oxide minerals is an important phenomenon exploited by the froth flotation process. This is apparent due to the use of ionic flotation collectors. Almost all

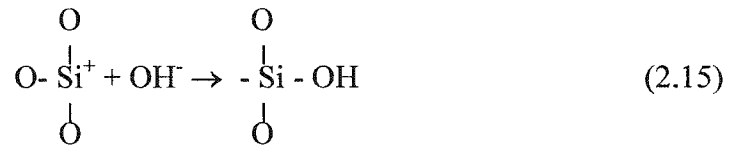
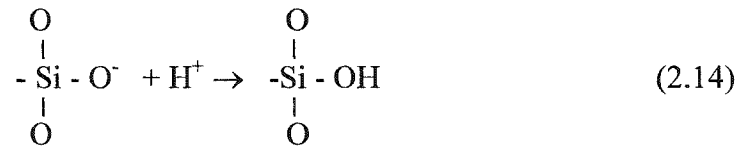
solids acquire a surface charge when brought into contact with a polar medium such as water (Shaw, 1992). Some of the common reasons are: the ionization of surface groups such as carboxyl and amino groups, the adsorption of ions such as surfactants, multivalent ions and polyelectrolytes, as well as the unequal dissolution of the ions comprising the surface molecules such as metal oxides and silver halides (Hunter, 1993). The manner in which the surface charge develops and changes also depends on solution conditions such as pH, ionic strength, addition of adsorbed ions, addition of surface active agents (ionic or nonionic), addition of reagents that chemically bond to the surface as well as the order of addition of these various species (Brookhaven Instruments Corporation, 1994).

The surface charge of the solid influences the distribution of nearby ions in the polar medium. Ions of opposite charge, called counter-ions, are attracted towards the surface and ions of like charge, called co-ions, are repelled away from the surface. This tendency, together with the mixing caused by Brownian Motion, leads to the formation of an electric double layer made up of the charged surface layer and a neutralizing excess of counter-ions over co-ions distributed in a diffuse layer in the polar medium. The theory of the electric double layer deals with the distribution of ions and with the magnitude of the electric potentials that arise in the vicinity of the charged surface.

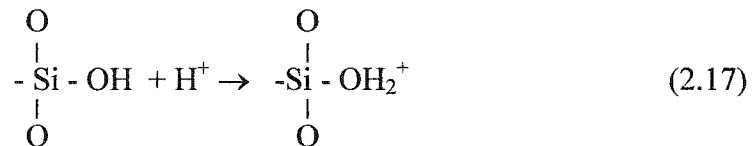
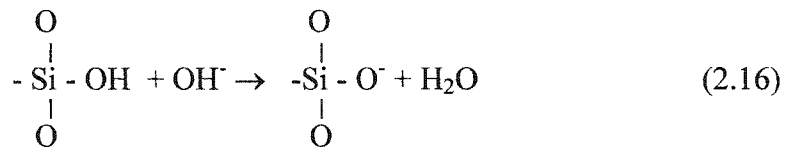
When oxide minerals are fractured by size reduction techniques in mineral processing such as crushing and grinding, metal-oxygen bonds are broken, which can be seen below using quartz as an example:



The broken metal oxygen bonds tend to react with ions present in an aqueous solution, most commonly H^+ and OH^- resulting from the dissociation of water molecules:



Thus, the quartz surfaces are covered with silanol groups $-OH$. When there is a change in solution pH, either additional hydrogen or hydroxyl ions are added depending on whether there is a decrease or an increase in pH, thus causing changes in surface charge:



From these reactions it can be seen that the surface Potential Determining Ions (pdi) for oxide minerals are hydrogen or hydroxyl ions and the surface charge on oxide minerals is a function of pH. When the surface charge is neutral, the corresponding pH is referred to as Point of Zero Charge (pzc). For oxide minerals this occurs when most of the surface is covered with uncharged hydroxyl groups. For quartz the pzc has been reported to be anywhere between 1.3 to 2.7 (Manser 1975). For rutile the pzc has been reported to be anywhere between 4.0 and 7.0 (Leja, 1982). The range of pzc that are reported can be attributed to the source of the oxide, trace impurities, etc. When the solution pH is below

the pzc for these oxides, the surface is positively charged and above this value, the surface is negatively charged.

2.3.1.5.2 The Electric Double Layer

The electric double layer can be regarded as consisting of two regions, an inner region that includes adsorbed ions that are held on the mineral surface, and a diffuse region in which ions are more mobile and are distributed according to the influence of electrical forces and random thermal motion (Shaw, 1992). The concentration of counter ions is high near the particle surface and decreases steadily to the concentration in the bulk liquid. Likewise, the co-ions are depleted near the surface, and their concentration increases until it reaches the level in the bulk liquid. Figure 7 shows a schematic representation of the diffuse part of the electric double layer (Shaw, 1992).

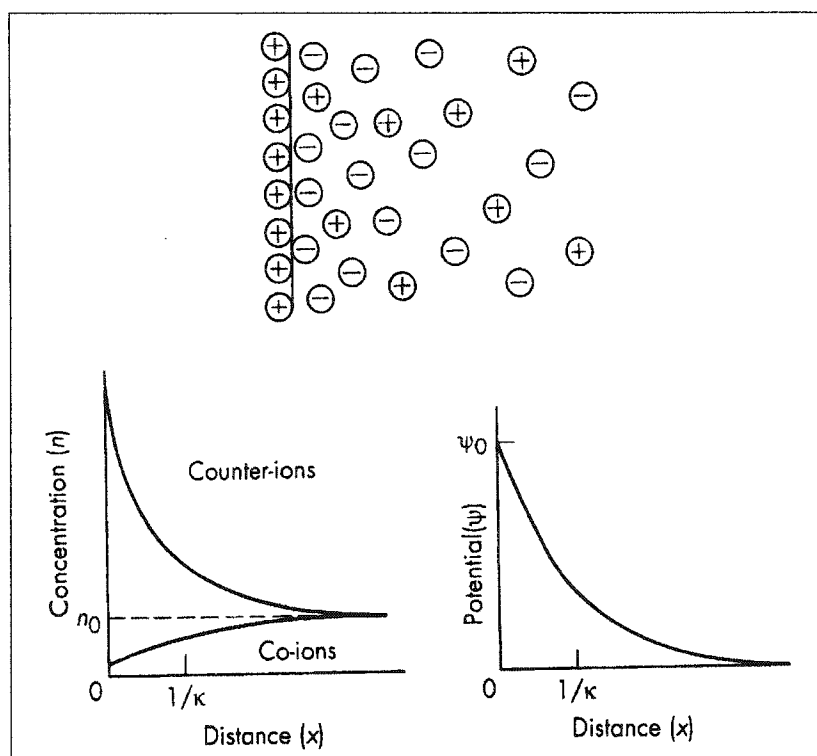


Figure 7 Schematic Representation of the Diffuse part of the Electric Double Layer (Shaw, 1992)

The simplest quantitative treatment of the diffuse part of the double layer was developed by Gouy (1910) and Chapman (1913), which is based on the following model:

1. The surface is assumed to be flat, of infinite extent and uniformly charged.
2. The ions in the diffuse part of the double layer are assumed to be point charges distributed according to the Boltzmann distribution.
3. The solvent is assumed to influence the double layer only through its dielectric constant, which is assumed to have the same value throughout the diffuse region.
4. A single symmetric electrolyte of charge number z will be assumed. This assumption facilitates the derivation while losing little owing to the relative unimportance of co-ion charge number.

If the electric potential is defined as ψ_0 at a flat surface, and ψ at a distance x from the surface in the electrolyte solution, then:

$$n_+ = n_0 \exp[-ze\psi/kT] \quad (2.18)$$

$$n_- = n_0 \exp[+ze\psi/kT] \quad (2.19)$$

where n_+ and n_- are the respective numbers of positive and negative ions per unit volume at points where the potential is ψ (where the electric potential energy is $ze\psi$ and $-ze\psi$, respectively) and n_0 is the corresponding bulk concentration of each ionic species.

The net volume charge density ρ at points where the potential is ψ is given by

$$\rho = z e (n_+ - n_-) \quad (2.20)$$

After some further assumptions, this model leads to the following equation for the electrostatic potential as a function of distance from the particle surface

$$\psi = \psi_0 \exp[-\kappa x] \quad (2.21)$$

where κ is a parameter that measures the decay of the potential from the surface with distance and can be defined as:

$$\kappa = [2e^2n_0z^2 / \epsilon kT] = [2e^2N_a cz^2 / \epsilon kT] \quad (2.22)$$

where ϵ is the permittivity of the solution, N_a is Avogadro's number and c is the concentration of the electrolyte. The double layer thickness is affected by electrolytes, and can be compressed as the concentration of the electrolyte is increased. For example, from equation 2.22, the double layer thickness is approximately 100 nm in 10^{-5} M KCl solutions, 10 nm in 10^{-3} M and 1 nm in 10^{-1} M. Thus at low concentrations, the double layer thickness is large and the resulting repulsive forces are long range. At high concentrations the double layer thickness is small and the resulting repulsive forces are short range.

The inner part of the electric double layer is separated from the diffuse part of the double layer by the Stern plane. The finite size of ions limits the inner boundary of the diffuse part of the double layer since the center of an ion can only approach the surface to within its hydrated radius without becoming specifically adsorbed (Hunter, 1993). The Stern plane is located at about a hydrated ion radius from the surface and can contain specifically adsorbed ions. Specifically adsorbed ions attach themselves to the surface by electrostatic and/or van der Waals forces strong enough to overcome thermal agitation. When specific adsorption takes place, counter-ion adsorption usually predominates over co-ion adsorption, a typical double layer situation can be seen in Figure 8, in which the Stern plane charge is defined as ψ_d (Shaw, 1992).

The electrokinetic behavior of a solid particle depends on the potential at the surface of shear between the charged surface and the electrolyte solution. This potential is called the electrokinetic or zeta potential ζ . The exact location of the shear plane is an unknown feature of the electric double layer. In addition to ions in the Stern layer, a certain amount of solvent will be bound to the charged surface and form a part of the

electrokinetic unit. The shear plane is assumed to be positioned at a small distance further out from the Stern plane and the ζ potential is slightly smaller than ψ_d . When there is specific adsorption or the solution phase contains a charged surface-active agent that can strongly adsorb onto the particle surface, the particle's surface charge can be profoundly altered, even reversed. This phenomenon can even occur at very small surfactant additions, in Figure 9, a negatively charged particle has an adsorbed surfactant which makes the particle appear to be positively charged (Hunter, 1993). Therefore, zeta potential measurements are critical in determining how a particle will interact with its surroundings and with other particles.

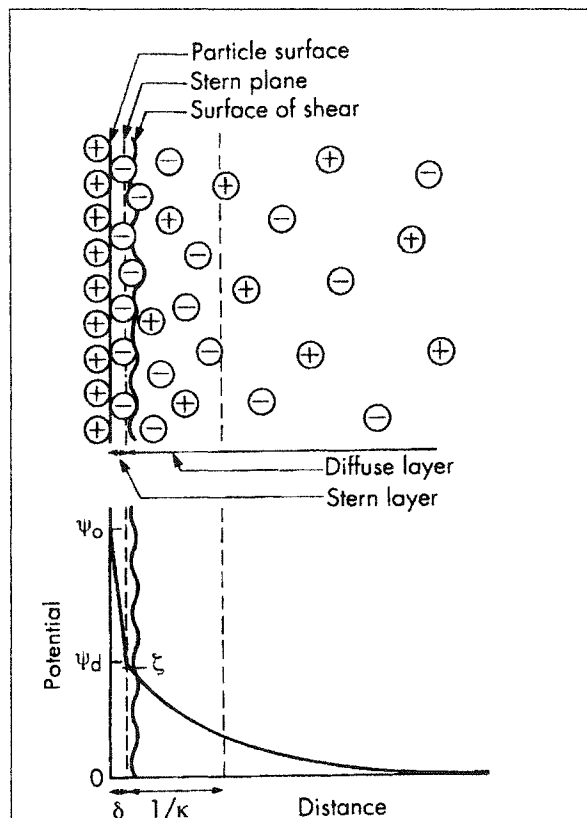


Figure 8 The Electric Double Layer According to Stern's Theory (Shaw, 1992)

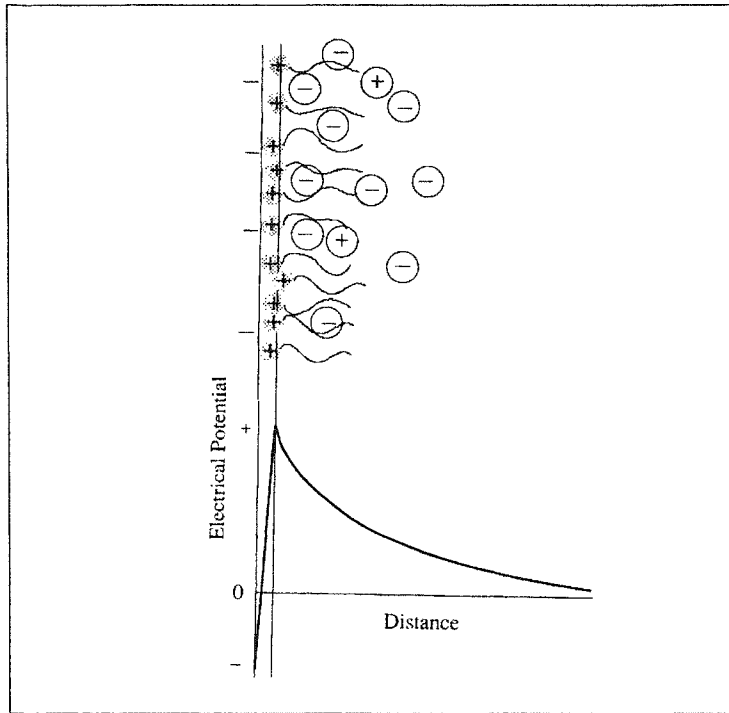


Figure 9 Particle Charge Reversal Due to the Presence of a Surfactant (Hunter, 1993)

The ζ potential is measured in the shear plane as the particle moves through a liquid. Experimentally, it is the velocity of a charged particle that is measured by its mobility in solution. From the mobility, the ζ potential of the charged particle can be calculated. The zeta potential is used to determine the magnitude of the electrostatic force. For curved surfaces the shape of the double layer can be described in terms of the dimensionless quantity ' κa ', which is the ratio of the radius of curvature to the double-layer thickness. When ' κa ' is small, a charged particle may be treated as a point charge; when ' κa ' is large, the double layer is effectively flat and can be treated as such. If electrolyte concentrations are in the order of 10^{-3} to 10^{-2} M, corresponding to a large ' κa ', then the Smoluchowski equation can be used to calculate the zeta potential from the measured particle mobility. In the Smoluchowski limit, the electrophoretic mobility, μ_e is related to the zeta potential through the following equation,

$$\mu_e = \varepsilon\zeta / \eta \quad (2.23)$$

where ε is the permittivity of the liquid and η is the viscosity of the liquid. One mobility unit is $1 \mu\text{s}^{-1}\text{V}^{-1}\text{cm}^2 = 10^{-8}\text{m}^2\text{s}^{-1}\text{V}^{-1}$. Therefore the zeta potential in water at 25°C is $\zeta = 12.83 \text{ mV}$ per mobility unit.

2.3.2 *Typical Processing Flowsheets for Heavy Minerals*

A heavy mineral processing flowsheet is an integration of the various separation techniques described in the previous section. These include gravity, magnetic, high-tension separators as well as froth flotation. The flowsheets vary according to the properties of the valuable (heavy) minerals present and the types of gangue minerals associated with them.

A generalized heavy mineral processing flowsheet can be seen in Figure 10 (Wills, 1997). In this flowsheet, a gravity pre-concentration step is employed to remove the majority of the light minerals such as quartz and clays so that the tonnage of feed can be substantially reduced. Afterwards, a low-intensity (magnetic) drum separator is used to remove any magnetite from the feed, followed by high-intensity wet magnetic separators, which separates monazite and ilmenite from the non-magnetic zircon and rutile. The two streams are dried separately followed by high-tension separation, which separates the zircon from rutile and ilmenite from monazite. Screen electrostatic separators are useful for cleaning the monazite and zircon concentrates by removing any fine conducting particles from these products. Similarly, plate electrostatic separators are utilized to reject coarse non-conducting particles from the rutile and ilmenite concentrates.

Associated Minerals Consolidated Ltd., located on the East Coast of Australia uses a process that is similar to the generalized process. The process flowsheet can be seen in Figure 11 (Wills, 1997). After the initial ore is upgraded on the dredge by the use of spirals and tables, the concentrate is dried and passed onto high-tension separators. After

several stages of cleaning, high-intensity induced roll (magnetic) separators are used to treat the conducting and non-conducting products. The conducting rutile concentrate is cleaned by the use of electrostatic plate separators and the non-conducting zircon concentrate is cleaned by electrostatic screen separators. Any remaining silica, being non-conducting, is recovered in the zircon concentrate. It is removed by a combination of pneumatic and wet tabling where a separation is achieved due to the density difference between these two minerals.

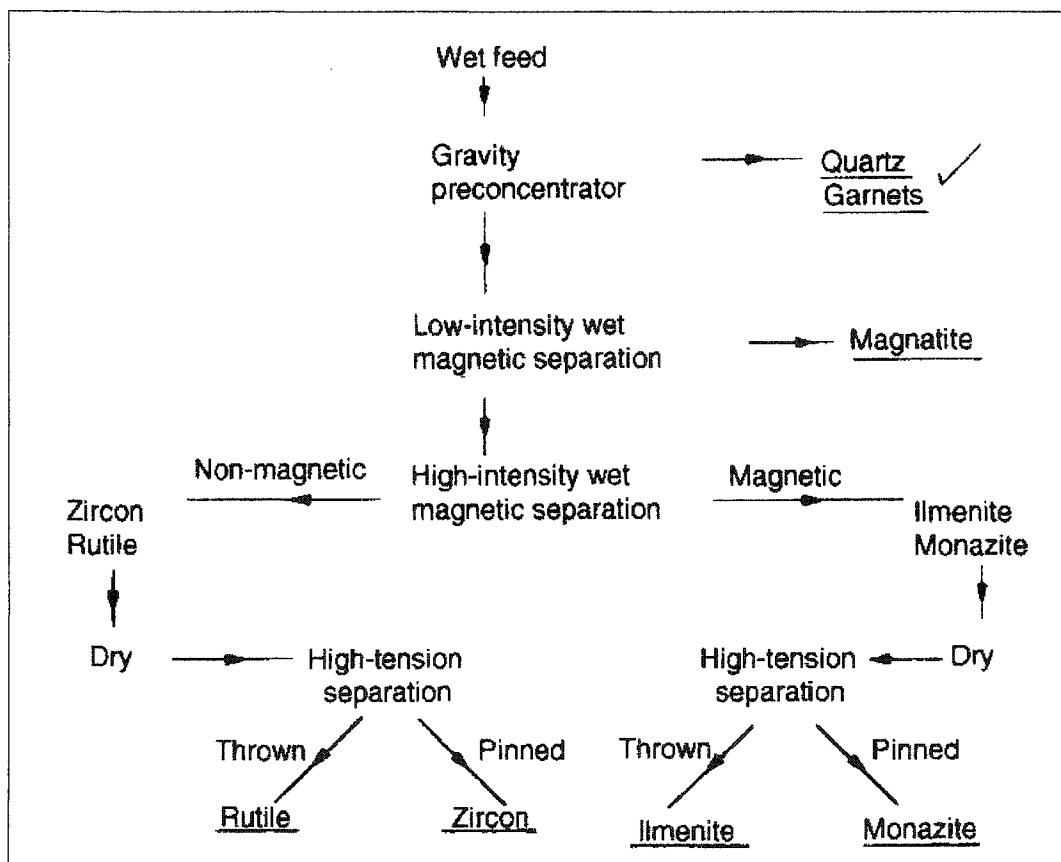


Figure 10 Generalized Mineral Processing Flowsheet of Heavy Minerals (Wills, 1997)

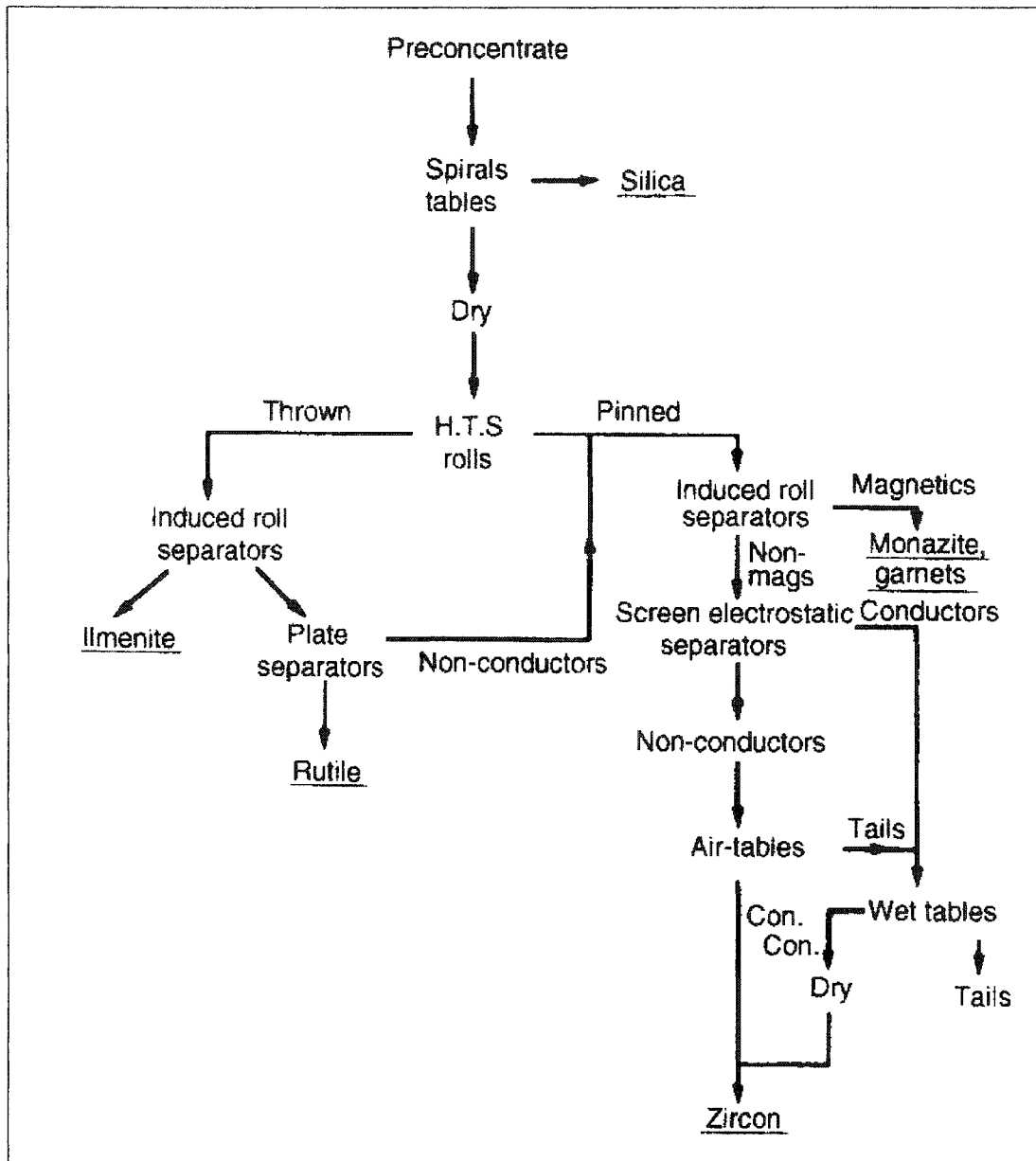


Figure 11 Associated Minerals Consolidated Ltd. of Australia (Wills, 1997)

Due to the high degree of liberation and uniformity in particle size, very good separation can be achieved in the mineral processing plants. Currently rutile concentrates containing over 91% TiO₂, typically around 96%, can be produced. The typical specification given in Table 4 represents the minimal composition of a rutile concentrate that can be processed by the chloride process (Garnar and Stanaway, 1994).

Table 4 Rutile Concentrate Specifications for the Chloride Process

Compound	Typical Specification	Current Production Grade
TiO ₂	85% min	> 91 %
Fe ₂ O ₃	N.A.	0.5 %
CaO	0.2% max	0.3 %
MgO	1-2% max	0.07 %
MnO	0.1-1% max	0.10 %
Al ₂ O ₃	1.0% max	< 0.5 %
SiO ₂	varies	< 1.0 %
U+Th	100 ppm max	50 ppm
Particle Size	-30 +200 mesh (-550 + 78µm)	Varies

2.3.3 Previous Studies to Recover Heavy Minerals from Alberta Oil Sand Tailings

Several research laboratories have performed basic studies to recover the heavy minerals from the Alberta oil sands tailings. This has not been an easy task compared to other heavy mineral recovery processes currently used around the world in beach sand processing. The minerals contained in the Alberta oil sands tailings are generally of altered forms and have associated impurity intergrowths that are not normally found in other alluvial or placer deposits. The solid particles in the tailings are still coated with bitumen, which by itself makes this deposit unique. The ilmenite minerals have been highly altered by weathering, which causes degradation in their magnetic properties. Among the heavy minerals contained in the Alberta oil sands tailings, rutile (anatase) is the most valuable and current sales prices of rutile (anatase) are about US\$400/tonne. Considering the transportation costs from potential heavy mineral producers in Fort

McMurray to the nearest ports, rutile would be the only titanium mineral concentrate that could be economically recovered from the oil sands tailings, although the relative amount of rutile (anatase) in the heavy mineral suite is still unclear. It has been reported to range between 4.0% and 36.6% of the total heavy mineral content.

The first systematic testwork to examine the options to recover the heavy minerals seemed to have started around 1976 by the research staff of Syncrude Canada Ltd., Trevoy and Schutte published the work in 1981. This was followed by the studies of several private and university research laboratories. A chronological list of the testwork to recover the heavy minerals from the oil sands tailings appears to be:

1. Syncrude Canada Ltd., Canada, 1981;
2. Mineral Deposits Ltd. (designated as MDL), Australia, 1982;
3. Western Ontario University (designated as WOU), Canada, 1987;
4. The Mineral Development Agreement Study (designated as MDA), Canada, 1996
5. Syncrude Canada Ltd and Lakefield Research Ltd. (designated as LRL), Canada, 2001.

A common feature of all these studies is that they all used the froth treatment tailings as the feed materials and they all used a burn-off to remove the residual bitumen.

In their pioneering study, Trevoy & Schutte (1981) used the conventional ore dressing techniques of alluvial deposits. Their process flowsheet is schematically shown in Figure 12. Following a burn-off step to remove the residual bitumen from the froth treatment tailings, they used gravity spirals to remove the light minerals and clays, and a high tension separator to produce a titanium mineral stream (conductors) and a zircon mineral stream (non-conductors). Magnetic separation was then employed to upgrade the titanium mineral concentrates, and a series of gravity, magnetic and high-tension separation were employed to upgrade the zircon concentrate. However, this work did not produce high-grade saleable titanium and zirconium mineral concentrates.

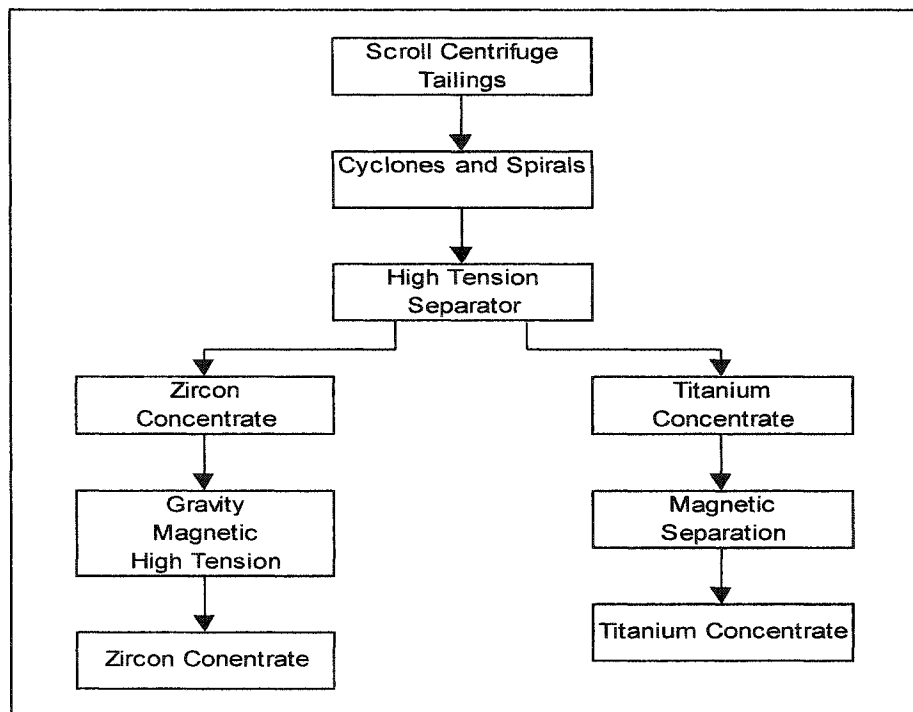


Figure 12 Trevoy & Schutte Flowsheet

Balderson of Mineral Deposits Ltd (1982) used a similar approach but his process was a more complicated combination of gravity, magnetic and electrostatic separations. A simplified flowsheet is shown in Figure 13. While the titanium mineral concentrates produced were inferior to the marketable grades, Balderson produced a near-market grade zircon concentrate (see Tables 5 to 7, “MDL”). However, the feed sample used in MDL’s testwork reported high mineral assays that were not reported in any other testwork then or since. This makes the MDL results unreliable.

Ityokumbul et al. of Western Ontario University (1987) developed and patented a process in which the froth treatment tailings were first subjected to flotation that resulted in the rejection of much of the light quartz minerals. The heavy minerals are enriched in a bulk flotation concentrate together with the residual bitumen. After calcining, which removed the bitumen, the bulk concentrate was processed by gravity and dense medium separators to further remove fines and quartz. The heavy mineral stream was then processed by

several stages of magnetic separation, each adjusted to different field intensities to produce Fe-bearing and non Fe-bearing Ti mineral concentrates. The non-magnetic product was claimed to be the zircon concentrate. However, none of the products were of marketable grades (Tables 5 to 7, “WOU”).

Table 5 Grades of rutile concentrates produced in previous studies

Compound	Weight % in rutile concentrate				
	MDL*	WOU	MDA	LRL	Typical market grade
TiO ₂	92.9	63.3	73.3	74.2	96.1
ZrO ₂	0.6	12.2	2.3	0.42	0.6
Fe ₂ O ₃	1.5	< 1.43	1.0	17.2	0.5
Al ₂ O ₃	0.6	NA [†]	NA	NA	0.4
SiO ₂	1.85	21.3	15.0	1.8	0.6

Table 6 Grades of ilmenite and leucoxene concentrates produced in previous studies

Comp.	Weight % in ilmenite concentrate					Weight % in leucoxene concentrate				
	MDL*	WOU	MDA	LRL	Market grade	MDL*	WOU	MDA	LRL	Market grade
TiO ₂	31.5	66.7	33.3	64.4	54.0	72.0	53.3	60.0	65.4	60.0
ZrO ₂	NA	< 0.07	0.5	0.24	NA	NA	< 0.07	0.5	2.45	NA
Fe ₂ O ₃	45.9	20.0	43.6	30.1	19.0	20.9	18.6	24.3	6.56	32.5
Al ₂ O ₃	5.8	NA	NA	NA	0.4	1.6	NA	NA	NA	1.2
SiO ₂	14.8	13.0	9.6	1.3	0.5	2.9	14.9	3.2	11.7	0.85
Cr ₂ O ₃	0.6	NA	NA	NA	0.4	0.6	NA	NA	NA	0.11

Table 7 Grades of zircon concentrates produced in previous studies

Compound	Weight % in zircon concentrate				
	MDL*	WOU	MDA	LRL	Typical market grade
ZrO ₂	66.3	39.0	59.5	65.1	66.2
TiO ₂	0.1	16.0	10.0	0.23	0.1
Fe ₂ O ₃	0.05	1.4	1.0	0.15	0.02
Al ₂ O ₃	0.3	NA	NA	NA	0.2

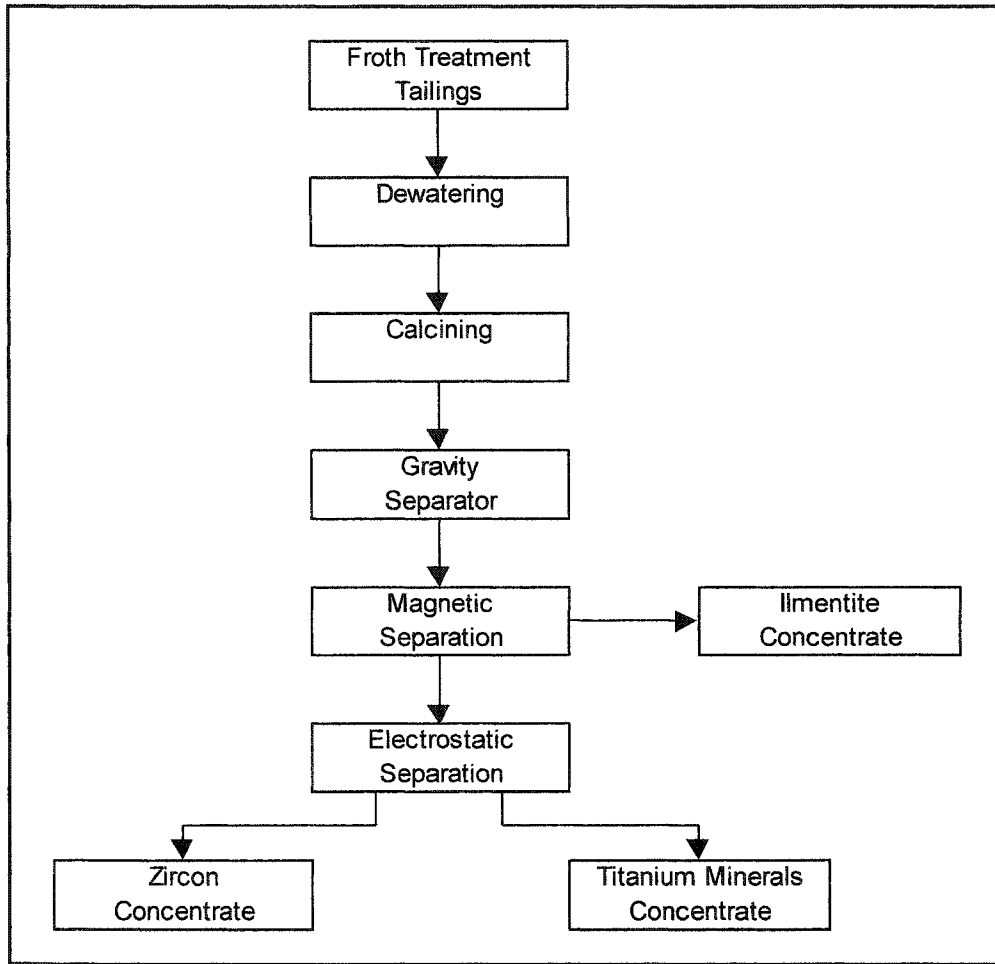


Figure 13 MDL Process Flowsheet

The Mineral Development Agreement (MDA) study initiated by the Federal and Alberta Provincial government followed generally established procedures in the flowsheet development testwork (Owen, 1996). The process flowsheet is shown in Figure 14. In this process a hydrocyclone was used to remove much of the fines and quartz. The hydrocyclone underflow was calcined to remove the residual bitumen and to decompose the secondary minerals such as pyrite and siderite. The calcine was separated into a titanium mineral stream and a zircon stream by gravity spirals. Each stream was then upgraded by magnetic separation and froth flotation. Electrostatic separation was not employed because it was considered ineffective. However, marketable grade concentrates were not produced (Tables 5 to 7, "MDA").

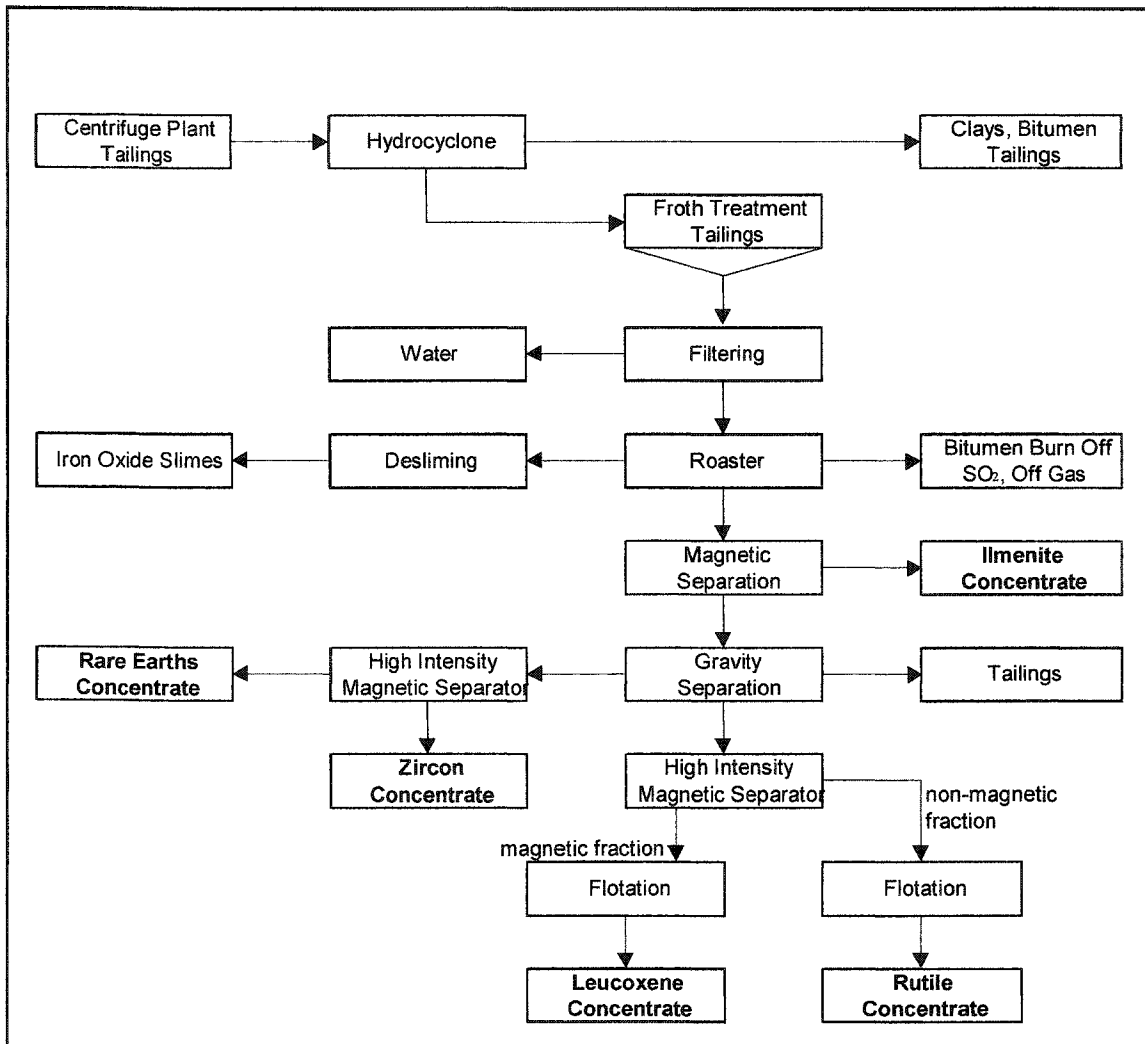


Figure 14 MDA Process Flowsheet

The most recent study on heavy mineral extraction from oil sands tailings was the work by Syncrude Canada Ltd and Lakefield Research Ltd. The process flowsheet from this study is schematically shown in Figure 15, which was constructed from Oxenford et al (2001). This process utilized a bulk flotation to produce a concentrate containing zircon and all the titanium minerals, including rutile, ilmenite and leucoxene. The procedure involved the use of a fatty acid and alcohol mixture as the collector at an elevated temperature of ~80°C. The hot pulp was conditioned with an alkali, a silica depressant and fatty acid mixture followed by flotation. The flotation recovery was found to be a

function of both pH and flotation temperature. The flotation concentrate contained between 4 - 8% residual bitumen by weight.

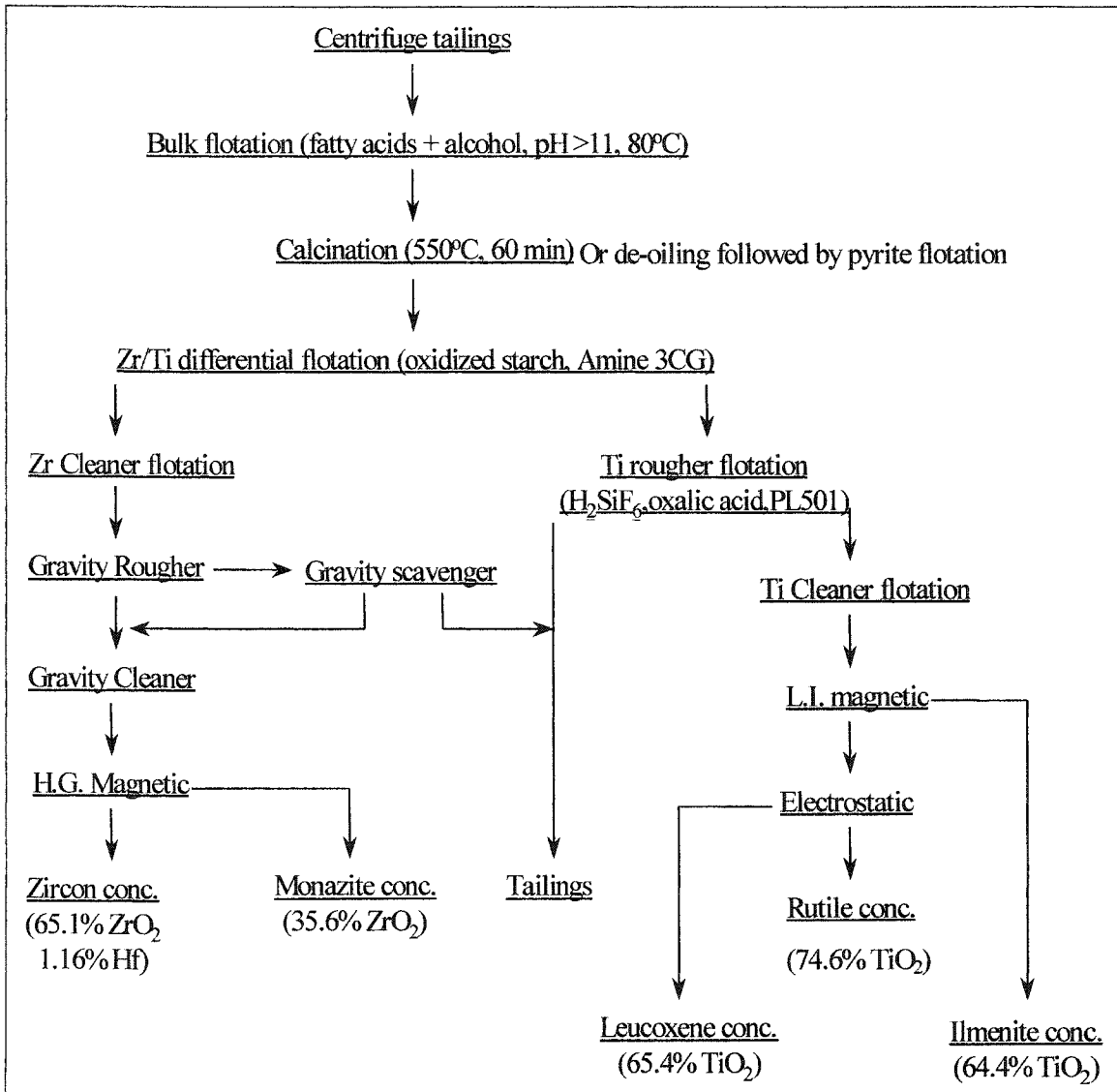


Figure 15 Lakefield Research Ltd. (LRL) Process Flowsheet (reconstructed from Oxenford et al (2001)).

Two options for bitumen removal were subsequently studied. The flotation product was either calcined at 550°C for 60 minutes or washed with organic solvent. Solvent extraction would allow for the recovery of the residual bitumen. The solvent extraction

involves scrubbing of the bulk concentrate in the presence of naphtha and a surfactant followed by removal of the naphtha/bitumen fraction in a cyclone. In this process, pyrite is recovered in the heavy mineral product and must to be removed by flotation with xanthate. On the other hand, calcination would convert the secondary minerals such as pyrite and siderite to hematite at the high temperatures used. The generated hematite can be removed by a magnetic separation. However, this option releases SO₂, which will require treatment so that it is not released into the atmosphere.

Following bitumen removal, zircon is separated from the titanium minerals by a differential flotation technique. To effect this separation several modified starches were tested of which an oxidized corn starch was found to be the most effective in depressing the titanium minerals. To float zircon, NaF was used as an activator together with an amine collector of which a mixture of primary and secondary amines gave the highest rate of zircon flotation along with the highest recovery.

The titanium bulk mineral concentrate was de-frothed and cleaned. Low-intensity magnetic separation was used to produce a highly magnetic mineral concentrate consisting of ilmenite. The remaining titanium minerals were dried and processed by electrostatic separation to produce a non-conducting concentrate consisting of leucoxene. The conducting stream is recovered as a rutile concentrate.

As can be seen from Tables 5 to 7, while the ilmenite and zircon concentrates produced from this study are saleable, the rutile concentrate does not satisfy the market grade requirements.

Comparatively, the Lakefield process is the most reasonable not only because it produced zircon and ilmenite concentrates that are saleable, but also because it used froth flotation for Ti/Zr separation. Traditionally, electrostatic separation is the routine technique for the separation of rutile from zircon. As is well known, out of the four major ore dressing techniques, electrostatic separation is intrinsically a dry process and requires less than a monolayer of mineral particles be spread on the separating drums. This requirement

limits its application in recovering heavy minerals from the oil sands tailings, which is mostly a wet process and is destined to be a large-scale operation. Gravity separation of zircon from the titanium minerals is not likely effective, because there is not a large enough gap between the densities of the titanium minerals (4.2 ~ 5.0) and zircon (4.6 ~ 4.7). Both zircon and rutile are non-magnetic, so magnetic separation cannot be used. This leaves froth flotation as the only choice. In fact, there seems to be a growing trend to use flotation as the separation method for titanium minerals from zircon (Mao et al, 1999).

Therefore, the process flowsheet in Figure 14 would be the basis for further metallurgical testwork to extract heavy minerals from the oil sands tailings.

3 OBJECTIVE

As described in the previous section, a process flowsheet recently developed by Lakefield Research Ltd and Syncrude Canada Ltd seems to be the most reasonable process that has been developed to recover the heavy minerals from the Alberta oil sands tailings. The process produced a saleable zircon concentrate and a saleable ilmenite concentrate and should serve as the basis for further metallurgical testwork. However, the rutile concentrate produced from this process was far below the saleable grade.

The objective of the current research project is to characterize the rutile concentrate produced by Lakefield Research Ltd and Syncrude Canada Ltd. and to examine the possibilities and limitations of upgrading it to a marketable high-grade. The scope of the project was limited to physical mineral processing techniques to achieve the upgrading since a hydrometallurgical process is not desirable.

The rutile concentrate produced by Lakefield Research Ltd. and Syncrude Ltd is referred to as “LR Rutile” in this thesis.

4 EXPERIMENTAL

4.1 Sample Characterization

Approximately two kilograms of a rutile concentrate produced by Syncrude Canada Ltd. and Lakefield Research Ltd. were received from Syncrude Edmonton Research Center on December 3, 1999. The sample was designated "LR Rutile" and was characterized by particle size, magnetic susceptibility, chemical composition and petrographical analyses.

The size distribution of the LR Rutile sample was determined by dry sieve analysis on a Ro-tap® machine. Sub-samples of the LR Rutile were sent to International Plasma Laboratories Ltd., Vancouver BC, for Whole Rock and multi-element ICP analyses, and to ACME Analytical Laboratories, also located in Vancouver, BC, for analysis on radioactive elements (thorium and uranium). Sub-samples of the LR Rutile were also sent to both Harris Exploration Services, Inc. Vancouver, BC and to Professor Jeremy Richards in the Department of Earth & Atmospheric Sciences at the University of Alberta, for petrographical analyses.

4.2 Magnetic Susceptibility Measurement

The magnetic susceptibility of the LR Rutile was measured in-house with a Frantz Isodynamic Separator. The transverse slope (θ) of the separator was set at 14.5° . It is known that the magnetic susceptibility of a material, χ , was related to the transverse slope θ and the electric current I by (McAndrew, 1957):

$$\chi = \frac{\sin \theta}{KI^2} \quad (4.1)$$

where K is a constant, and was found to be 3.15×10^6 by calibrating the separator using substances with known magnetic susceptibility, i.e., ferrous ammonium sulfate with $\chi = 32.4 \times 10^{-6} \text{ m}^3/\text{kg}$ and copper sulfate with $\chi = 5.88 \times 10^{-6} \text{ m}^3/\text{kg}$.

4.3 Magnetic Separation

Both low intensity and high intensity magnetic separation tests were conducted to separate the iron-bearing minerals from the LR Rutile. Low intensity dry magnetic separation tests were conducted using a Carpco Dry Roll Magnetic Separator. The magnetic field intensity of this separator could be adjusted by varying the electric current from 0 to 3 amperes, and the corresponding magnetic field intensity varied from 0 to 6700 Gauss.

High intensity dry magnetic separation was performed in a Frantz Isodynamic Separator. The maximum electric current in this separator was 1.9 amperes, which corresponded to a magnetic field strength of 12,000 Gauss.

4.4 Electrostatic Separation

Electrostatic separation tests were conducted using a Carpco Dry Roll Electrostatic Separator. In these tests the DC voltage applied across the electrodes was set between 30 and 40 kV. The LR Rutile sample was fed at a very low feed rate to ensure a monolayer of particles on the separation drum.

4.5 Froth Flotation

Froth flotation was used to remove the small amount of quartz from the LR Rutile. Due to the small amount of LR Rutile sample available, some preliminary flotation tests were conducted with purchased high purity minerals. These tests were conducted in a modified Hallimond flotation tube. Separation tests of the LR Rutile were also required to be conducted on a small scale, for this purpose, a small laboratory suspension flotation machine was constructed in our lab.

4.5.1 *Flotation of Quartz and Rutile Single Minerals*

High purity quartz mineral for flotation testwork was purchased from Ward's Scientific Establishment, Inc. and originated from Hot Springs, Arkansas, USA. Lumps of the quartz crystals were crushed in laboratory jaw crushers and ground in a stainless steel laboratory pulverizer. The ground sample was then screened into -105 + 74 μm and -74 μm size fractions. The -105 + 74 μm size fraction was used in the flotation testwork. Before use, the size fraction was leached in a 0.1 M HCl solution for 24 hours and then washed until no chloride ions could be detected. The washed sample was then filtered, dried and stored.

The rutile sample was a powdered concentrate produced by the Zaoyang Rutile Mine in China. The concentrate assayed over 93% TiO_2 which was all in the form of rutile. The concentrate was produced through gravity and magnetic separation techniques. The sample was screened and the -105 + 74 μm size fraction was used in the single mineral flotation testwork and the -74 + 38 μm size fraction was used in the artificial mixture testwork. The -38 μm size fraction was used in zeta potential and polysaccharide adsorption measurements.

The cationic collector used in the single mineral and artificial mineral mixture flotation testwork was dodecylamine, which was purchased from Aldrich Chemicals and used without purification. The stock solution of the dodecylamine was prepared by blending in a stoichiometric amount of acetic acid and then diluting to the mark on the volumetric flask.

A commercial cationic collector, Armeen 18D[®], was kindly provided by Akzo Noble and was used without purification. The stock solution of Armeen 18D[®] was prepared by adding a stoichiometric amount of hydrochloric acid to solubilize the amine and then diluting to the mark on a volumetric flask. When preparing the sample, the Armeen 18D[®] was assumed to be pure aliphatic amines with 18 carbon atoms.

Various polysaccharides were purchased from several sources and were tested as selective flotation depressants for the titanium minerals. Table 8 lists the names and sources of the polysaccharides used in the testwork.

The polysaccharide stock solutions were prepared in several different ways. CMC solutions were prepared by sprinkling the dry powder onto a stirring vortex followed by gentle stirring for 30 minutes. Dextrin and starch were prepared by making a paste with cold water, then dissolving with boiling water. It was observed that starch solutions prepared in this way still contained un-dissolved precipitates. In later stages of the testwork, 0.5 N sodium hydroxide (20 g/L) solutions were used to fully digest the starch.

Table 8 Polysaccharides used in the testwork

Reagent	Supplier
CMC (carboxymethyl cellulose)	Polysciences Inc.
CMS (carboxymethyl starch)	Charles Tennant & Co.
Guar Gum	Polysciences Inc.
Citric acid	Fisher Scientific
Corn starch	Sigma Chemicals
Potato Dextrin	Sigma Chemicals
Potato starch	Sigma Chemicals
Rice starch	Sigma Chemicals
Unmodified Wheat starch	Sigma Chemicals

The flotation testwork was conducted in a flotation tube that was substantially modified from the Hallimond tube. The tube was made up of two pieces. The bottom piece is similar to the base of a P/S flotation cell that had a flat sintered glass frit, so that a magnetic stir bar could be used to agitate the pulp. The top part is a straight column with a side-collecting chamber joined by a narrow throat. Only the mineral particles that attached to the gas bubbles can pass the throat and be collected as a concentrate. This minimizes mechanical entrainment.

In a typical test of the single minerals, 2 grams of the mineral sample was conditioned in a 250-ml beaker with 110 ml of solution. The pH was adjusted to the desired value with HCl or NaOH. A selected depressant was added (if used) and conditioned for 5 minutes,

followed by the addition of dodecylamine acetate and three more minutes of conditioning. The conditioned pulp was then transferred to the flotation tube and floated for five minutes with 10 ml/minute of N₂ gas. The concentrate and tailings were filtered, dried and weighed to calculate the flotation recovery.

After establishing the flotation responses of the quartz and rutile single minerals, artificial mixtures of quartz and rutile, using a 1:1 weight ratio (1 g -74 + 38 μm rutile and 1 g -105 + 74 μm quartz) were blended and floated using the established conditions for the Modified Hallimond flotation tube. The concentrate and tails were each wet screened on a 200-mesh (74 μm) sieve. The +200 mesh (+74 μm) material was quartz and the -200 mesh (-74 μm) material was rutile. Each flotation test generated four screen products. The four products were filtered, dried and weighed to calculate the flotation recovery of quartz and rutile and the concentrate grade.

4.5.2 *LR Rutile Flotation*

The flotation tube was ideal for fundamental investigations to study the hydrophobicity of minerals. But due to the inadequate agitation and the absence of a frother in the tube, it was not a good representation of the mechanical flotation machines. In order to make the tests more representative of a mechanical flotation machine, a miniature suspension-cell flotation machine was constructed and used in the remainder of the testwork. The machine consisted of a mechanical stirrer and a specially designed flotation cell. By changing the propeller, different sizes of flotation cells could be fitted ranging from 20-ml to 250-ml. A 40-ml cell was used in this testwork. The cells were constructed out of Plexiglas and were designed in such a way that the insertion of a baffle plate resulted in the formation of a quiescent froth layer that could be scraped off. Without the baffle plate the pulp could only be agitated which served the purpose of conditioning. The procedure utilized for this testing was the same as discussed above except that 4 grams of the LR Rutile (after a magnetic separation) was used and all the conditioning took place in the suspension cell and a frother was used with a conditioning time of 2 minutes before flotation. Since the cell volume was 40-ml rather than 115-ml, the solid/liquid ratio was

about 3 times higher than in the flotation tube testing. The agitation speed of the impeller was fixed at 1800 rpm.

4.5.2.1 Scaling up Suspension-Cell Flotation Machine

The suspension-cell flotation machine used in the LR Rutile flotation testwork provided a good approximation of the conditions that are necessary in commercial flotation machines. The flotation conditions may change when further testwork in a larger bench scale Denver flotation cell could be conducted. Conditions such as pulp density, reagent additions, flow characteristics and agitation intensity would have to be tested and further optimized before larger scale testwork could begin. The reagent concentrations were much higher in the suspension-cell than those required for the fundamental investigations in the modified Hallimond tube to achieve the same results and are expected to need further optimization when the process is scaled up.

4.6 Zeta Potential Measurements

Zeta potential measurements were conducted in a ZetaPlus zeta potential meter manufactured by Brookhaven Instruments Corporation. In this instrument, the electrokinetic mobility of the dispersed mineral particles was measured with the laser Doppler technique and the zeta potential was calculated from the mobility using the Smoluchowski equation.

High purity quartz and rutile mineral samples were prepared by further grinding the - 400 mesh (- 38 μm) sample in a corundum mortar and pestle. One gram of the ground mineral sample was dispersed into 1 liter of a 10^{-2} M KNO_3 solution. For each measurement, a 50 ml aliquot of the mineral suspension was taken and adjusted to the desired pH with either hydrochloric acid or sodium hydroxide. When dodecylamine acetate was used, the collector was added and conditioned for 3 minutes. In some measurements wheat starch was also used and was conditioned for 5 minutes. A small volume of the suspension was then transferred into the sample cuvet of the ZetaPlus and

allowed to equilibrate to 25 °C inside the instrument. Ten measurements were taken for each sample and the average was reported as the zeta potential value for the sample.

4.7 Adsorption Measurements

The adsorption density of unmodified wheat starch on both quartz and rutile mineral samples was determined as a function of both pH and residual concentration of the wheat starch. The polysaccharide concentrations were determined by the phenol-sulfuric acid method as described by Dubois et al (1956). For the adsorption test, the - 400 mesh (- 38µm) mineral samples of quartz and rutile were further ground in a corundum mortar and pestle, and the wheat starch solution was prepared by digesting 0.1 g in 0.5 N NaOH solution for 30 minutes. The solution was then transferred to a one-liter volumetric flask and diluted to the mark. In the adsorption test, one gram of the mineral sample was mixed with 25 ml of a 10^{-2} M NaCl solution. An aliquot of 25 ml of the polysaccharide solution was taken, the pH adjusted with either hydrochloric acid or sodium hydroxide to the desired value and then mixed with the 25 ml mineral suspension. The 50 ml suspension was then placed in a Jeio Tech SI-600 Shaking Incubator, and agitated for 60 minutes at 200 rpm and 25°C. Afterwards, the solution pH was checked and recorded. A sub-sample of the mineral suspension was taken and centrifuged in a Sorvall Instruments GLC-4 General Laboratory Centrifuge at 2200 rpm for 4 minutes, and the residual concentration of wheat starch in the supernatant was determined. For this, 4 ml of the centrifuged solution was taken and placed in a test tube. 1.5 ml of a 5% phenol solution was added to the test tube, followed by 10 ml of concentrated sulfuric acid that was injected quickly along the wall of the test tube so that there was adequate mixing inside the tube. The phenol-sulfuric acid solution was allowed to cool for 10 minutes in air, then placed in a water bath and equilibrated at 25°C for 15 minutes. The absorbance of the solution was measured at 490 nm against distilled water and a blank standard of the phenol-sulfuric acid solution with a Jenway Model 6405 UV-VIS spectrophotometer. Polysaccharide concentrations were determined using a calibration curve. The difference between the original and residual polysaccharide concentration was taken as the amount adsorbed by the mineral. Appendix I shows an example of this calculation.

4.8 SEM/EDX Analysis

Scanning electron microscopic measurements were performed in a Hitachi S-2700 scanning electron microscope with energy dispersive x-ray analysis capabilities by Tina Barker. The rutile concentrate samples from the flotation testwork were coated with carbon to make them electrically conductive. An accelerating voltage of 20.0 kV was used to acquire both back-scattered electron images and secondary back-scattered electron images. EDX analysis was used for semiquantitative analysis to identify elemental composition of localized areas on the top layer of the rutile particle surfaces.

5 RESULTS AND DISCUSSION

5.1 Characterization of the LR Rutile

5.1.1 Particle Size

The size distribution of the LR Rutile sample was determined by dry sieve analysis on a Ro-tap® machine. It was found that the 80% passing size of the concentrate was 145 µm, and over half of the particles were between 105 and 149 µm.

5.1.2 Chemical Analysis

Table 9 lists the results of whole rock analysis together with the concentrations of radioactive elements. The contents of TiO₂, Fe₂O₃ and SiO₂ were in good agreement with the reported assays of Lakefield Research Ltd. The major contaminating elements in the LR Rutile appeared to be Fe₂O₃, SiO₂, and Al₂O₃. The LR Rutile was also found to contain 474.3 ppm Th and 88.8 ppm U. These contaminants all exceeded the maximum limit set for marketable rutile concentrate (see Table 4). Further upgrading has to focus on the removal of these impurities.

Table 9 Whole rock analysis of the LR Rutile

Compound	Weight %
Al ₂ O ₃	1.03
BaO	0.29
CaO	0.27
Fe ₂ O ₃	18.71
K ₂ O	0.18
MgO	0.32
MnO	0.60
Na ₂ O	0.27
P ₂ O ₅	0.43
SiO ₂	1.94
TiO ₂	75.54
U + Th, ppm	563.1
Loss on ignition	----
Total	99.58

5.1.3 Petrographical Analyses

Harris Exploration Services' report indicated that the majority of the grains in the LR Rutile were probably ilmenite and leucoxene, and only a minor proportion of the grains were identified as rutile, or its polymorph, anatase. Generally, the amount of rutile and anatase was small, estimated at about 5% and 12%, respectively. Zircon, monazite, and apatite were recognizable trace accessories. Figure 16 shows a typical photomicrograph of the grain-mounted LR Rutile sample.

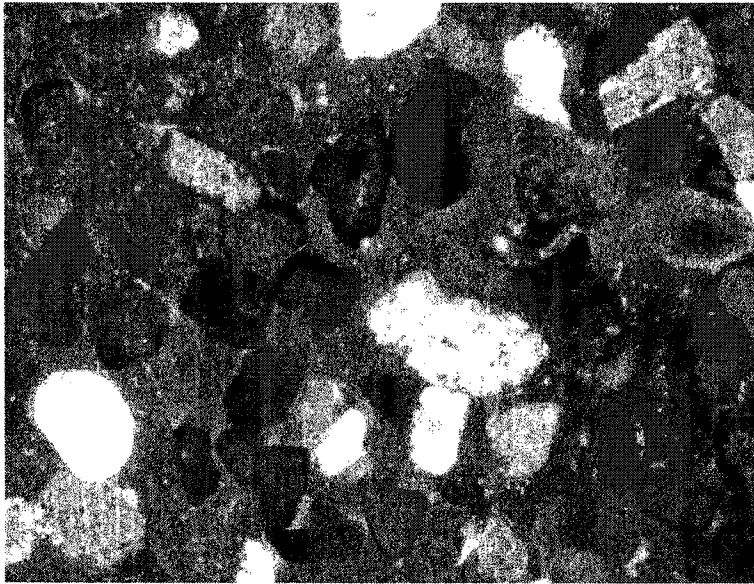


Figure 16 A typical field of LR Rutile under cross-polarized light.

The rutile grains are translucent, whitish to light brown in appearance. Grains that appear white to red translucent are probably anatase and/or leucoxene. The remaining grains show weak anisotropism with colors ranging from dark tan to near black – these are probably ilmenite.

An x-ray diffraction (XRD) analysis was conducted by Harris Exploration Services, Inc. The XRD spectrum showed the peaks due to rutile. The major peaks due to ilmenite

were absent. Although the sensitivity of ilmenite in XRD analysis is inherently low, the absence of ilmenite peaks indicated that the ilmenite was present mainly as the altered non-crystalline forms such as leucoxene.

The XRD spectrum also contained 4 relatively minor peaks at $d = 3.4219 \text{ \AA}$, 3.3295 \AA , 2.2938 \AA and 1.8316 \AA that could not be identified. These 4 peaks did not fit the patterns of any of the Fe and Ti-Fe oxide minerals.

Similarly, Professor Richards's analysis identified rutile in various forms, ilmenite in various forms, as well as zircon, monazite, staurolite and chromite. He observed that pure, crystalline rutile (and anatase) was not abundant, probably accounting for less than 10% of the entire sample. Most of the rutile (anatase) appeared to be impure or polycrystalline grains with inclusions of silicates and other oxides. The majority of the ilmenite was not crystalline ilmenite but present as its altered form, probably leucoxene.

Professor Richards also conducted electron microprobe analysis on the LR Rutile. This analysis again indicated that a significant amount of the rutile particles contained inclusions of other minerals. The resulting TiO_2 contents for different rutile grains were found to vary from 77% to 99%.

The results of the petrographical analyses indicate that the extent of upgrading of the LR Rutile could be limited by the complex interlocking of the rutile (anatase) with other minerals.

5.2 Upgrading of the LR Rutile by Magnetic Separation - Removal of Iron

5.2.1 Low Intensity Dry Magnetic Separation

In the first trial test, approximately 84 grams of the LR Rutile were separated using the Carpc Dry Roll Magnetic Separator at a field intensity of 2000 Gauss. The sample was split into a magnetic fraction and a non-magnetic fraction following the flowsheet shown

in Figure 17. Both fractions were analyzed for TiO_2 and Fe_2O_3 . Table 10 shows the results. As can be seen, about one quarter of the material was recovered in a non-magnetic product that assayed 85.5% TiO_2 and the grade of the non-magnetic product was 10 percent higher than the original LR Rutile.

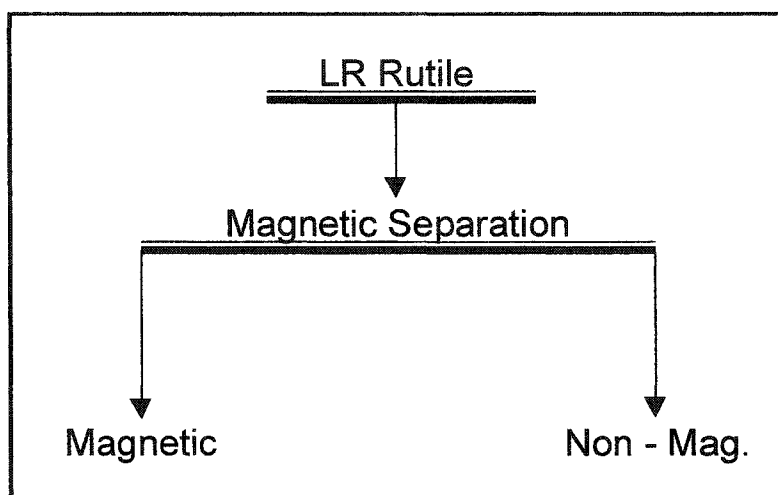


Figure 17 Low Intensity Magnetic Separation

Table 10 Magnetic separation of LR Rutile at 2000 Gauss

Products	Weight		Assay (%)		Distribution (%)	
	(g)	(%)	TiO_2	Fe_2O_3	TiO_2	Fe_2O_3
Non-mag fraction	20.5	24.4	85.5	8.83	26.7	12.1
Magnetic fraction	63.5	75.6	75.6	20.7	73.3	87.9
Total	84.0	100.0	78.0	17.8	100.0	100.0
Measured			75.5	18.7		

When the non-magnetic product was passed through the separator again, further removal of the Fe-bearing minerals was possible. Figure 18 shows the flowsheet used for the separation and Table 11 shows the results of a similar magnetic separation test that was conducted at 6000 Gauss. After the initial stage of separation, the non-magnetic product was cleaned twice in order to remove as much of the iron bearing minerals as possible by the technique.

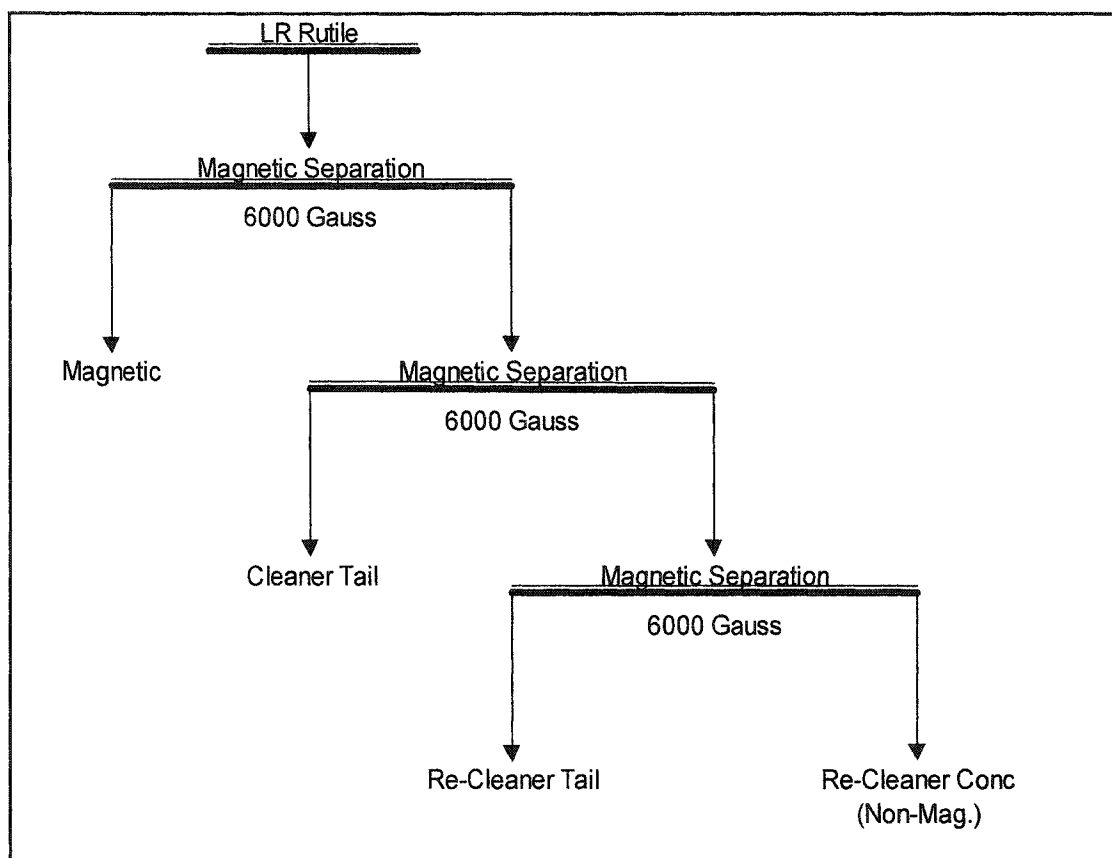


Figure 18 Low Intensity Magnetic Separation with Cleaning

Table 11 Magnetic separation of LR Rutile at 6000 Gauss, with cleaning

Products	Weight		Assay (%)		Distribution (%)	
	(g)	(%)	TiO ₂	Fe ₂ O ₃	TiO ₂	Fe ₂ O ₃
Re-cleaner concentrate (rutile)	7.0	5.7	89.2	2.30	6.5	0.8
Re-cleaner tail	3.7	3.0	85.6	7.29	3.3	1.3
Cleaner concentrate (Non-mag)	10.7	8.7	88.0	4.03	9.8	2.1
Cleaner tail	14.1	11.4	81.0	13.8	11.8	9.3
Non-mag fraction	24.7	20.1	84.0	9.56	21.6	11.4
Magnetic fraction	98.5	79.9	76.6	18.7	78.4	88.6
Total	123.2	100.0	78.1	16.9	100.0	100.0
Measured			75.5	18.7		

Similar separation results were obtained whether the magnetic field intensity was set at 2000 Gauss or 6000 Gauss. The non-magnetic product assayed 84% - 85% TiO₂ and the

weight recovered into the non-magnetic fraction was about 20% to 24%. After two stages of cleaning, the TiO₂ content was only slightly upgraded from 84% to 89%. However, this was accompanied by severe losses of the weight - total TiO₂ recovery dropped from 26.7% to 6.5%.

After the magnetic separation, the content of radioactive elements in the non-magnetic product was also significantly reduced. The re-cleaner concentrate (rutile) shown in Table 11 was found to contain 96.6 ppm Th and 83.3 ppm U (the initial LR Rutile contained 474.3 ppm Th and 88.8 ppm U). This indicates that the radioactive elements are mostly associated with the magnetic minerals, possibly monazite.

5.2.2 High Intensity Dry Magnetic Separation

High intensity dry magnetic separation using a Franz Isodynamic separator showed similar results as the low intensity magnetic separation testwork. Table 12 shows the test results after one pass in a Frantz separator at 12000 Gauss and Table 13 shows complete whole rock analyses of the LR Rutile (feed) as well as the magnetic and non-magnetic fractions produced from this test. The data contained in Table 13 shows that while the magnetic separation significantly lowered the Fe₂O₃ content in the LR Rutile (from 18.7% to 0.77%), there was a slight increase in the Al₂O₃ content (from 1.03% to 1.59%) and a significant increase in the SiO₂ content (from 1.94% to 6.01%) in the non-magnetic product (i.e., the rutile concentrate). The TiO₂ grade was determined to be 86.4% with a recovery of 18.0%. There is a tradeoff between the recovery and grade of the rutile concentrate produced by magnetic separation.

Table 12 Magnetic separation of LR Rutile at 12000 Gauss

Products	Weight		Assay (%)		Distribution (%)	
	(g)	(%)	TiO ₂	Fe ₂ O ₃	TiO ₂	Fe ₂ O ₃
Non-mag fraction (rutile)	173.2	14.9	86.4	0.77	18.0	0.6
Magnetic fraction	993.3	85.1	68.7	21.1	82.0	99.4
Total	1166.5	100.0	71.3	18.1	100.0	100.0
Measured			75.5	18.7		

While there was still room to optimize the magnetic separation conditions to further lower the Fe₂O₃ content in the rutile concentrate, it seemed that the high SiO₂ and Al₂O₃ content needed to be dealt with first. The subsequent research work was therefore focused on the removal of the contaminating silica and aluminosilicate minerals. The non-magnetic fraction shown in Table 12 was used in the subsequent flotation tests to remove the siliceous minerals.

Table 13. Whole rock analyses of the magnetic separation products. Values expressed as weight % unless otherwise stated

Compound	LR Rutile	Non-magnetic Fraction	Magnetic Fraction
Al ₂ O ₃	1.03	1.59	1.20
BaO	0.29	0.15	0.33
CaO	0.27	0.22	0.21
Fe ₂ O ₃	18.71	0.77	21.12
K ₂ O	0.18	0.28	0.40
MgO	0.32	0.12	0.37
MnO	0.60	0.02	0.71
Na ₂ O	0.27	0.36	0.39
P ₂ O ₅	0.43	0.16	0.44
SiO ₂	1.94	6.01	0.86
TiO ₂	75.54	86.42	68.69
ZrO ₂		1.35	0.28
U+Th, ppm	563.1	108	456
Loss on ignition	-	2.69	2.05
Total	99.58	98.79	96.77

5.3 Upgrading of the LR Rutile by Electrostatic Separation-Removal of Siliceous Minerals

In the upgrading of heavy mineral sands, electrostatic separation is typically used to remove non-conducting quartz from conducting rutile. This separation is based on the differences between the electrical conductivities of the minerals. In this series of tests the

non-conducting quartz is pinned to the separation drum while the rutile particles are thrown from the drum. Several trial tests were conducted on the non-magnetic fraction of the LR Rutile. The products were not assayed but examined under a stereomicroscope. The results of the electrostatic separation testwork did not yield satisfactory results primarily due to the severe mechanical entrainment during the separation. Rutile, the major constituent in the sample, was being thrown from the drum and as a result it formed a conducting stream with a high flowrate. This resulted in significant amounts of non-conducting quartz to be mechanically carried with the conducting rutile stream.

5.4 Upgrading of the LR Rutile by Froth Flotation - Removal of Siliceous Minerals

5.4.1 Quartz Single Mineral Flotation

The flotation response of quartz single mineral using dodecylamine acetate (DDAA) as the collector was determined as a function of both pH and collector concentration. The results are presented in Figure 19. From this figure, it can be seen that quartz can be effectively floated with DDAA between pH 5 and 12 and at a concentration above 4.4×10^{-5} mol/liter. When the solution pH was below 2 or above 12, quartz could not be floated by DDAA. When the DDAA concentration was at or below 8.7×10^{-6} mole/liter, quartz flotation depended on pH and increased with increasing pH with a maximum flotation around pH 10 to 11.

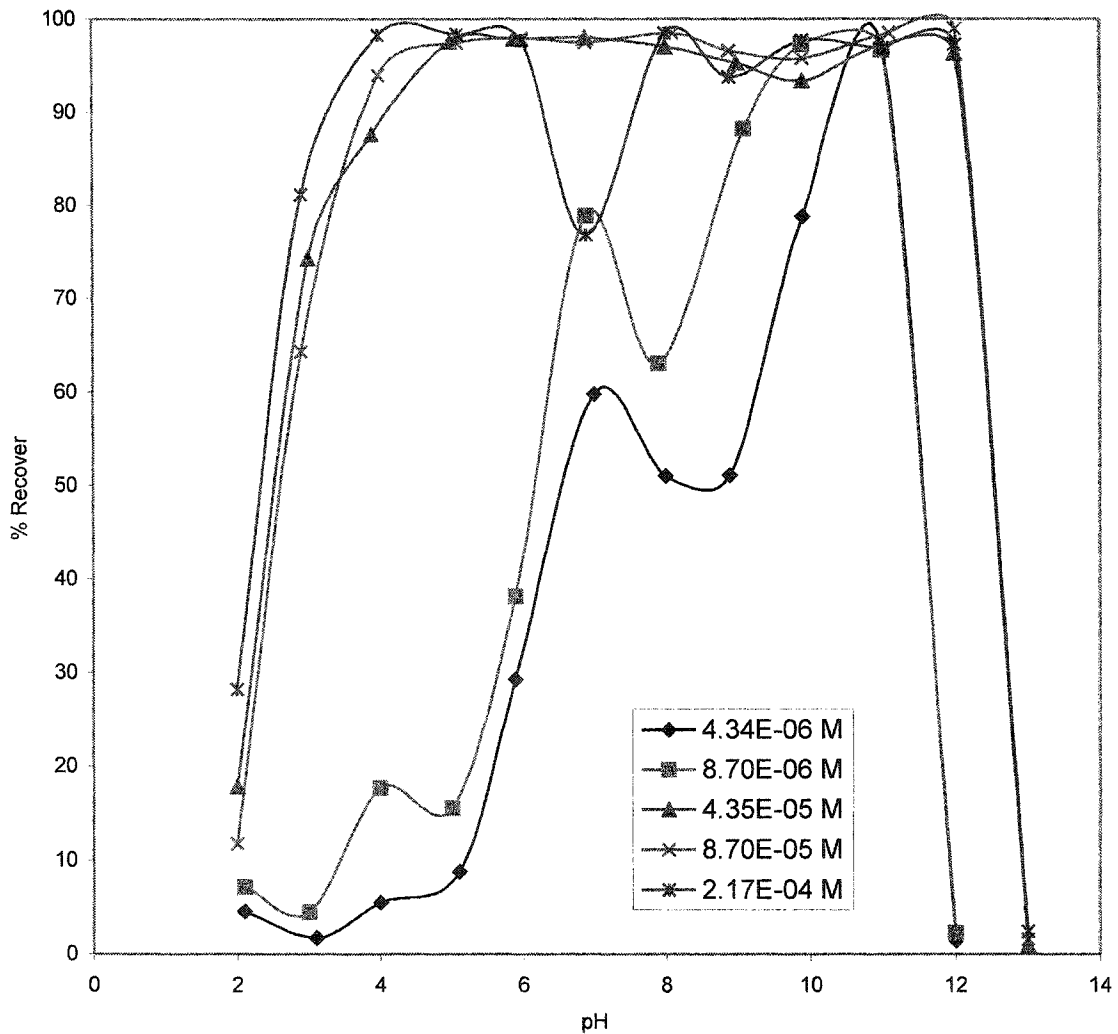


Figure 19 Flotation recovery of quartz single minerals

These results indicate that quartz flotation is possible over a wide range of pH values with DDAA. A collector concentration of 10^{-4} mol/liter was chosen for subsequent flotation testwork. It is assumed that this concentration would provide a good basis for maximizing quartz flotation without adding a considerable dose into the system. The optimum DDAA concentration will depend on the conditions necessary to depress rutile flotation.

5.4.2 *Rutile Single Mineral Flotation*

Rutile is completely floated by DDAA in the absence of a depressant. A suitable depressant had to be found that selectively allowed for quartz flotation while significantly depressing rutile. Of the seven different polysaccharides tested from Table 8, only potato starch, rice starch and unmodified wheat starch were potential selective depressants for rutile. Figure 20 shows the effect of these depressants on both quartz and rutile single mineral flotation using a DDAA concentration of 10^{-4} mol/liter. From this figure it can be seen that there exists windows of separation between pH 7 to 10 where it is possible to float quartz from rutile without losing a significant amount of rutile.

From Figure 20, it can be seen that quartz flotation is limited at pH values below 7. Compared to Figure 18, this is due to the presence of the polysaccharide depressants, which seemed to depress quartz flotation at lower pH values.

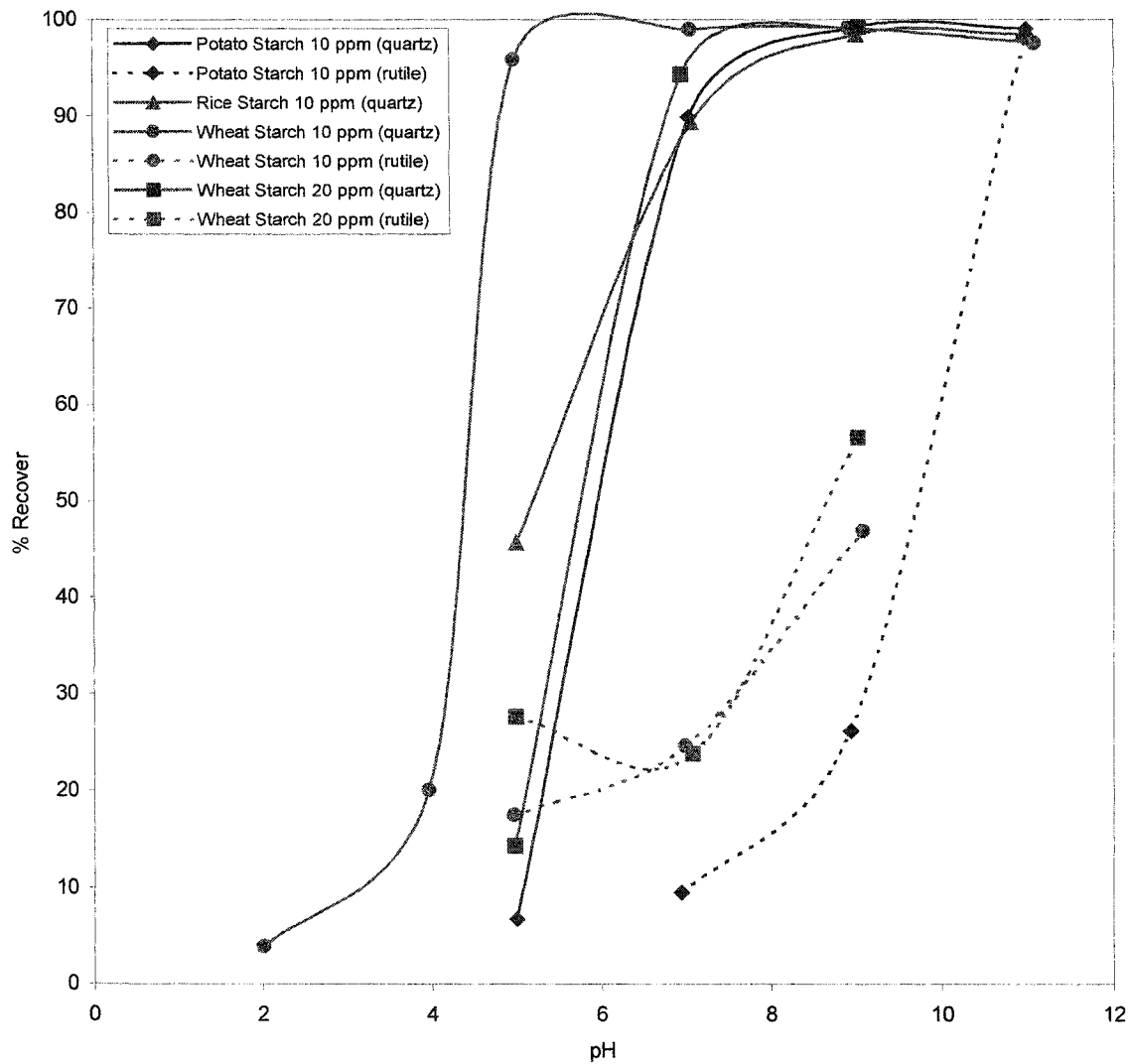


Figure 20 Flotation Recovery of Quartz and Rutile Single Minerals with Selected Depressants

5.4.3 Flotation of Artificial Mineral Mixtures

After establishing the flotation responses of quartz and rutile single minerals, artificial mixtures of quartz and rutile were blended and floated using the established conditions in the flotation tube. The DDAA concentration was fixed at 10^{-4} mol/liter and the depressant concentration was fixed at 10 ppm. The results can be seen in Figure 21.

Figure 21 indicates that there are still windows of separation available using either potato starch or unmodified wheat starch, although the effective flotation pH range increased to

between 10 and 12 for potato starch and between 8 and 12 for wheat starch. This increase from the single mineral experiments indicates that by blending the minerals together interactions between them have occurred. These interactions affected the flotation conditions and moved the windows of separation to higher pH values. Unmodified wheat starch had a wider pH range where a separation was possible. As a result, the unmodified wheat starch was chosen as a suitable depressant for rutile.

It was realized that flotation testing in a modified Hallimond tube only represented theoretical conditions. Frothers and intensive agitation, which are typical in commercial flotation machines, were not used in the flotation tube testing. To represent more closely the commercial flotation machines, a suspension-cell flotation machine was constructed and used in subsequent tests on artificial mineral mixtures. It was found that both the flotation tube testing and the suspension-cell flotation machine testing showed similar separation results, except that the required reagent concentrations (both the collector and the depressant) were much higher in the suspension-cell. This is probably due to a combination of the high solid/liquid ratio and the high agitation intensity.

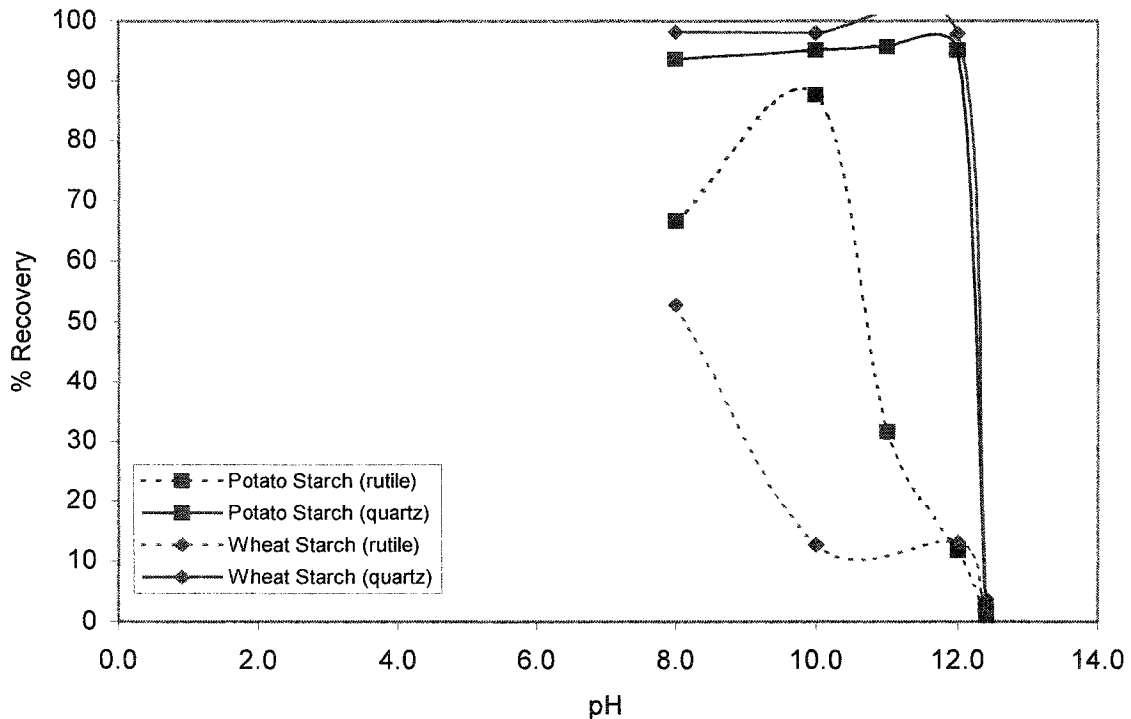


Figure 21 Flotation Recovery of Quartz and Rutile Artificial Mixtures with Selected Depressants. The tests were conducted in a flotation tube.

Figure 22 shows the effect of the concentration of unmodified wheat starch on the separation of artificial mixtures of quartz and rutile at pH 11 and a DDAA concentration of 2×10^{-4} mol/liter. It can be seen that as the concentration of the wheat starch is increased to 20 ppm, rutile recovery to the froth product decreases rapidly from about 90% to below 10%. Quartz recovery only slightly decreases as the wheat starch concentration is increased. The results indicate that, at conditions close to commercial flotation machines, wheat starch is still an effective selective depressant for quartz/rutile separation.

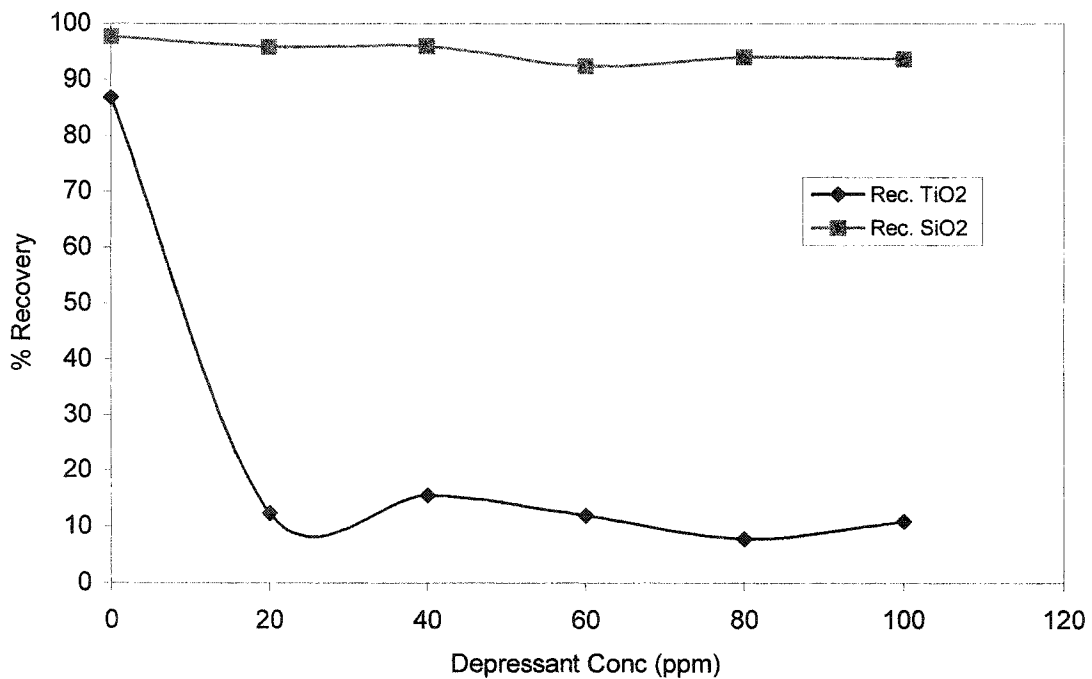


Figure 22 Flotation Recovery of Quartz and Rutile Artificial Mixtures as a Function of Wheat Starch Concentration. The flotation tests were conducted in a suspension-cell flotation machine.

5.4.4 Mechanisms of the Flotation Separation of Quartz from Rutile

The results presented in the previous sections indicate that using a cationic collector and at a pulp pH between 8 and 12, quartz can be floated from artificial quartz/rutile mixtures leaving rutile in the flotation cell. This occurs as long as a certain concentration of wheat starch is present in the flotation pulp. It is believed that this process would be best suited to remove minor amounts of contaminating quartz from rutile concentrates.

To understand why the separation between quartz and rutile was achieved by using the flotation procedures, the zeta potentials of the minerals and adsorption densities of the wheat starch on the minerals were determined.

5.4.4.1 Zeta Potential Measurements

Figure 23 shows the zeta potentials of quartz and rutile single minerals dispersed in 10^{-2} M KNO_3 . As can be seen, at the same pH, the rutile surface showed a more positive charge. The isoelectric points for quartz lie between pH 2.2 and 2.8. For rutile, the iep lie between pH 5.1 and 6.6. The reported values in the literature for quartz and rutile are 1.3 to 3.7 (Manser, 1975) and 4.0 to 7.0 (Leja, 1982), respectively. The zeta potential values determined in the measurements fall between the values reported in the literature. It is easy to see that, since a cationic collector was used in the flotation, at any pH quartz would interact more strongly with the collector since its surface is more negatively charged.

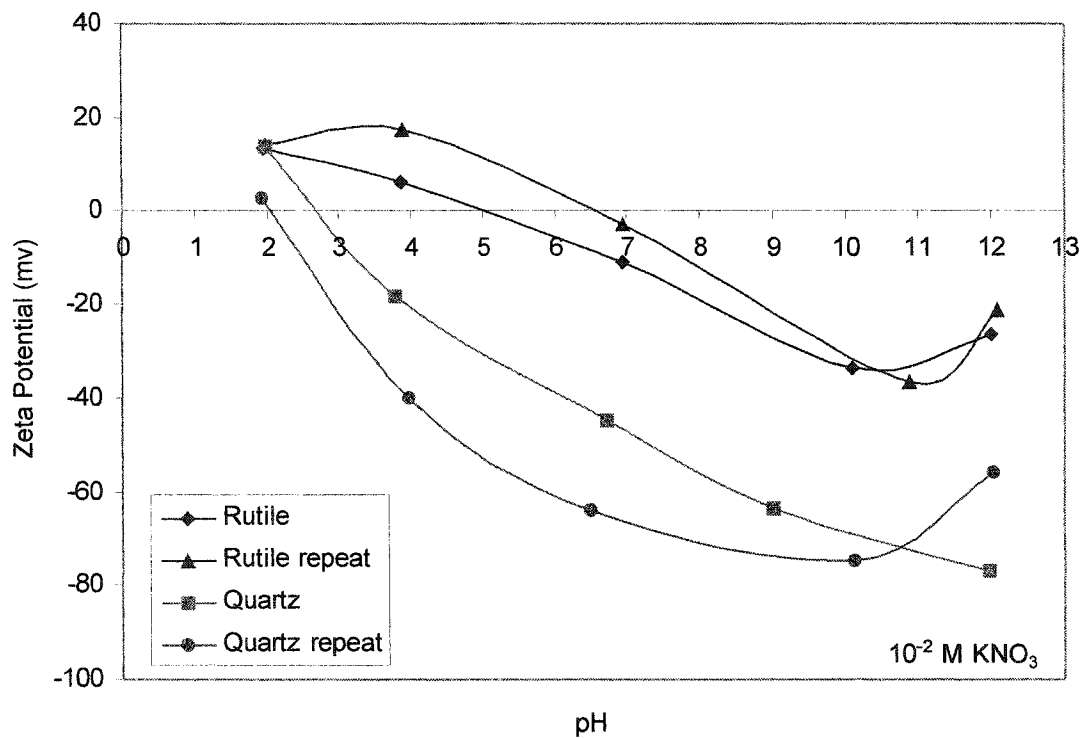


Figure 23 Zeta Potential Measurements of Quartz and Rutile

Next, the effects of the dodecylamine acetate on the zeta potentials of the minerals were determined and the results are shown in Figure 24. Two dodecylamine acetate concentrations were used, i.e., 10^{-4} M and 10^{-6} M. As can be seen, the presence of the dodecylamine acetate moved the zeta potential of both quartz and rutile to more positive values, which resulted in an increase in the iep of both minerals. For quartz, the iep moved to between 2.9 and 3.1, and for rutile, the iep moved to between 7.5 and 7.6. This indicates that at any given pH, the mineral surface is more positively charged in the presence of the collector. Obviously, this is due to the adsorption of the collector cations, which increased the zeta potential of the minerals.

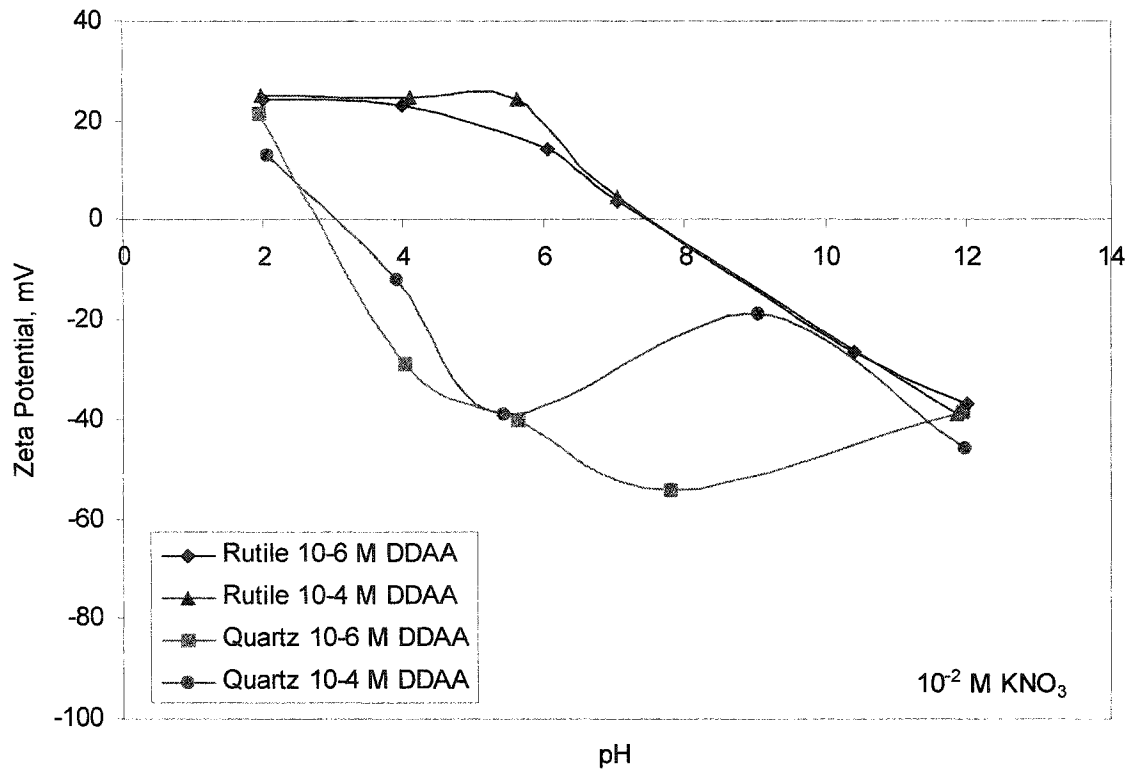


Figure 24 Effect of DDAA on Zeta Potential for Quartz and Rutile

The addition of 10 ppm wheat starch resulted in a decrease in the magnitude (absolute values) of the zeta potentials on both quartz and rutile (Figure 25). The decrease is more pronounced at acidic pH. Also, when the two minerals are compared, the decrease in magnitude is more pronounced for rutile. This is caused by adsorption of the wheat starch. Obviously, as the large starch molecules are adsorbed on the mineral surfaces, they stretched the “shear plane” further away from the mineral surface, thus causing a drop in the zeta potential since the potential across the interface decays exponentially. The further away the shear plane, the lower the absolute value of the zeta potentials. The effect of a combination of 10 ppm digested unmodified wheat starch and 10^{-6} M dodecylamine acetate on the zeta potential was also measured and the results presented in Figure 26. Again, there was a significant drop in the magnitude of the zeta potentials on both quartz and rutile.

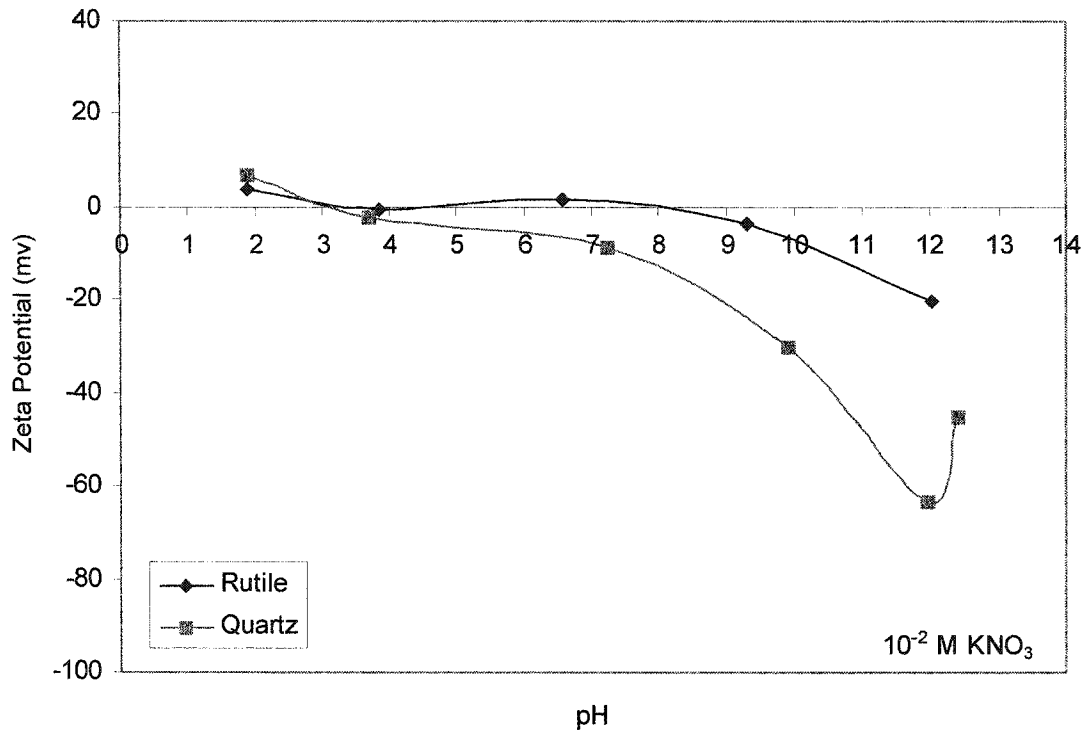


Figure 25 Effect of 10 ppm Wheat Starch on Zeta Potential for Quartz and Rutile

In the pH range of interest for flotation, i.e., between pH 10 and 12, the zeta potential measurements coincide with the results obtained in the flotation testwork. In this pH range, quartz has a much more negatively charged surface than rutile. This is the case even when starch is present in the solution. In the presence of starch, both quartz and rutile have a surface charge that is near zero up to pH 10; thus no cationic collector can electrostatically interact with the mineral surface. Without a cationic collector, quartz cannot be separated from rutile. As the pH becomes more alkaline, the quartz surface becomes much more negative than the surface of rutile. As the flotation results indicated, the cationic collector will have a preference to electrostatically interact with the quartz surface over rutile at reasonable collector dosages. If the dose is increased, then all the minerals will be floated.

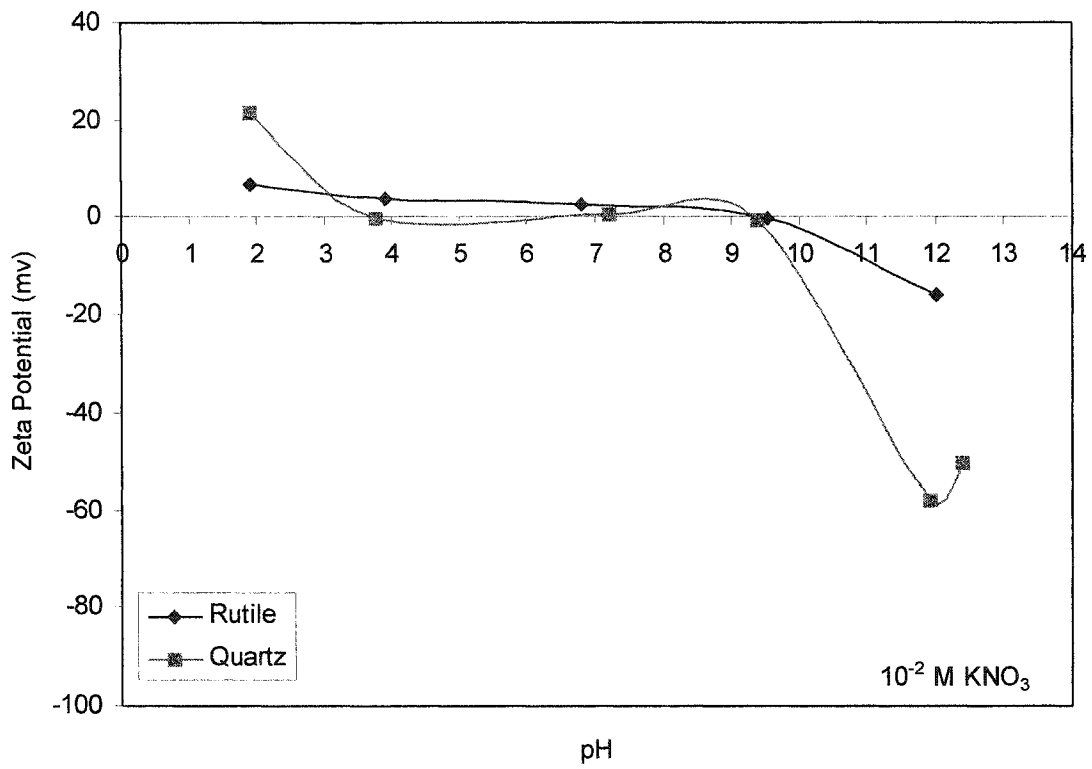


Figure 26 Effect of 10 ppm Wheat Starch and 10⁻⁶ M DDAA on the Zeta Potential for Quartz and Rutile

5.4.4.2 Adsorption Density of Starch

The adsorption density of the wheat starch on quartz and rutile was measured as a function of pH. The results were found to be fairly reproducible. Generally, the accuracy of the adsorption density was within reason and repeatable across the entire pH range of testing. The results are presented as mg of starch adsorbed per gram of mineral. Since the samples were prepared in the same manner, it is assumed that the resulting particle size is similar and since quartz and rutile minerals exhibit little porosity the adsorption mechanisms would be similar.

Figure 27 shows the adsorption of the wheat starch on rutile and quartz as a function of solution pH. As can be seen, between pH 2 and 4, both rutile and quartz strongly adsorb wheat starch. Between pH 4 and 7, the adsorption of wheat starch on quartz is consistent until pH 7.4 where a dramatic increase in the adsorption density takes place. This peak was verified by several measurements in the neutral pH range. At pH 8, the adsorption on quartz decreases steadily until pH 12.4. The adsorption of the wheat starch on rutile is generally higher than on quartz and only decreased slightly with increasing pH.

The optimum separation of quartz from rutile in the artificial flotation testwork was in the pH range between 10 and 12. This is also where the largest difference in adsorption densities occurred. This, coupled with the zeta potential measurements, explains why quartz/rutile separation could be achieved between pH 10 and 12. With the stronger adsorption of the wheat starch on rutile surfaces than quartz, rutile would be more hydrophilic than quartz. In this pH range quartz is also much more negatively charged than rutile which would enable the quartz to preferentially adsorb the cationic collector.

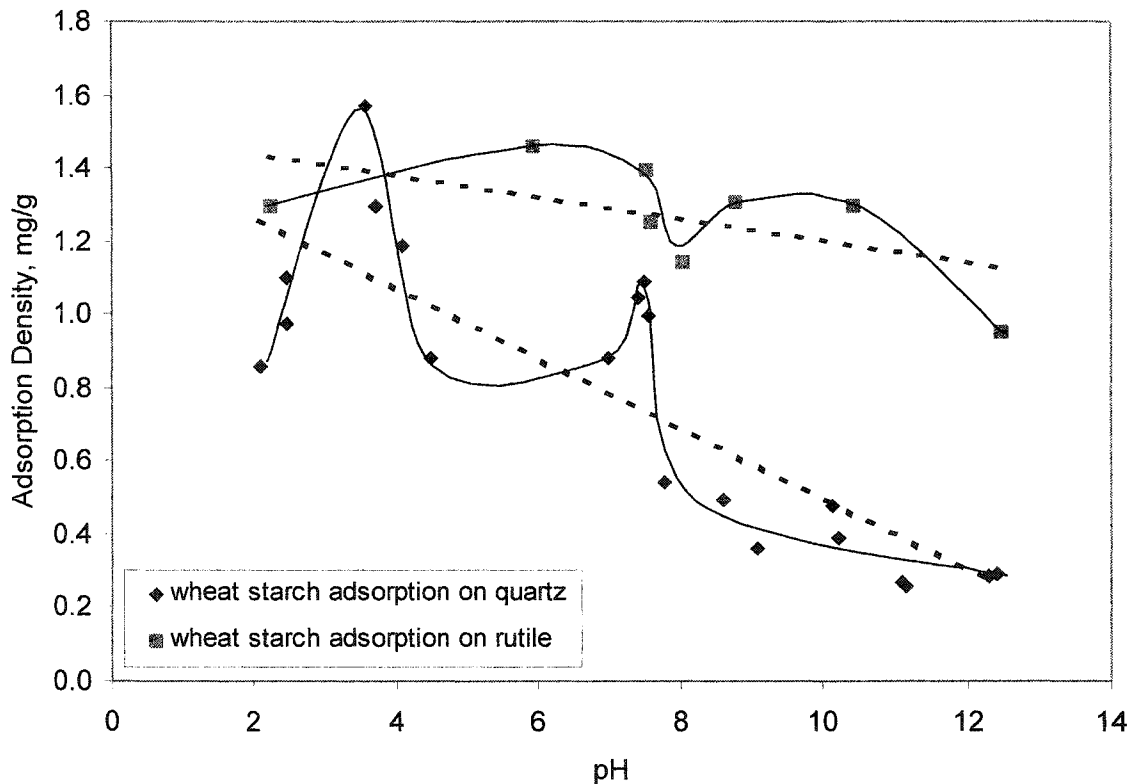


Figure 27 Adsorption Density of Wheat Starch on Quartz and Rutile

5.5 Reverse Flotation of Siliceous Minerals from the LR Rutile

Finally, the established quartz/rutile separation procedures were applied to the LR Rutile. The LR Rutile had gone through a high intensity magnetic separation so that the majority of the Fe-bearing minerals had been removed. The flotation feed was therefore the non-magnetic fraction from the LR Rutile, and was designated LRNM. This sample, which contained 86.4% TiO₂ and 6.01% SiO₂, was subjected to reverse flotation using the established conditions. The test products were examined under an optical stereomicroscope and only those products considered worthwhile were sent out for assays of TiO₂ and SiO₂. This pre-examination was possible since the siliceous minerals were mostly translucent while the rutile (anatase) grains were opaque. Whole rock analyses were also conducted on selected flotation products to determine the contaminating minerals in the final concentrate. The following variables were tested to maximize the separation:

- Concentration of the collector (dodecylamine acetate);
- The use of a commercial cationic collector Armeen[®] 18D (Akzo Noble);
- Concentration of the depressant (wheat starch);
- Flotation time;
- Pretreatment of the sample by washing with hydrochloric acid (to remove any surface contamination resulting from previous treatment in Lakefield Research's process)
- Type of frothers. Initially MIBC was used. DF250 was later tested to maintain the stability of the froth layer.

5.5.1 The Effect of Concentration of Dodecylamine Acetate (DDAA)

In this series of tests, the other flotation conditions were fixed while the concentration of the collector, dodecylamine acetate, was varied. The concentration of wheat starch (rutile depressant) was fixed at 20 ppm, pH at about 11, MIBC at 0.15 g/L and flotation time 5 minutes for each float concentrate. Table 14 shows the results.

Table 14. Effect of DDAA Concentration on the Reverse Flotation of Rutile Concentrate

Test #	Product	Sample ID	pH before flotation	Collector (mol / L)	Float time (min)	Weight		Assay, %	
						(g)	%	SiO ₂	TiO ₂
1	Feed					3.9931	100.0		
	Con 1	LRNM # 1C	11.15	4.0x10 ⁻⁴	5.0	0.1350	3.4		
	Con 2		10.44	4.0x10 ⁻⁴	5.0	0.0859	2.2		
	Tail	1 - 4C				3.7722	94.5		87.0
2	Feed					3.9870	100.0		
	Con 1	LRNM # 2C	10.91	6.0x10 ⁻⁴	5.0	0.2369	5.9		
	Con 2		9.42	6.0x10 ⁻⁴	5.0	1.5162	38.0		
	Tail	2 - 6C				2.2339	56.0		88.6
3	Feed					3.9861	100.0		
	Con 1	LRNM # 3C	11.09	8.0x10 ⁻⁴	5.0	0.3375	8.5		
	Con 2		9.48	8.0x10 ⁻⁴	5.0	1.9153	48.0		
	Tail	3 - 8C				1.7333	43.5		87.5
4	Feed					3.9783	100.0		
	Con 1	LRNM # 4C	10.96	10.0x10 ⁻⁴	5.0	0.1486	3.7		
	Con 2		8.65	10.0x10 ⁻⁴	5.0	2.9278	73.6		
	Tail	4 - 10C				0.9019	22.7		87.3

Obviously, as the concentration of the DDAA collector was increased, the weight of the flotation tails, i.e., the rutile concentrate, decreased sharply. This is accompanied without any gain in the TiO₂ grade. The concentration of DDAA was then fixed at 5x10⁻⁴ M based on the slightly better TiO₂ grade and recovery of test #2.

5.5.2 The Effect of Concentration of Rutile Depressant – Wheat Starch

In this series of tests, the DDAA concentration was fixed at 5x10⁻⁴ mol/liter, pH at about 11, MIBC at 0.15 g/L, and a flotation time of 5 minutes for each concentrate. The results are presented in Table 15.

Table 15 Effect of Wheat Starch Concentration on the Reverse Flotation of Rutile Concentrate

Test #	Sample	Sample ID	pH before flotation	Depressant	Float time (min)	Weight		Assay, %	
						(g)	%	SiO ₂	TiO ₂
5	Feed			10 mg / L		3.9906	100.0		
	Con 1	LRNM # 5D	11.23	Unmodified wheat starch	5.0	0.4803	12.0		
	Con 2		11.14		5.0	0.6698	16.8		
	Tail	5 - 1D				2.8405	71.2		89.5
6	Feed			20 mg / L		3.9956	100.0		
	Con 1	LRNM # 6D	11.20	Unmodified wheat starch	5.0	0.2677	6.7		
	Con 2		11.11		5.0	0.3204	8.0		
	Tail	6 - 2D				3.4075	85.3		88.2
7	Feed			40 mg / L		3.9946	100.0		
	Con 1	LRNM # 7D	11.03	Unmodified wheat starch	5.0	0.2298	5.8		
	Con 2		11.13		5.0	0.3174	7.9		
	Tail	7 - 4D				3.4474	86.3		89.1
8	Feed			60 mg / L		3.9810	100.0		
	Con 1	LRNM # 8D	10.96	Unmodified wheat starch	5.0	0.1856	4.7		
	Con 2		8.65		5.0	0.2398	6.0		
	Tail	8 - 6D				3.5556	89.3		88.7

As can be seen from Table 15, the weight yield of the flotation tail, i.e., the rutile concentrate, increased with increasing depressant concentrations. However the grade of the rutile concentrate was not affected. Based on the results, a depressant concentration of 50 ppm wheat starch was selected since both the weight recovery and the grade were deemed high at this concentration.

5.5.3 Other Test Conditions

The results shown in Tables 14 and 15 indicated that there was no significant upgrading of the rutile concentrate, and that the TiO₂ content in the flotation tails (rutile) stayed at around 87 - 89%. Apparently, some drastic measures had to be taken in order to upgrade the rutile. First of all the flotation feed was cleaned by washing with a diluted hydrochloric acid solution to remove any possible surface contaminants. Secondly, a commercial cationic collector, Armeen[®] 18D, obtained from Akzo Noble, was used in place of DDAA. Armeen[®] 18D has 18 carbon atoms in the hydrocarbon chain and was expected to have a stronger collecting power than DDAA, which has only 12. Thirdly, the solution pH was raised from 11 to close to 12 to keep the losses of rutile at a minimum. Finally, the total flotation time was increased and DF250 was used to replace MIBC to maintain a stable froth layer during the extended flotation period. The froth was scraped for 30 minutes, although it appeared quite barren throughout the tests. It was reasoned that the small amount of quartz contained in the rutile would be floated slowly into the flotation concentrate. In some tests, the froth would become unstable during the extended flotation period and further addition of DF250 could not restore it. A second and third dose of Armeen[®] 18D rejuvenated the froth. The additional collector doses served a similar purpose to additional flotation stages. Table 16 shows the results of the flotation tests under these conditions. The flotation products were again examined under a stereomicroscope and some were assayed for SiO₂ and TiO₂. These assay results are also shown in Table 16.

Obviously, irrespective of the change of flotation conditions, the SiO₂ content in the rutile concentrate stayed at 4.8 – 6.0% and the TiO₂ content at 87 – 89%. There was no obvious upgrading of the LRNM using the reverse flotation procedures.

Systematic analyses of the flotation tails (i.e., the rutile concentrate) were then performed to find out the reason behind these observations.

Table 16 Reverse Flotation of Rutile Concentrate using Armeen® 18D

Test #	Pretreatment	Sample	Sample ID	pH before flotation	Depressant	Armeen® 18D (mol / L)	Float time (min)	Weight		Assay, %	
								(g)	%	SiO ₂	TiO ₂
9	Acid Wash 2 drops DF 250	Feed			50 mg / L			3.9857	100.0		
		Con 1	LRNM # 9 C1	12.09	Unmodified	5.0×10^{-4}	7.0	0.0482	1.2		
		Con 2	LRNM # 9 C2	11.89	Wheat starch	5.0×10^{-4}	10.0	0.1087	2.7		
		Tails	LRNM # 9 T		20 g/L NaOH			3.8288	96.1		
10	Acid Wash 1 drop DF 250	Feed			50 mg / L			3.9746	100.0		
		Con 1	LRNM # 10 C1	11.99	Unmodified	5.0×10^{-4}	16.0	0.0810	2.0		
		Con 2	LRNM # 10 C2	11.53	Wheat starch	5.0×10^{-4}	14.0	0.2647	6.7		
		Tails	LRNM # 10 T		20 g/L NaOH			3.6289	91.3		
11	Acid Wash 1 drop DF250	Feed			50 mg / L			3.9342	100.0		
		Con 1	LRNM # 11 C1	11.97	Unmodified	5.0×10^{-4}	15.0	0.1602	4.1		
		Con 2	LRNM # 11 C2	11.14	Wheat starch	5.0×10^{-4}	8.0	0.4419	11.2		
		Tails	LRNM # 11 T		20 g/L NaOH			3.3321	84.7		
12	Acid Wash 1 drop DF250	Feed			50 mg / L			3.9646	100.0	5.22	
		Con 1	LRNM # 12 C1	12.03	Unmodified	7.5×10^{-4}	11.0	0.0475	1.2	6.48	
		Con 2	LRNM # 12 C2	11.73	Wheat starch	1.25×10^{-4}	7.0	0.0390	1.0	11.76	
		Con 3	LRNM # 12 C3	11.58	20 g/L NaOH	2.5×10^{-4}	8.0	0.0915	2.3	10.78	
		Con 4	LRNM # 12 C4	N.A.		2.5×10^{-4}	8.0	0.2459	6.2	7.29	
		Tails	LRNM # 12 T					3.5407	89.3	4.84	87.4
13	Acid Wash 1 drop DF250	Feed			50 mg / L			3.9735	100.0	5.69	
		Con 1	LRNM # 13 C1	12.00	Unmodified	5.0×10^{-4}	12.0	0.0739	1.9	5.20	
		Con 2	LRNM # 13 C2	11.55	Wheat starch	5.0×10^{-4}	13.0	0.2139	5.4	7.63	
		Con 3	LRNM # 13 C3	10.87	20 g/L NaOH	5.0×10^{-4}	7.0	0.6789	17.1	5.87	
		Tails	LRNM # 13 T					3.0068	75.7	5.52	89.0
14	Acid Wash 1 drop DF250 +400 mesh	Feed			50 mg / L			3.9455	100.0	6.31	
		Con 1	LRNM # 14 C1	12.03	unmodified	5.0×10^{-4}	12.0	0.0797	2.0	6.65	
		Con 2	LRNM # 14 C2	11.60	wheat starch	5.0×10^{-4}	12.0	0.2106	5.3	12.31	
		Con 3	LRNM # 14 C3	10.99	20 g/L NaOH	5.0×10^{-4}	8.0	0.6740	17.1	5.57	
		Tails	LRNM # 14 T					2.9812	75.6	6.04	89.1
16	Acid Wash 1 drop DF250 +400 mesh	Feed			50 mg / L			3.9898	100.0		
		Con 1	LRNM # 16 C1	12.05	unmodified	5.0×10^{-4}	9.5	0.0590	1.5		
		Con 2	LRNM # 16 C2	11.76	wheat starch	5.0×10^{-4}	11.0	0.1240	3.1		
		Con 3	LRNM # 16 C3	11.39	20 g/L NaOH	5.0×10^{-4}	10.0	0.4679	11.9		
		Tails	LRNM # 16 T					3.3389	84.6	6.83	85.7
17	Acid Wash 1 drop DF250 +400 mesh	Feed			50 mg / L			4.0005	100.0		
		Con 1	LRNM # 17 C1	12.04	unmodified	5.0×10^{-4}	8.0	0.0404	1.0		
		Con 2	LRNM # 17 C2	11.79	wheat starch	5.0×10^{-4}	9.0	0.0846	2.1		
		Con 3	LRNM # 17 C3	11.56	20 g/L NaOH	5.0×10^{-4}	9.5	0.1432	3.6		
		Tails	LRNM # 17 T					3.7323	94.6		SEM/EDX

5.6 Analysis of the Flotation Products

5.6.1 Optical Analysis

The observations under the optical stereomicroscope yielded semi-quantitative information about the flotation products. Under transmitted light, quartz was a clear and colorless crystal and the titanium minerals were opaque or semi-opaque; thus it was relatively easy to distinguish the two minerals. Generally, in each flotation test, the first flotation concentrate contained abundant free quartz grains, either as large individual

grains, or as aggregated flocs that contained many small quartz grains. The subsequent flotation concentrates contained fewer quartz grains, which were mainly interlocked with rutile in the edges, rims, and trelliswork structures. The flotation tails usually contained very few free quartz grains, although interlocked grains were occasionally observed.

5.6.2 Chemical Analyses

These semi-quantitative observations were confirmed by the chemical assays of SiO₂ in the flotation concentrates, as shown in Table 17 for tests #12, #13 and #14. As can be seen from Table 16, there was a certain degree of selective quartz flotation, especially in tests #12 and #14, for the flotation concentrates assayed higher SiO₂ content than the tails.

Table 17 Whole Rock Analysis of Typical Flotation Tails (rutile concentrates), Weight %

Compound	LRNM#12T	LRNM#13T	LRNM#14T
Al ₂ O ₃	1.34	1.43	1.39
BaO	0.11	0.13	0.13
CaO	0.35	0.39	0.33
Fe ₂ O ₃	0.66	0.72	0.70
K ₂ O	0.49	0.18	0.17
MgO	0.33	0.34	0.33
MnO	0.01	0.01	0.01
Na ₂ O	0.37	0.38	0.32
P ₂ O ₅	0.17	0.17	0.16
SiO ₂ *	4.83	5.52	6.04
TiO ₂	87.41	88.95	89.06
ZrO ₂	1.14	1.04	1.09
U+Th, ppm	112	80	165
Total	97.21	99.26	99.73

* Average of three assays

However, as can be seen from Table 17, all three typical flotation tails (which were rutile concentrates) still contained 4.8% to 6.04% SiO₂, although virtually no quartz grains were observed through the stereomicroscope. To verify these assay results, the procedures of test #14 were repeated in tests #15 and #16. The flotation products of test #15 were sent for mineralogical analyses, the flotation tail of test #16 was sent to a different assay lab (Dynatec Corp.'s Metallurgical Technologies Division, Fort

Saskatchewan, AB) to check the SiO₂ and TiO₂ assays. The assay results of the flotation tail of test #16 were also shown in Table 16, i.e., 6.83% SiO₂ and 85.7% TiO₂, which were very close to the assays of the flotation tail of test #14, performed by International Plasma Laboratories Ltd. in Vancouver, BC.

5.6.3 Petrographical Analyses

Harris Exploration Services, Inc., who also performed the analyses on the original LR Rutile, conducted the mineralogical analysis. In general, the mineralogical assessment results seemed to confirm the observations under the stereomicroscope but were at odds with the chemical assays. While some free and interlocked quartz grains were observed in the flotation concentrate, no quartz grains could be detected in the flotation tails. Harris Exploration Service estimated that the flotation tail of test #15 contained 86.0% rutile (TiO₂), 10.0% opaque minerals which were initially thought to be Fe-bearing titanium minerals, 0.5% quartz (SiO₂), 3.0% zircon (ZrO₂.SiO₂), and 0.5% of other silicate minerals. They performed SEM/EDX analyses on about 20 opaque grains and found that in all cases titanium was the only elemental response and no iron was detected, and concluded that these opaque minerals were all some forms of TiO₂. They could not explain why the chemical assays indicated 5 - 6% SiO₂.

The disparity between the mineralogical analysis and the chemical assays may be the result of the interlocking between quartz (and other silicates) and rutile. In fact, mineralogical analysis on the LR Rutile sample showed that some of the rutile particles were polycrystalline aggregates of rutile and minor silicates. When these types of particles stayed in the flotation tails, they would increase the SiO₂ assays but may not be completely detected by optical observations although some may be observed. In fact, one of the slides prepared by Harris Exploration Services on the test #15 tail showed such interlocked rutile and quartz grains (Figure 28).

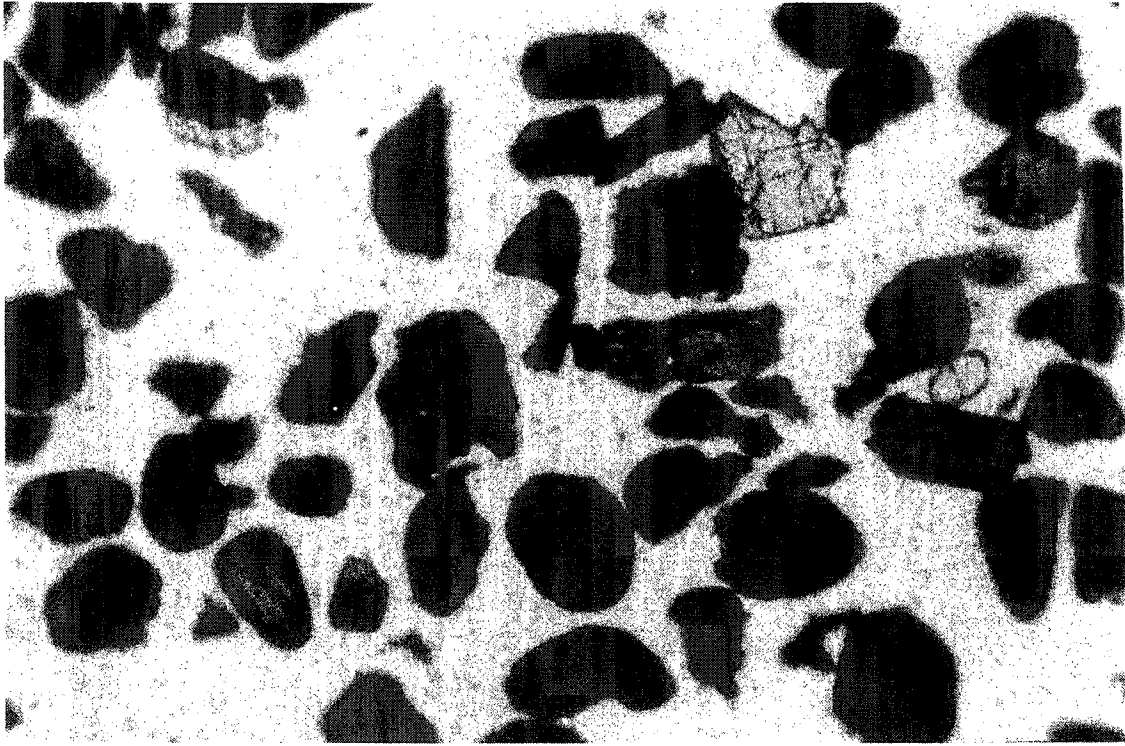


Figure 28 Typical field of flotation tail by plane polarized light. Dominant opaque (black) to translucent brown constituent is TiO_2 . High relief transparent grains (dark rim) in upper right quadrant are zircon. TiO_2 grain at upper left is a middlings, with a partial selvedge of quartz (colorless).

5.6.4 SEM/EDX Analysis

The flotation tail (which was the rutile concentrate) of test #17 was analyzed with a scanning electron microscope (SEM) with energy dispersive x-ray fluorescence (EDX). Some of the SEM images and EDX spectra are presented in Figures 29 to 32.

Figure 29a shows the back scattering image of a rutile particle surface. Elements with low atomic numbers appear darker in this type of image. As can be seen, the surface showed a rough texture where the lighter color was found to be titanium. There were several round-shaped darker grains embedded on the surface (Figure 29a). An EDX spectrum was taken from grain P1. As shown in Figure 29b, the EDX spectra for the

mineral grain responded with Si and O, revealing that it was predominantly quartz. Similarly, the other darker grains in the lower left part of the image were also quartz.

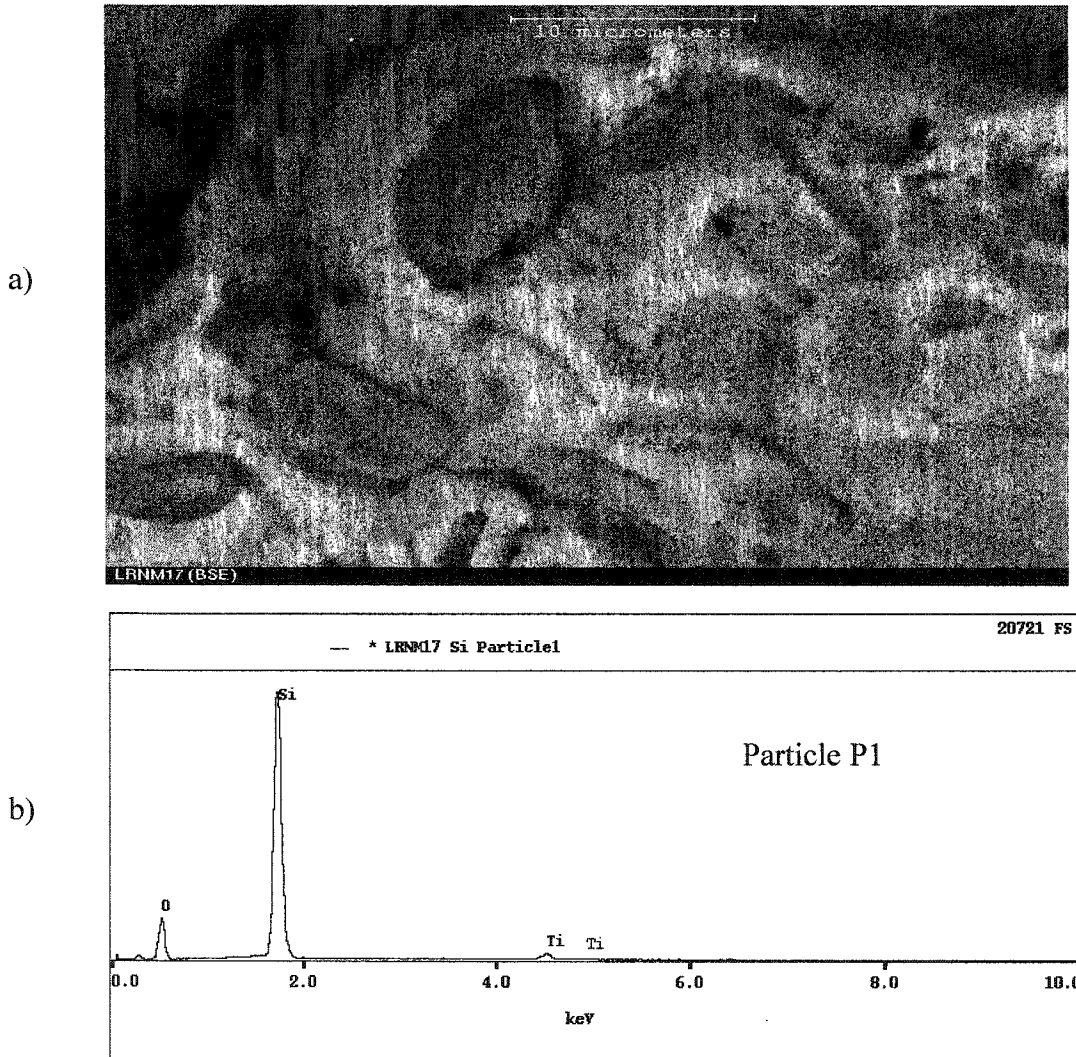


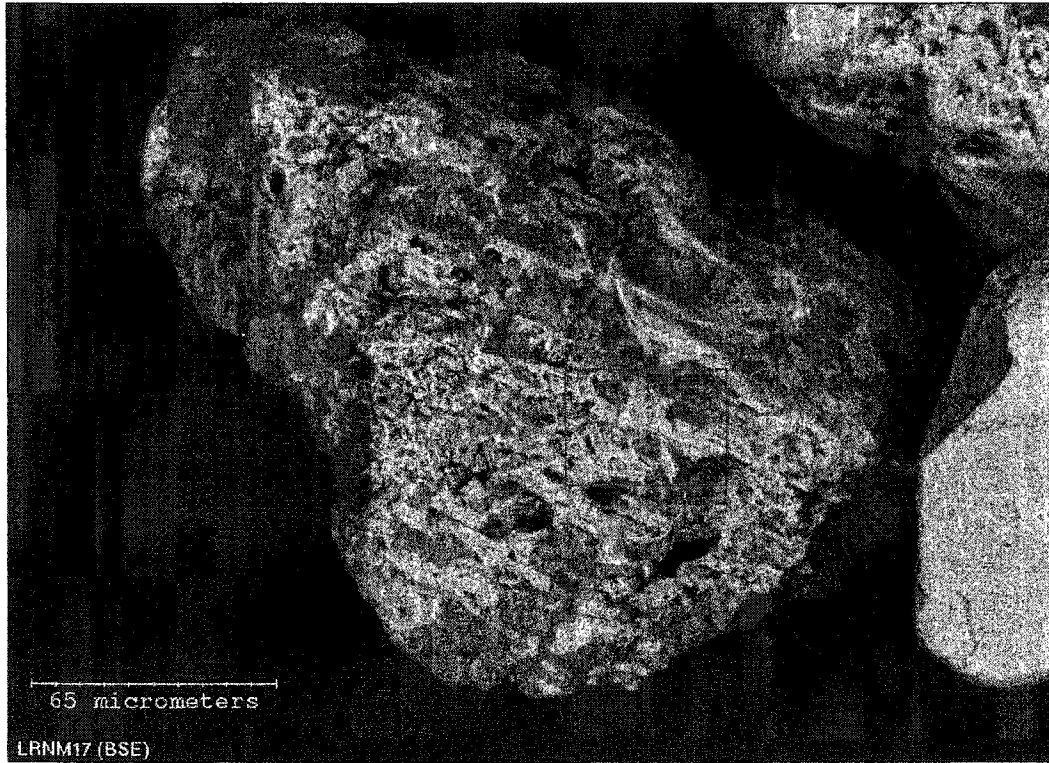
Figure 29 a) SEM image of the surface of a rutile particle;
b) EDX spectrum of P1, which shows that P1 is a siliceous mineral grain.
The other three darker round-shape embedded grains in the lower left are also siliceous minerals.

Figure 30a shows a composite rutile particle with a very complex trelliswork structure. The light colored, needle-like crystals were found to be titanium minerals. However, there were numerous darker grains embedded throughout the structure. Figure 30b shows a magnified view of a small area marked in Figure 30a. Apparently, the embedded grains P2 and P3 were siliceous minerals, as shown by their EDX spectra in Figure 30c and 30d. An area marked in Figure 30b shows complex texture and the EDX spectrum recorded for this area showed the presence of Ti, Si, O and Al. Clearly, this is an area where the titanium minerals are intimately intergrown with the silicate/aluminosilicate minerals.

Generally, particles like those shown in Figure 29a and Figure 30a were common in the rutile concentrate. Figures 31 and 32 show two typical views of the rutile concentrate. As can be seen, some of the particles in the rutile concentrate appeared well crystallized and their surfaces were smooth. EDX analyses of these well-crystallized grains showed titanium as the only elemental response. However, a significant number of the particles showed rough surface textures indicating that these minerals are not well crystallized. These particles usually contain embedded grains that were composed of Si and O, as marked in Figures 31 and 32.

There were no free grains of quartz observed in the SEM/EDX analysis of the flotation tails, the rutile concentrate. This indicates that the developed flotation procedure functioned to remove the well-liberated quartz grains. It is believed that the intimate association of the titanium minerals with the siliceous minerals was the main reason why the SiO_2 content in the rutile concentrate could not be lowered using the reverse flotation procedures.

a)



b)



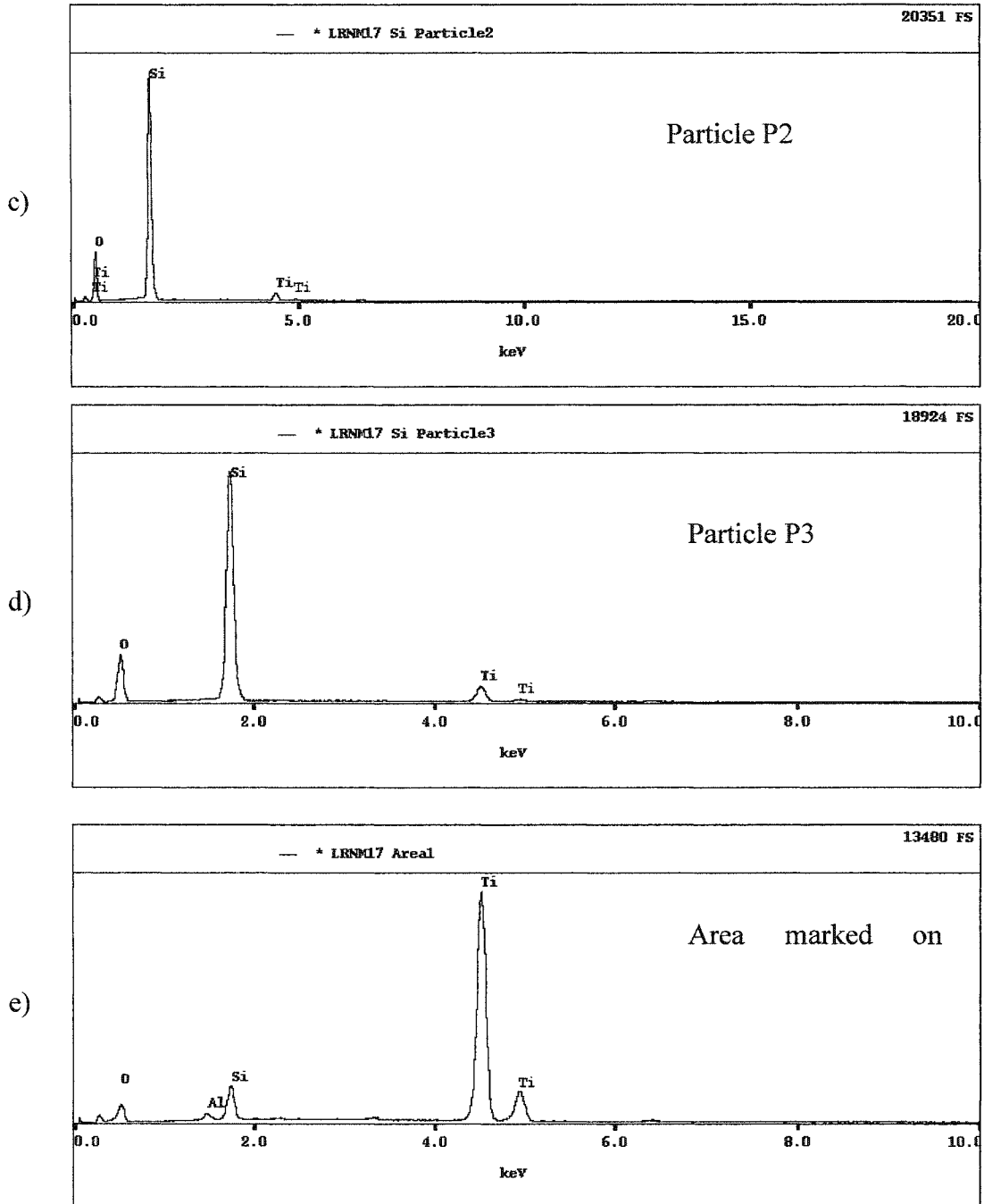


Figure 30 a) SEM image of a rutile particle, showing the trelliswork of rutile with embedded darker siliceous mineral grains;
 b) An enlarged view of the area marked in a;
 c) EDX spectrum of grain P2 in b;
 d) EDX spectrum of grain P3 in b;
 e) EDX spectrum of the area marked in b.



Figure 31 A typical SEM image of the rutile concentrate. The marked areas show embedded darker grains, which are siliceous minerals. The smooth crystal in the upper right corner is pure rutile.

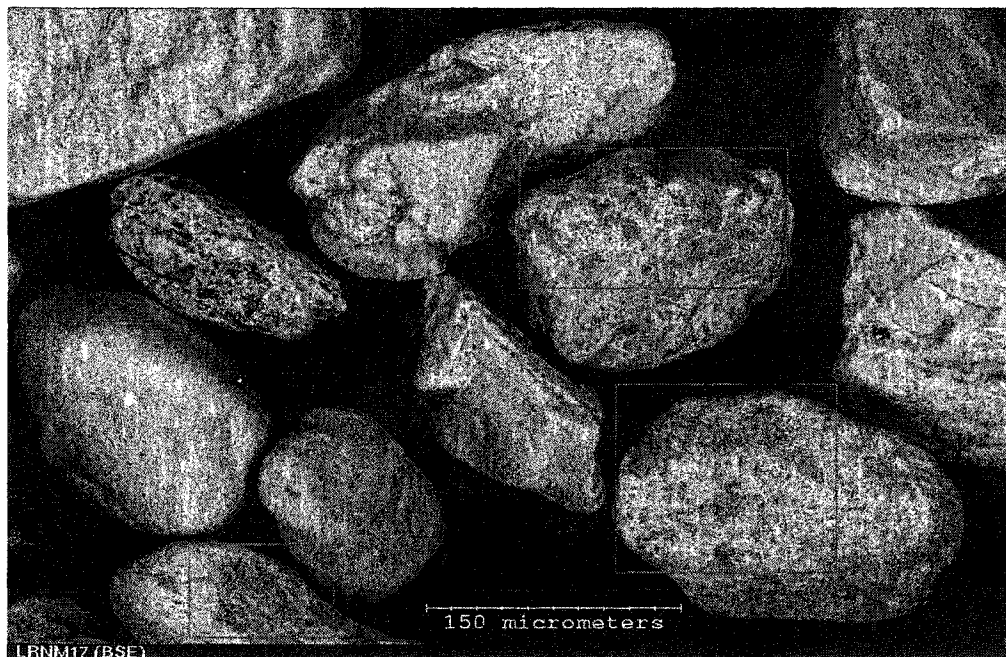


Figure 32 Another SEM image of the rutile concentrate, showing similar features as Figure 31. The smooth crystals are high purity rutile (anatase).

6 CONCLUSIONS

Recently, a rutile concentrate (designated LR Rutile) was produced from the oil sands froth treatment tailings by Lakefield Research Ltd. and Syncrude Canada Ltd. and, based on a novel process that was developed from a complete knowledge of previous studies. The most significant feature of the process is the use of froth flotation for the separation of titanium minerals from zircon. Since the process is most likely viable, the current project has been designed to build upon it with the objective of characterizing and upgrading the rutile concentrate (LR Rutile) it produced.

The major findings of this project are:

1. The LR Rutile has a dominant particle size around 120 μm with an 80% passing size of 145 μm .
2. The LR Rutile contained 75.5% TiO_2 , 18.7% Fe_2O_3 , 1.03% Al_2O_3 , 1.94% SiO_2 , and 563 ppm Th+U. Mineralogical analyses confirmed the presence of rutile (and anatase) as well as ilmenite in various altered forms. The estimated amount of rutile (and anatase) in the LR Rutile was between 10% and 17%, and the major part of the rutile (anatase) grains were impure or polycrystalline, with inclusions of siliceous minerals or other oxides. In fact, electron microprobe analysis showed that the TiO_2 content in the rutile (anatase) grains ranged from 77 to 99%.
3. The majority of the Fe-bearing titanium minerals (altered ilmenite) in the LR Rutile were found removable by dry magnetic separation. At a low magnetic field strength (2000 Gauss), about 88% of the Fe was removed from the LR Rutile in a single pass, resulting in an upgraded non-magnetic rutile product that assayed 85.5% TiO_2 and 8.83% Fe_2O_3 , with 24% weight recovery. At a high magnetic field strength of 12,000 Gauss, over 99% of the Fe was removed, resulting in an upgraded non-magnetic rutile product that assayed 86.4% TiO_2 , 0.77% Fe_2O_3 , 1.59% Al_2O_3 , 6.01% SiO_2 , and 180 ppm Th+U, with 15% weight recovery. The

increase of SiO₂ content in the rutile product indicated that the majority of the siliceous minerals in the LR Rutile were non-magnetic.

4. To remove the contaminating SiO₂ in the rutile concentrate, a reverse flotation process was developed. It was found that cationic collectors, dodecylamine acetate and Armeen[®] 18D, could be used to float quartz and rutile, but the latter could be selectively depressed by various polysaccharides, amongst which a wheat starch was found the most effective.
5. The developed reverse flotation process was tested on the upgraded non-magnetic rutile fraction from the magnetic separation. While it was found that the free liberated quartz was completely floated into the flotation concentrates, the flotation tails, which were the rutile products, still contained substantial amount of SiO₂ that ranged from 4.84% to 6.04%. The TiO₂ content in the flotation tails ranged from 87% to 89%.
6. Adsorption and zeta potential measurements support the results for the flotation procedure developed to float quartz from rutile. In alkaline pH, between 10 and 12, quartz is much more negatively charged than rutile resulting in a stronger cationic collector adsorption. Also in this pH range wheat starch adsorbs much more strongly on rutile mineral surfaces than on quartz resulting in a strong depressive effect on titanium minerals.
7. Mineralogical analyses, and more significantly the SEM/EDX analyses, indicated that the siliceous minerals in the rutile concentrate were intimately associated and interlocked with the rutile (anatase). Such interlocking makes it impossible to lower the SiO₂ content by physical ore dressing techniques without significant particle size reduction.

7 RECCOMENDATIONS FOR FURTHER RESEARCH

The maximum grade of rutile concentrate that could be produced from the oil sands tailings by physical mineral dressing techniques is 90% TiO₂. The typical specifications for the chloride titanium pigment feedstock requires >85% TiO₂, < 1.0% Al₂O₃, varying amounts of SiO₂ and <100ppm U+Th (Garnar and Stanaway, 1994). The upgraded rutile concentrate from this project meets most of these requirements except for the Al₂O₃ and U+Th content (1.34 - 1.43% and 80-165 ppm, respectively).

To upgrade the rutile concentrate to a premium grade (>96% TiO₂), two possible process routes could be followed:

1. A size reduction of the LR Rutile followed by physical separation processes.
2. A selective leaching process for the quartz and aluminosilicate minerals, such as a caustic leach. This may be done with or without a size reduction.

However, neither process route is appealing at this stage due to the already finer sizes of the rutile product than other available rutile concentrates produced from beach sands resources, and due to the costs and potential environmental problems associated with caustic leaching.

The radioactive elements (U and Th) in the LR Rutile are most likely associated with magnetic minerals such as monazite, as shown by the significant reduction in their concentration after the removal of magnetic minerals. More tests to optimize the magnetic separation conditions would further lower the content of both Fe and the radioactive elements in the rutile concentrate.

8 REFERENCES

1. Alberta Chamber of Resources, 1996. Mineral Development Agreement – Co-product Study. Executive Summary.
2. Balderson, G.F., 1982. Test work on scroll centrifuge tailings from Syncrude Canada Ltd., Mineral Deposits Limited Report No. 46.123.1/1.
3. Banford, Johnathan, Maud, Geoffrey Elliott, and Demosthenous, Maria Leonida, July 28, 1998. U.S. Patent 5,785,748, Titanium Dioxide Pigments.
4. Birkeland, Peter W., Larson, Edwin E., 1989. Putnam's Geology, 5th Edition, Oxford University Press, New York.
5. Blair, S M, 1950. Development of the Alberta Bituminous Sands - Report On The Alberta Bituminous Sands, Report, Bechtel Corp and UOP, Edmonton.
6. Borowiec, Krzysztof, Grau, Alfonso E., Gueguin, Michel and Turgeon, Jean-Fran.cedilla.ois, Nov. 3, 1998. U.S. Patent 5,830,420, Method to Upgrade Titania Slag and Resulting Product.
7. Brookhaven Instruments Corporation, 1994. Instruction Manual for the Zeta Potential Meter.
8. Chao, Tze, and Senkler, George H. Jr., February 4, 1992. U.S. Patent 5,085,837, E.I. Du Pont de Nemours and Company.
9. Deura, Tetsushi N., Wakino, M., Matsunaga, T., Suzuki, Ryosuke O. and Ono, K. Dec. 1998. Titanium Powder Production by $TiCl_4$ Gas Injection into Magnesium Through Molten Salts, Metallurgical and Materials Transactions B, Vol. 29B, 1167-1174.
10. Dubois, M., Gilles, K., Hamilton, J. K., Rebers, P.A., and Smith, F., 1956. Analytical Chemistry, 28, 350.
11. Fukushima, Seitaro, Saito, Ariyoshi, and Kaneko, Fukuzo, 1976. U.S. Patent 3,961,940, Post-Treatment of Ilmenite Ore Subjectoed to Selective Chlorination Treatment, June 8, 1976.
12. Gambogi, Joseph, January 2002. U.S. Geological Survey, Mineral Commodity Summaries: Titanium Mineral Concentrates.

13. Garnar, T. E. and Stanaway, K. J., 1994. Titanium Minerals, in Industrial Minerals and Rocks, 6th Ed., Edited by D.D. Carr. Society of Mining Engineers, Inc., AIME, New York, 1071-1090.
14. Gurav, Abhijit S., Kodas, Toivo T., and Anderson, Bruce M., Nov. 10, 1998. U.S. Patent 5,833,892, Formation of TiO₂ Pigment by Spray Calcination.
15. Hiew, Michael and Chegwidan, Philip, Jan. 29, 2002. U.S. Patent 6,342,099, Coated Titanium Dioxide Pigments and Processes for Production and Use.
16. Hollitt, Michael John March 23, 1999. U.S. Patent 5,885,536, Process for Alkaline Leaching a Titaniferous Material.
17. Hunter, Robert J., 1993. Introduction to Modern Colloid Science.
18. Ityokumbul, M.T., Bulani, W. and Kosaric, N., 1987. Economic and environmental benefits from froth flotation recovery of titanium, zirconium, iron and rare earth minerals from oilsand tailings. *Wat. Sci. Tech.*, Vol 19, Rio, 323-331.
19. Lefond, Stanley J., 1983. Industrial Minerals and Rocks (Nonmetallics other than Fuels), 5th Ed., Society of Mining Engineers, American Institute of Mining, Metallurgical, and Petroleum Engineers, Inc., New York, New York.
20. Leja, Jan, 1982. Surface Chemistry of Froth Flotation, Plenum Press, New York.
21. Manser, R M, 1975. Handbook of Silicate Flotation.
22. Mao, M., Fornasiero, D., Ralston, J., and Sobieraj, S., 1999. Use of Depressants in the Separation of Zircon from Rutile and Ilmenite, Ian Wark Research Institute, University of South Australia. 38th Annual Conference of Metallurgists of CIM.
23. McAndrew, John, 1957. Calibration of a Frantz Isodynamic Separator and its application to mineral separation. *Proceedings of the Australian Institute of Mining and Metallurgy*, No 181, 59-73.
24. McCosh, R., 1996. Geology executive summary from Mineral development Agreement, Final Report, Alberta Chamber of Resources.
25. Mineral Sands, www.minerals.org.au, 1999. Minerals Council of Australia and Australian Geological Survey Organization.
26. Mishra, Brajendra and Kipouros, Georges J., 1996. Titanium: extraction and processing: proceedings of the symposium sponsored by the Reactive Metals Committee of the Light Metals Division of the Minerals, Metals & Materials Society,

- 1997 Materials Week in Indianapolis, Indiana, September 14-18, 1997 / sponsored by the Reactive Metals Committee, Light Metals Division, TMS: Minerals, Metals & Materials Society.
27. National Energy Board, October 2000. Canada's Oil Sands: A Supply and Market Outlook to 2015. Cat. No. NE23-89/2000E.
 28. Orth-Gerber, Jurgen, Elfenthal, Lothar and Blumel, Siegfried, Jan. 22, 2002. U.S. Patent 6,340,387, Organically Post-Treated Pigments and Methods for their Production.
 29. Owen, M., 1996. Mineral Development Agreement, Final Report, Alberta Chamber of Resources.
 30. Oxenford, J., Coward, J.E. and Bulatovic, S., 2001. Heavy minerals from Alberta's oil sands. CIM Annual General Meeting, Quebec City, April 30 – May 2, 2001.
 31. Padmanabhan, N.P.H., Sreenivas, T., and Rao, N.K., 1990. "Processing of Ores of Titanium, Zirconium, Hafnium, Niobium, Tantalum, Molybdenum, Rhenium, and Tungsten: International Trends and the Indian Scene." High Temperature Materials and Processes, Vol. 9, Nos 2-4, 217-247.
 32. QIT, www.qit.com, Fer et Titane, 2001.
 33. Rhee, K.I. and Sohn, H.Y., 1990. The Selective Carbochlorination of Iron from Titaniferous Magnetite Ore in a Fluidized Bed, Metallurgical Transactions B, Vol. 21B, April, 341-347.
 34. Richards Bay Minerals Inc., www.richardsbayminerals.co.za, 2002.
 35. Rosskill, www.roskill.co.uk/timet.html, 2001. The Economics of Titanium Metal, 2nd. Ed.
 36. Scotland, W A and Benthin, H, 1952-1954. Exploration of the Alberta Bituminous Sands. Unpublished report of the Alberta Department of Energy.
 37. Shaw, Duncan J., 1992. Colloid and Surface Chemistry, 4th Edition.
 38. Smith, William F., 1993. Structure and Properties of Engineering Alloys, 2nd. Ed. McGraw-Hill, Inc.
 39. Sohn, Hong Yong and Zhou, Ling, Dec. 1998. The Kinetics of Carbochlorination of Titania Slag, Departments of Metallurgical Engineering and of Chemical and Fuels

- Engineering, University of Utah, Salt Lake City, UT, The Canadian Journal of Chemical Engineering, Vol. 76, Dec. 1998.
40. Suncor Energy Inc., www.suncor.ca, 2002.
 41. Svoboda, J. 1987. Magnetic Methods for the Treatment of Minerals. Elsevier, New York.
 42. Syncrude Canada Ltd., www.syncrude.ca, 2001.
 43. Trevoy, L.W. and Schutte, R., 1981. A new source of heavy minerals from Canadian oil sands mining operations. Preprint No. 81-20, Annual Meeting of SME/AIME.
 44. Weast, Robert C. and Astle, Melvin J., 1981. CRC Handbook of Chemistry and Physics, 61st Edition, Boca Raton, Florida.
 45. Wills, Barry A., Mineral Processing Technology, 6th Edition, Butterworth-Heinemann, Oxford, 1997.
 46. Winter, Mark, www.webelements.com, 1993. [The University of Sheffield and WebElements Ltd., UK].
 47. Yang, Fenglin and Hlavacek, Vladimir Dec. 1998. Carbochlorination Kinetics of Titanium Dioxide with Carbon and Carbon Monoxide as Reductant, Metallurgical and Materials Transactions B, Vol. 29B, 12971307.

9 APPENDIX

9.1 Appendix I: Adsorption Measurements

The concentration of wheat starch in aqueous solutions was determined by the colorimetric method of Dubois et al (1956). In this method, a certain amount of phenol is added to the polysaccharide solution, followed by the rapid addition of concentrated sulfuric acid. This produces a stable orange color whose intensity is proportional to the concentration of the polysaccharide.

According to Dubois et al, the amount of phenol and the wavelength to be used to measure the intensity of the orange color are critical parameters that must be determined empirically. A preliminary test showed that addition of 1.5 ml of a 5% phenol solution plus 10 ml of concentrated sulfuric acid to 4 ml polysaccharide solution provided the optimum conditions which can be seen below in Figure A1. The adsorbance of the colored complex was determined at 490 nm. Figure A2 shows the resultant linear calibration curve for various polysaccharide concentrations using the above conditions.

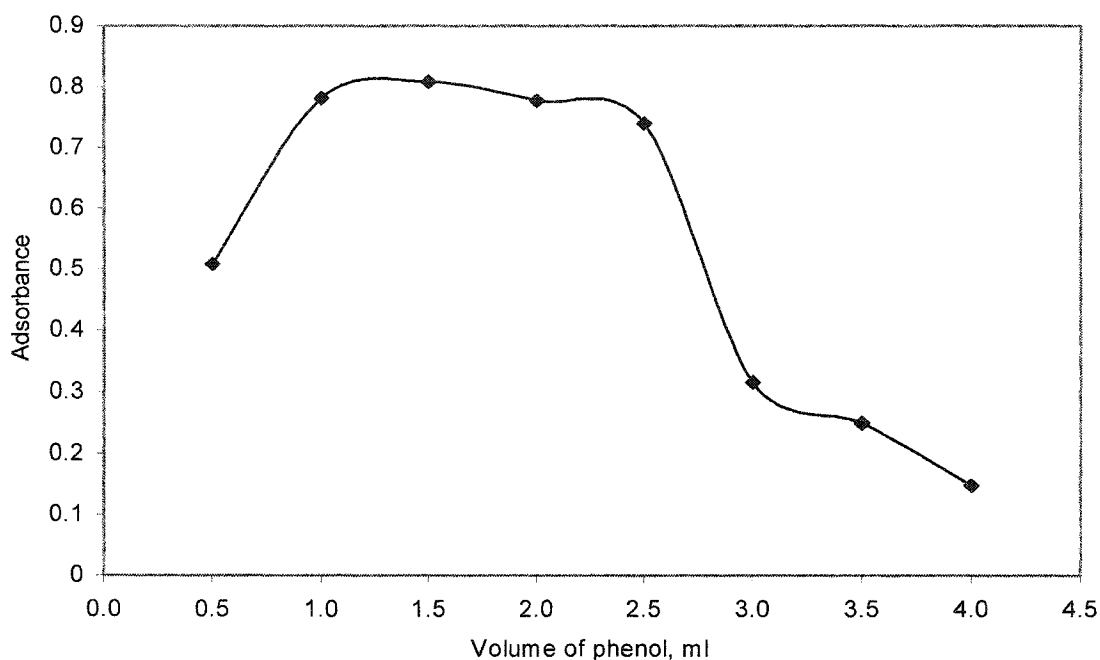


Figure A1 Effect of Phenol addition on the adsorbance of wheat starch using the sulfuric acid - phenol method

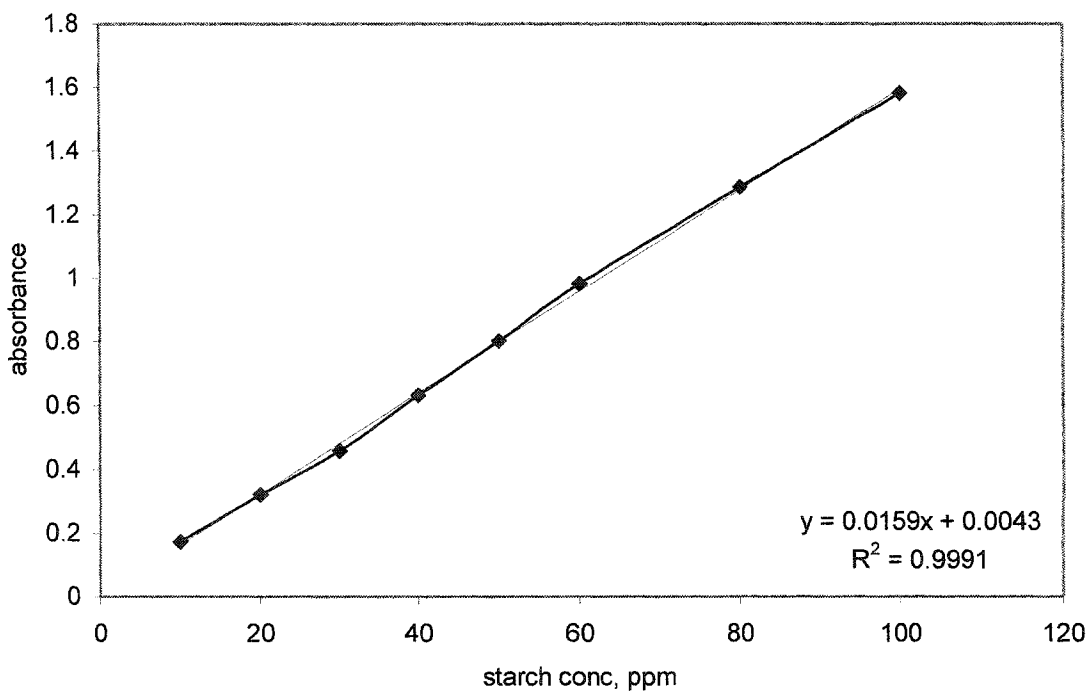


Figure A2 Calibration curve of wheat starch

9.1.1 Determination of Adsorption Density

The regression equation shown in Figure A2 can be transformed to:

$$C = k_1 \cdot \text{abs} + k_2 \quad (9.1)$$

In the calculation of polysaccharide concentration, the slope of the regression line (k_1) was assumed to be constant, and the second parameter k_2 , was determined in every batch of tests by one or several blank points.

For example, for wheat starch:

$$C = 62.89 \cdot \text{abs} - 0.2704 \quad (9.2)$$

When the adsorption test was conducted with the -400 mesh (-38 μ m) rutile at different pH values (original concentration of wheat starch was 50 ppm; 1 gram of -400 mesh rutile in a 50 ml solution), four measurements were taken to ensure accuracy of the measurements. This can be seen below in Table A1. After two measurements, a blank phenol-sulfuric acid solution was run to ensure there was no instrument drift. The following results were obtained:

Table A1 Measured adsorbance of wheat starch on rutile as a function of pH

final pH	abs 1	abs 2	abs 3	abs 4	avg. abs
2.23	0.335	0.332	0.367	0.367	0.350
5.94	0.279	0.283	0.313	0.313	0.297
7.53	0.308	0.309	0.327	0.328	0.318
7.58	0.358	0.357	0.362	0.364	0.360
8.03	0.400	0.400	0.390	0.392	0.396
8.77	0.371	0.371	0.384	0.385	0.378
10.42	0.374	0.375	0.390	0.388	0.382
12.48	0.484	0.487	0.498	0.500	0.492
blank 1	0.740	0.740	0.790	0.789	0.765
blank 2	0.790	0.789	0.803	0.804	0.797
blank 3	0.765	0.764	0.761	0.758	0.762

The initial concentration of wheat starch C_0 , 50 ppm, was adjusted using the calibration curve. Substituting this value into equation 9.2 allows the residual concentration of wheat starch to be calculated. This can be seen below in Table A2.

Table A2 Residual concentration of wheat starch

final pH	abs 1	abs 2	abs 3	abs 4	avg. abs	residual conc. ppm
2.23	0.335	0.332	0.367	0.367	0.350	21.697
5.94	0.279	0.283	0.313	0.313	0.297	18.369
7.53	0.308	0.309	0.327	0.328	0.318	19.681
7.58	0.358	0.357	0.362	0.364	0.360	22.322
8.03	0.400	0.400	0.390	0.392	0.396	24.525
8.77	0.371	0.371	0.384	0.385	0.378	23.416
10.42	0.374	0.375	0.390	0.388	0.382	23.666
12.48	0.484	0.487	0.498	0.500	0.492	30.572
blank 1	0.740	0.740	0.790	0.789	0.765	47.603
blank 2	0.790	0.789	0.803	0.804	0.797	49.588
blank 3	0.765	0.764	0.761	0.758	0.762	47.431

Once the residual concentration was found, the amount of starch that had been adsorbed by the rutile was calculated according to the following equation:

$$\Gamma = ((C_o - C)*V) / (W*S) \quad (9.3)$$

Where Γ is the amount adsorbed (mg/m^2), C_o and C are the original and residual concentrations of wheat starch (ppm), V is the volume of the suspension (L), W is the sample weight (g) and S is the specific surface area of the sample (m^2/g). Since the surface area of the minerals could not be determined, the assumption that S is equal to unity will be made and the resultant measurements will be reported on a basis of mg starch adsorbed per gram of mineral.

$$\text{At pH 2.23, } \Gamma = ((47.603 - 21.697)*0.05) / (1*1) = 1.30 \text{ mg/g}$$

The rest of the adsorption densities for rutile can be calculated accordingly as shown below in Table A3:

Table A3 Adsorption densities of wheat starch per gram of rutile

final pH	abs 1	abs 2	abs 3	abs 4	avg. abs	residual conc. ppm	Γ (mg/g)
2.23	0.335	0.332	0.367	0.367	0.350	21.697	1.30
5.94	0.279	0.283	0.313	0.313	0.297	18.369	1.46
7.53	0.308	0.309	0.327	0.328	0.318	19.681	1.40
7.58	0.358	0.357	0.362	0.364	0.360	22.322	1.26
8.03	0.400	0.400	0.390	0.392	0.396	24.525	1.15
8.77	0.371	0.371	0.384	0.385	0.378	23.416	1.31
10.42	0.374	0.375	0.390	0.388	0.382	23.666	1.30
12.48	0.484	0.487	0.498	0.500	0.492	30.572	0.95
blank 1	0.740	0.740	0.790	0.789	0.765	47.603	
blank 2	0.790	0.789	0.803	0.804	0.797	49.588	
blank 3	0.765	0.764	0.761	0.758	0.762	47.431	